REMOVAL OF MIXED CONTAMINANTS FROM WASTEWATER BY MULTISTAGE FLOTATION PROCESS

by

Fan Shi

B. S., Nanjing University of Chemical Technology, China, 1995

M. S., Nanjing University of Chemical Technology, China, 1998

Submitted to the Graduate Faculty of

School of Engineering in partial fulfillment

of the requirements for the degree of

Doctor of Philosophy

University of Pittsburgh

2005

UNIVERSITY OF PITTSBURGH

SCHOOL OF ENGINEERING

This dissertation was presented

by

Fan Shi

It was defended on

October 26, 2005

and approved by

George E. Klinzing, Professor, Department of Chemical and Petroleum Engineering

Badie I. Morsi, Professor, Department of Chemical and Petroleum Engineering

Ronald D. Neufeld, Professor, Department of Civil and Environmental Engineering

Ralph R. Lai, Senior Scientist, Dr., National Energy Technology Laboratory

Dissertation Director: Shiao-Hung Chiang, Professor, Department of Chemical and Petroleum Engineering

REMOVAL OF MIXED CONTAMINANTS FROM WASTEWATER BY MULTISTAGE FLOTATION PROCESS

Fan Shi, PhD

University of Pittsburgh, 2005

Wastewater discharged by industrial plants, including paper mills, petroleum refineries, chemical processing and other manufacturing facilities pose serious environmental concerns. In order to effectively remove mixed types of pollutants, including fine solids, emulsified oil and dissolved chemicals, a multi-stage loop-flow flotation column (MSTLFLO) has been developed. The loop flow action in the MSTLFLO column provides favorable hydrodynamic conditions, which promotes local in-stage mixing and enhances the bubble-particle contacts. It overcomes the slow collection problems normally encountered in conventional column flotation. Furthermore, with the addition of suspended adsorbent particles, the MSTLFLO column can function as an adsorptive flotation device to remove dissolved chemicals from wastewater.

In this study, an experimental investigation on a simulated wastewater system containing emulsified mineral oil, suspended particles (powdered activated carbon or glass beads), and dissolved phenol (as a representative chemical) has been carried out using the MSTLFLO flotation column. Test results show that the separation efficiencies of emulsified oil and fine particles are greater than 90% while the phenol removal approaches the limiting value of equilibrium adsorption. Thus, the potential application of MSTLFLO process for simultaneous removal of mixed pollutants from industrial wastewater has been demonstrated.

The rate of oil/fine particle separations in MSTLFLO column obeys the non-linear kinetics. The kinetic constants are correlated in terms of a two-parameter (gas holdup and bubble size) expression. A process simulation program based on the classic tank-in-series model

has been established. Experimental results for the removal of both individual and mixed components in MSTLFLO process are shown to be in excellent agreement with values predicted by the numerical simulation. In addition, a comparative study of oil removal in a 4-in and a 12-in MSTLFLO column has yielded a simple geometric scale-up scheme in term of the ratio of column diameters.

The findings of this study are intended to provide an engineering design basis in exploring future applications of the MSTLFLO flotation process for industrial wastewater treatment.

DESCRIPTORS

Draft tube

Fine particle separation

Kinetic correlation

Multi-stage flotation

Oily water treatment

Phenol adsorption

Process simulation

Scale-up

Simultaneous removal of mixed pollutants

Wastewater treatment

TABLE OF CONTENTS

LIST OF TABLES

LIST OF FIGURES

NOMENCLATURE

a, b, c, d, and *e*	Empirical constants
B, M, T	Bottom, Middle and Top stage, respectively
C	Concentration
d_{50}	Average particle diameter
d_b	Bubble size
d_e	Distance between two electrodes
d_p	Particle size
$E_{a,\,c,\,K}$	Attachment, Collision and Overall collection efficiency, respectively
H	Height of liquid
H_B	Liquid surface height
H_L	Distance between two pressure probes
H_m	Manometer reading
K	Kinetic constant
K_{ads}	Freundlich constant for adsorption of phenol on PAC
n	Order of the flotation or constant
O.D.	Outside diameter
PAC	Powered Activated Carbon
q	Chemical concentration in adsorbent
Q	adsorption amount per PAC
R_c	Overall recovery rate
$R,\ R^2$	Determination coefficient
SGV	Superficial Gas Velocity

t	Residence time
$\bar{t}_c$	Fluid mean residence time
u_L	Average liquid linear velocity
U_L	Superficial liquid velocity
V_g	Superficial Gas Velocity

GREEK LETTERS

θ	Contact angle
ε	Gas holdup

SUBSCRIPTS

0	Initial
4, 12	4-in, 12-in column
∞	Infinity
b	Bubble
d	Downcomer
eq	Equilibrium state
F	Frother
g	Gas
i	the *i*th
L	Liquid
p	Particle
r	Riser

PREFACE

The author would like to take this opportunity to express his sincere appreciation to his advisor Professor S. H. Chiang for his very valuable guidance, advice and contribution through the course of present study. Many thanks are also due to Professor Badie I. Morsi, Professor George E. Klinzing, Professor Ronald D. Neufeld, and Dr. Ralph R. Lai, members of author's dissertation committee, for their time and helpful comments

The author expresses his deep sorrow for the passing of Professor F.G. Pohland. He also wishes to express sincere gratitude to Professor Pohland for serving as one of the original members of his thesis committee.

The great technical assistance on the equipment by Mr. Larry Herman is acknowledged. Thanks are also extended to Dr. Zhong Zhou, Dr. Hongming Li and Mr. Deliang Shi, for their helps during the construction of equipment.

Finally, the author would like to thank his wife and parents for their encouragement and understanding throughout his academic pursuits.

1.0 INTRODUCTION

Wastewater discharged by industrial plants, including paper mills, petroleum refineries, chemical processing and other manufacturing facilities pose serious environmental concerns. To meet the strict government regulations, the industrial effluents have to be treated to remove contaminants, including different types of pollutants, prior to discharge into the environment. To achieve such a goal, we have developed a multi-stage loop-flow flotation column (MSTLFLO), which provides favorable hydrodynamic conditions by inducing loop flow action in the column. Furthermore, with the addition of suspended adsorbent particles, the MSTLFLO column can function as an adsorptive flotation device to remove dissolved chemicals from wastewater.

1.1 DEVELOPMENT OF FLOTATION PROCESS

The importance of the flotation process to the entire industrial world cannot be over emphasized. The process of flotation is based on the generation of gas bubbles within a solid-liquid or liquid-liquid suspensions and subsequent attachment and removal of solid particles or immiscible liquid droplets from the liquid medium by the rising gas bubbles.

The "modern" floatation technology was introduced to mineral industries in early 18^{th} centuries. It is estimated that up to 95% base-metal ores were treated by the flotation processes

[1]*: At present, the flotation technique has been applied not only in the mineral industry, but also the non-mineral industries, including pulp mills, rubber and waste battery. More recently, the environment engineers are using flotation processes to treat the contaminated sands[2], polluted soils[3] and different types of wastewaters[4, 5, 6].

The effectiveness of flotation mostly depends on the interfacial properties of components in the mixtures to be separated. These interfacial properties can be modified by adding different surface active reagents, named as surfactants. The introduction of various surfactants to modify the interfacial properties of different minerals led to major advances in the development of the flotation process. Researchers tested a large number of surfactants to improve the flotation separation efficiency[7]. For example, $Ca(OH)_2$ was used as a depressant to prevent pyrite from attaching to gas bubbles; SO_2 could depress sphalerite, which is liable to float along with the galena in the copper, lead and silver ores. Others materials, like coal tar, impure oleic acid and crude oil, were proved to be successful reagents in mineral selecting flotation.

Bubble generation is an essential step in flotation, because rising bubbles provide the lift force for those components (in the form of fine particles or droplets) to be separated. Based on the methods of bubble generation, flotation can be classified into three categories[8]:

- ***Dispersed air flotation***: Gas bubbles are introduced into the flotation compartment by suction induced by agitation or by injection of compressed gas through a sparger. Gas bubbles thus generated are usually large. This method has been widely used in mineral processing for upgrading ore concentrates.
- ***Dissolved gas flotation***: When a pressurized feed stream saturated with dissolved gas is introduced to a flotation device that operated at ambient pressure, gas bubbles are generated

* References are listed in numerical order in the Bibliography section

due to a sudden reduction of pressure. Typically, the saturator pressure goes as high as 5 atm. The gas bubbles so generated are very small at high expense.

- ***Electrolytic flotation***: Hydrogen and oxygen bubbles are generated by electrolysis. The gas bubbles are generally smaller than 30 μm. The operating cost is even higher (due to high energy cost) than dissolved gas flotation.

Although there are many different types of flotation devices, agitated cell and bubble column are the two most widely used configurations. A typical design of mechanical (agitated) cell is shown in Figure 1[9]. Slurry is fed into a cell. An impeller is installed in the flotation cell. Air is sucked into the cell through a hollow shaft of an agitator, and then air stream is broken by the agitating impeller, so that small bubbles are emitted from the end of impeller blades. Then, rising bubbles together with attached particles/droplets form a foam layer on the top of the dispersion phase. The foam layer is skimmed off mechanically from the top. Non-flotated components are withdrawn from the bottom of the cell. It should be noted that rotating impeller of the agitator not only introduces air bubbles into the flotation cell, but also mechanically breaks them up into small sizes. In addition, agitation induces turbulent mixing to promote particle-bubble collisions.

Mechanic flotation cells work well in mineral processing systems. However, large space requirement and high power consumption are their main drawbacks. The invention of flotation column in the early 1960s is considered to be the beginning of a new trend in flotation separation. This column flotation design was first patented in Canada and thus it was often referred as Canadian or conventional column [10]. A schematic of a conventional column is shown in Figure 2, with typical operating parameters.

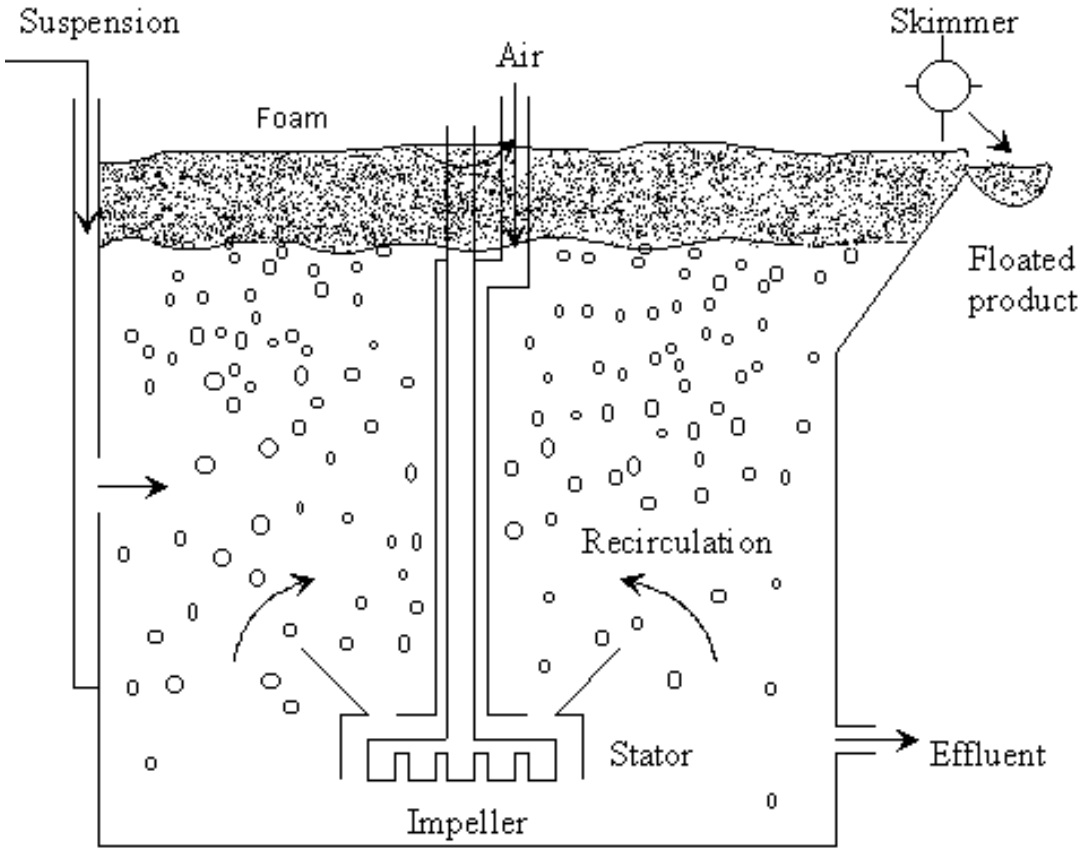

Figure 1 Illustration of a Mechanical Cell

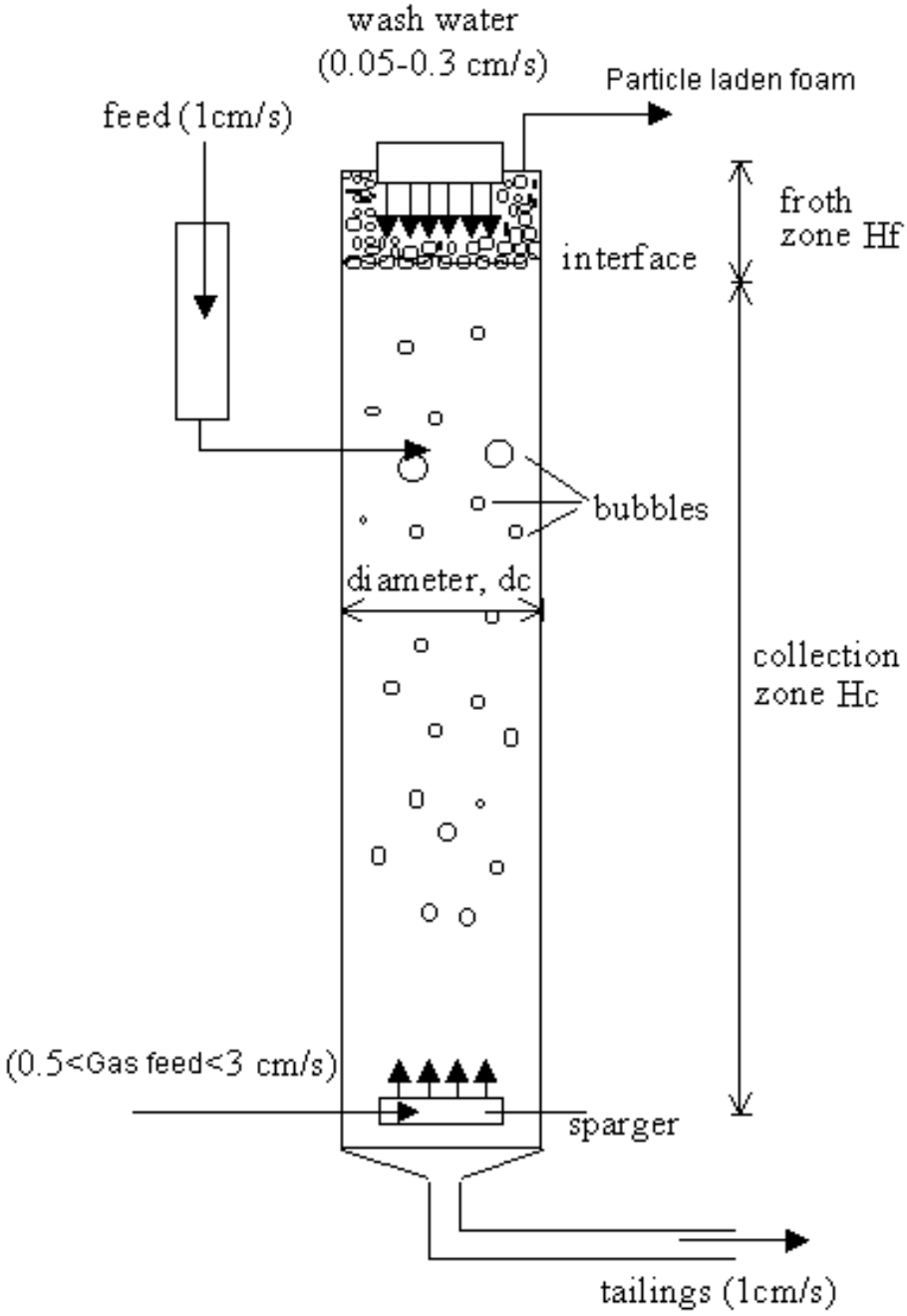

Figure 2 Schematic of Canadian or Conventional Column

Since the first flotation column was employed in mineral industry, this technique has been spread to many other fields, including petroleum refineries, chemical processing and manufacturing plants. The commercial applications of column flotation have surged since late 1970's. More recently, several different designs based on the idea of conventional flotation column were reported in the literatures. These include:

- ***Jameson's flotation column***[11]: it is a high throughput design for the beneficiation of mineral ores. Jameson's flotation column consists of two columns: the first column is installed inside the second column. Mineral ore slurry is fed into the top of the first column under pressure and air is entrained into slurry and forces foam moving downward. Foam passes through the bottom of the first column then into the second column where valued ores are carried up by froth to the surface and liquid together with tailings is drained through the bottom of the second column.
- ***Yoon's micro-bubble flotation column***[12]: it has been used for fine coal beneficiation. In Yoon's column, two types of bubble spargers are used in generating small bubbles: an external porous tube and an internal high-shear agitator. The sizes of microbubbles are in the range from 50 to 400 μm. This microbubble column is found to be very effective in processing the particles less than 20 μm in diameter.
- ***Yang's packed column***[13]: it provides an economical packed column for separating floatable particles from a mixture of floatable or non-floatable particles. This device is filled with a large number of circuitous flow passages, which are conducing flows between the upper and lower sections of the column. When pressurized air flow is passing through the packed flow passages, it is broken into small bubbles. These small bubbles collide with floatable particles and form a foam concentrate which overflows from the top.

- ***Miller's cyclonic column***[14] is a kind of flotation column with a tangential inlet on the top and an annular outlet at its bottom. Slurry is directed into the column in a swirling motion so that slurry develops a thin fluid layer around the inner wall of the column. Gas is injected through porous wall and into a thin slurry layer. Bubble and particle aggregates congregate at the axial center of the column and form a froth column, which can be removed with a vortex finder at the top of the column axially.
- ***Lai's Cyclonic Flotation Column (CFC)*** provides an effective way for the deep cleaning of pyrite in coal [15]. Slurry is mixed by impellers located at the center of the column, and heavy pyrite particles are more likely move towards the wall than light foam and coal particles, because of the centrifuge force. CFC gives a higher pyretic sulfur rejection, 88.3%, than that of a conventional Wemco cell, 63.8%. CFC also has potential application in separating heavy fine particles, such as metal oxides, from wastewater.

In our laboratory, a **M**ulti-**ST**age **L**oop-**FLO**w ***(MSTLFLO)*** flotation column [16] has been developed by incorporating draft tubes in a conventional flotation column to achieve "true" multistage operation. In addition, the MSTLFLO process has several important advantages, as compared with conventional flotation processes, which include: reduction in back mixing, increase in interfacial area and improvement of mixing and contact between bubbles and particles. A brief description of the MSTLFLO process is given in the following section.

1.2 MSTLFLO PROCESS

A typical three-stage MSTLFLO flotation column, as applied to oily wastewater treatment, is shown in the Figure 3. Air is introduced into the bottom stage of column, after passing through a regulator, a flow meter and a porous sparger with a mean pore size of 10 μm. A stable simulated oil-water emulsion, which is prepared by passing through a static mixer, is pumped to the top of column via a liquid distributor. Treated clean water leaves the column from the bottom discharge pipe, while oil-laden foam overflows from the top of the column into a foam discharge tank. Three draft tubes are installed concentrically in the column as stages. Each stage can be viewed as a subset of a bubble column similar to that in an air-lift reactor.

In addition to wastewater treatment, this simple, low cost and high throughout flotation column is also found to be a very effective separation device for other applications. It has been applied for the removal of metal oxide precipitates from nuclear power plant DECON water[17] and for fine coal beneficiation[18]. Other potential applications include de-inking of recycled paper pulp and removal of emulsified oil/grease droplets from produced water.

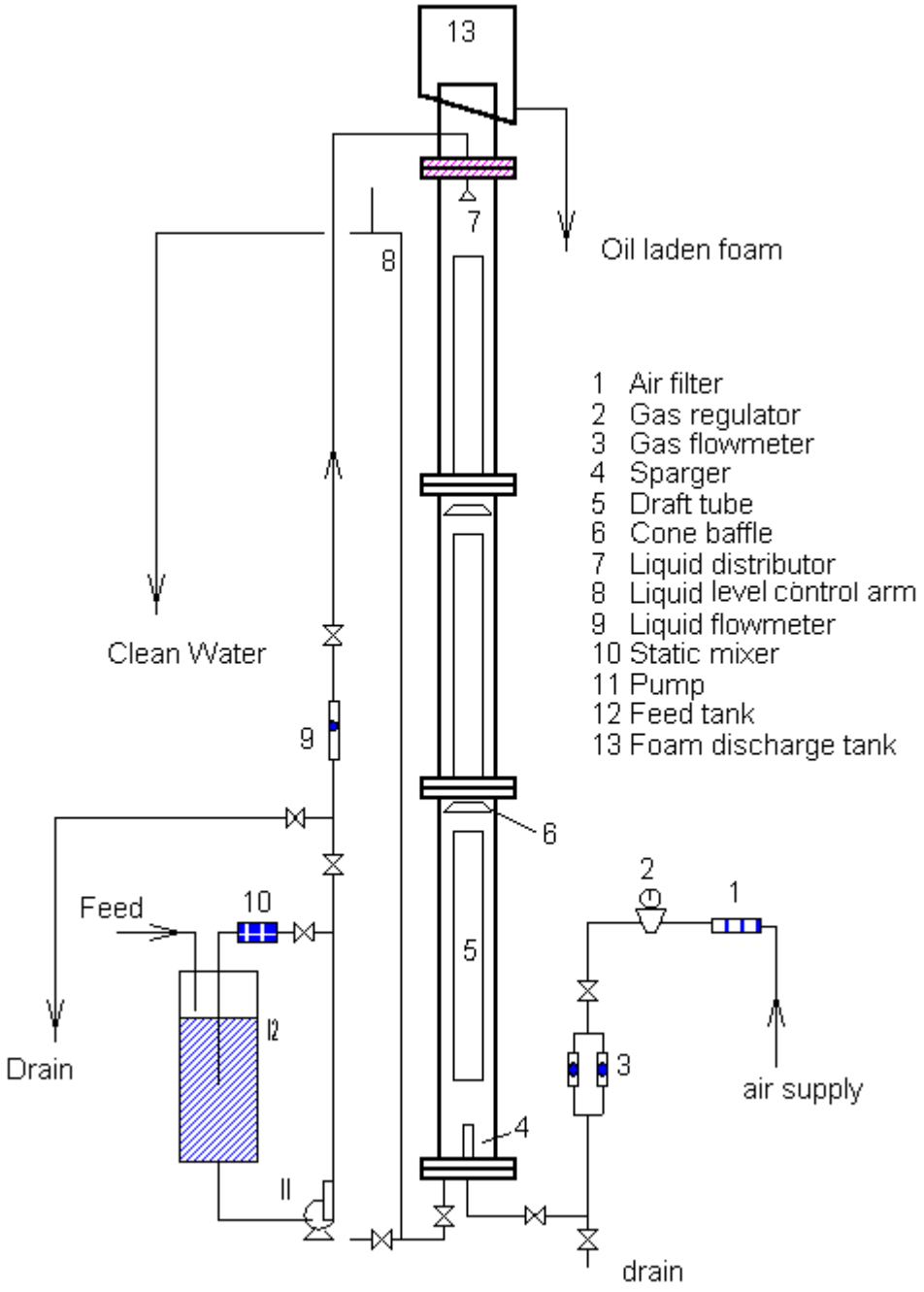

Figure 3 A Multi-stage Loop-Flow Flotation Column for Oily Wastewater Treatment

1.3 NEEDS IN WASTEWATER TREATMENT

There are trillions of gallons of wastewater produced annually by industrial operations in the United States. Oil-water emulsions can be found in wastewater effluent streams from many sources, including metal fabrication plants, petroleum refineries, chemical processing/ manufacturing facilities and paper mills. In 1983, there was more than 400 billion gallons wastewater discharged by oil and gas extraction industry, including nearly 150 billion gallons untreated wastewater. Petroleum and coal products manufacturing industry produced 700 billion gallons wastewater, in which there were 323 billion gallons of untreated wastewater[19]. In the past twenty years (see Table 1), water consumption by heavy industries, including manufacturing, minerals industry and steam/electricity generation, has been increased from 79,794 billion gal (~302.0 billion m^3) in 1985 up to 83,697 billion gal (~316.8 billion m^3) in 2000 [20].

Due to stringent US Environmental Protection Agency (EPA) regulations for wastewater discharge, and a large amount of untreated industrial wastewater, task for the clean-up of industrial and commercial wastewater presents a very serious challenge. For example, the maximum permissible limit of total oil/grease in water prior to discharge to the environment is 40 ppm (parts per million)[19]. In order to meet this and other mandated regulatory limits, there is a pressing need to develop efficient and economical techniques for treating industrial wastewater to protect the environment.

Table 1 Water Usages in the United States

Functional Group	Water Usage (billion gallons/Yr)	
	1985	2000
Heavy Industry		
Manufacturing	8,646	7,179
Steam/electricity generation	34,623	29,015
Minerals Industry	3,224	4,135
Saline water *	33,301	43,368
Subtotal:	**79,794**	**83,697**
Domestic	9,601	11,066
Agriculture	61,497	57,085
Commercial	2,208	2,457
Total:	**153,100**	**154,305**

*Saline water is used mainly in manufacturing and steam electric generation.

2.0 BACKGROUND

Depending on the types of contaminants in discharged fluids, different separation methods are applied in wastewater treatment. Currently, in industrial applications, most of typical separation processes are designed for dealing with only one specific type of contaminants in wastewater. Generally, sedimentation separation is effective only when solid particle size is larger than 50 μm. Membrane separation is found successful in removing micron-size particles. Bio-remediation is used for the removal of dissolved organic pollutants from water when certain operating conditions are applied. Adsorption is also employed to deal with removing organic contaminates from wastewater. However, to treat wastewater containing mixed types of contaminants, a multiple step process, including pre-treatment, is often required. For example, the waste stream is first treated using sedimentation, filtration and disinfection prior to be fed to an adsorption bed [21].

2.1 CONTAMINANTS IN WASTEWATER

Wastewater contains a myriad of organic and inorganic pollutants. In general, major pollutants in wastewater include oily waste, suspended solid particles, and dissolved chemicals. Most of the oily wastes, including greases as well as oils, such as light/heavy hydrocarbons,

lubricants and fats and fatty oils, are naturally hydrophobic. It was reported[22] that oily wastes have been produced from many industries, including petroleum refineries, metals manufactures, food and machine processors. These industrial oily wastes are either emulsified or non-emulsified (floating) oils. Floating oil can be removed economically and efficiently by using gravity separation, however, the treatment of emulsified oil is found to be more complex and costly. Depending on chemical composition and surface charge, fine solid particles can be either hydrophobic or hydrophilic. Generally, many ores are hydrophilic in varying degrees. However, there are still several types of minerals hydrophobic, including sulfide minerals, graphite and certain gold ores[1]. Dissolved chemicals include organic and inorganic chemicals. Phenolic wastes are among the most common organic pollutants in wastewater. Phenolic wastes include a variety of similar chemicals, such as phenols, chlorophenols and phenoxyacids. Biological process and chemical oxidation process are successfully applied as pre-treatment and polishing processes for phenol removal. Activated carbon adsorption is currently the best separation method to remove dilute phenol from water. As indicated before, a MSTLFLO flotation column has been successfully applied to solid separations (as in metal oxide removal and fine coal beneficiation) and oily water treatment. Thus the possibility of applying MSTLFLO flotation column to deal with mixed contaminants in water in a one-step operation has been suggested.

2.2 PRINCIPLE OF FLOTATION

Flotation is a process to separate particles (including oil droplets) from aqueous phase with the help of air bubbles. First applied in mineral processing, fine particle flotation separations began in the early twentieth century. As a separation process involving collisions

between bubbles and particles (or droplets), the principle of flotation is stated in the conception of flotability, which is discussed in the following section.

2.2.1 Flotability

For a given particle or droplet, flotability means its ability to attach onto an air bubble and to be floated to the surface of liquid. It can be measured indirectly in terms of the surface properties of particle, including hydrophobicity and zeta potential.

2.2.2 Hydrophobicity

Particles are said to be hydrophobic when they are easily attachable to gas bubbles. Otherwise, they are hydrophilic. So the floatability of a particle is determined by the hydrophobicity of particles. Hydrophobic particles can be easily captured and carried upward by gas bubbles to the surface of slurry, while hydrophilic particles can not.

Contact angle is the most commonly used parameter to indicate the hydrophobicity of particles. The measurement of contact angle in pure water is used to serve as a measurement of hydrophobicity of solid particles. Hydrophobic particles are associated with large contact angles, while hydrophilic particles are coupled with small contact angles. Usually, only particle with contact angle larger than 30 degree can be separated efficiently by flotation method [23].

2.2.3 Induction Time

While contact angle reveals equilibrium property of particle and bubble adhesion, induction time indicates the kinetic basis for breaking thin-film (of water) in between bubbles

and particles. Induction time[24] is the minimum period of time required to overcome resistances before particles and bubble can attach to each other, which is mainly determined by the hydrodynamic conditions at the bubble-particle interface.

2.2.4 Zeta Potential

In addition to hydrophobicity and induction time, zeta potential can also be viewed as another criterion for flotability. Zeta potential is a measure of surface charge of solid particles, which is directly related to the ability of particles to form aggregates with themselves or with gas bubbles, therefore, the stability of solid suspension.

Due to small size of suspended particles, surface force (electrostatic force in this case) often plays a more important role in controlling particle behavior than gravity. General relationship between the values of zeta potential and the stability of particles, particularly for hydrophobic colloids, is given in Table 2 [25]. It is seen that large zeta potential promotes stable particle suspensions.

2.2.5 Surface Modification

The majority of minerals is found to be hydrophilic in their natural state and need to be modified in order to make them floatable. Previous studies [26] showed that naturally hydrophilic particles could be made hydrophobic by adsorbing non-polar groups on the site of polar groups at the surface of particles. In order to modify the interfacial properties of particles, appropriate chemicals must be added into the particle suspension. Based on different functions, these chemicals are classified into two groups [27]:

- ***Collector:*** It is a chemical adsorbed on particle's surface to make it hydrophobic and easy to attach to air bubbles
- ***Regulator:*** In practice, regulator are often divided into three subdivisions:
  Depressant: a reagent to lower particle's flotation activity
  Activator: a reagent to aid the adsorption of collectors
  Modifier: a substance, which regulates hydrogen ion concentration in the pulp, and modifies the zeta potential of suspended particles.

Table 2 Stability of Suspension and Zeta Potential

Stability Characteristics	Average ZP in mV
Maximum agglomeration and precipitation	+3 to 0
Excellent agglomeration and precipitation	-1 to –4
Fair agglomeration and precipitation	-5 to –10
Threshold of agglomeration	-11 to –20
Plateau of slight stability (few agglomerates)	-21 to –30
Moderate stability (no agglomerates)	-31 to –40
Good stability	-41 to –50
Very good stability	-51 to –60
Excellent stability	-61 to –80
Maximum stability	-81 to -125

2.2.6 Mechanism of Capture of Particles

Besides the floatability of the particles, there are other factors affecting flotation efficiency. For a given type of particles and a set of operation conditions, the chance of flotation can be expressed in terms of three probabilities, as shown in following equation [1]:

$$\text{Chance of flotation} = \text{probability of particle-bubble collision} \times \text{probability of attachment} \times \text{probability of retention of attachment}$$

The probability of collision between particles and bubbles is controlled by hydrodynamic conditions of flotation process. There are three ways contact between bubbles and particles:

- **Collision** – collision is induced by turbulent mixing or caused by direct contact between a rising bubble and a sedimenting particle.
- **Entrapment** – bubbles are entrapped in a growing floc structure.
- **Precipitation** - a particle precipitates onto a bubble or into a floc.

The probability of attachment is affected by interfacial properties, including zeta potential of particles, interfacial tensions, etc. The retention of attachment is affected by turbulent condition and adhesive force of attached particles on bubbles. In general, the probability of attachment and the retention of attachment are considered as one factor, the efficiency of attachment. Figure 4 shows the aggregation of fine solid particles and air bubbles in a flotation process[28].

2.2.7 Flotation Process

Flotation in a single dispersed air flotation cell is usually treated as a first-order kinetic process in a perfectly mixed stirred tank [29]. In practice, two or more flotation cells are connected in series to increase recovery and avoid backmixing. Hence, if n individual identical flotation cells were arranged in series, then as long as the kinetic constant, K, remains the same in all cells, the overall solids recovery R_c^n is given by:

$$R_c^n = 1 - \frac{1}{\left(1 + \frac{K\bar{t}_c}{n}\right)^n} \qquad (1)$$

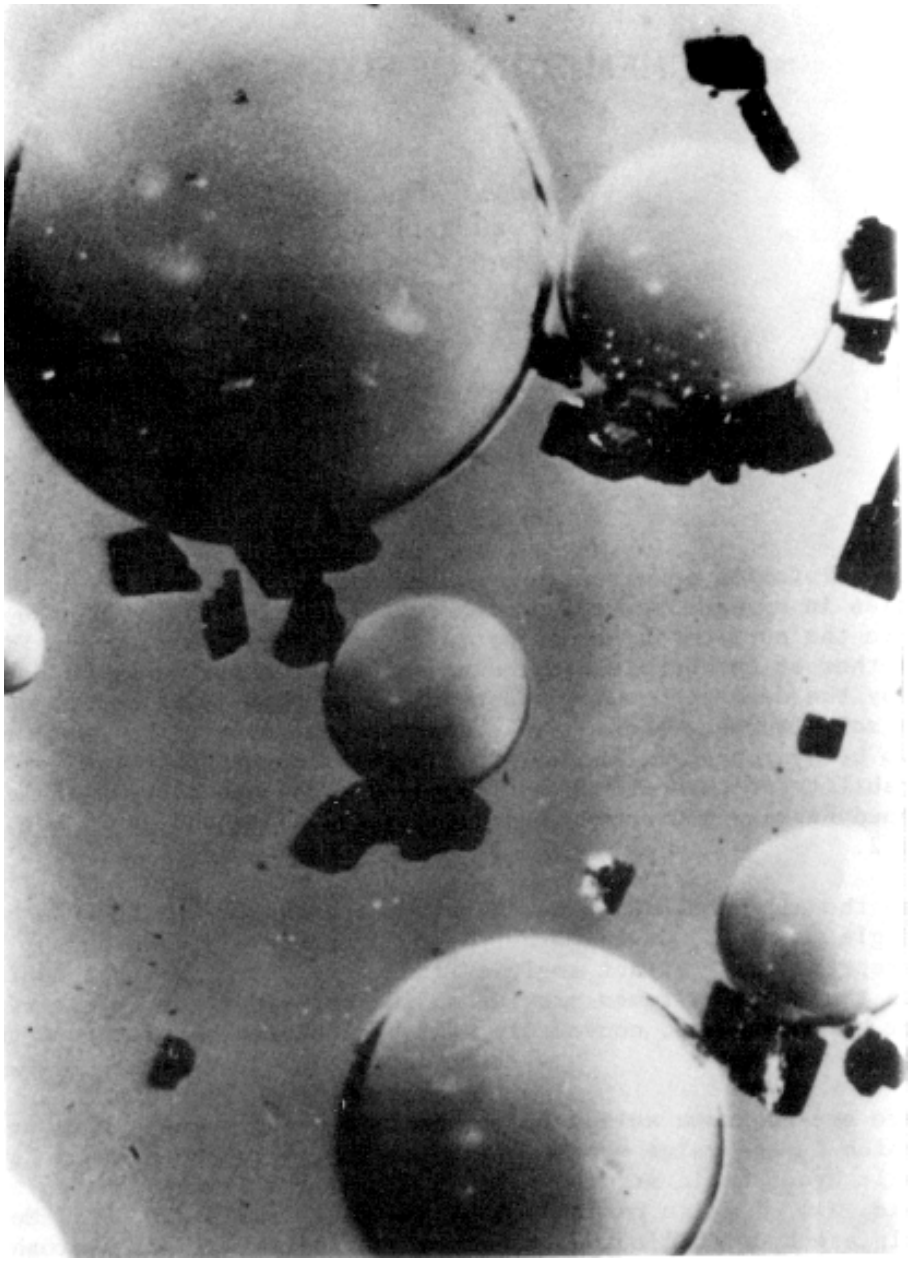

Figure 4 Attachment of Fine Particles on Bubbles (by Fuerstenau [28])

$$\frac{\bar{t}_c}{t} = \frac{n}{Kt}\left[\exp(\frac{Kt}{n}) - 1\right] \quad (2)$$

where t is residence time, and $\bar{t}_c$ is mean residence time in each individual flotation cell.

a. Solid Particle Flotation

An approach has been successfully used to describe a flotation system in analogous to a stir tank chemical reactor. Assuming bubble concentration is constant, experimental results [29] show that a simple overall flotation removal rate of solids follows a first-order kinetics in the form of:

$$X\,(\text{particles}) \rightarrow z\,(\text{floated aggregates}) \quad (3)$$

It was found that the recovery of particles over 200 μm and below 10 μm was poor. Particles of an intermediate size range show the best results, although there are different optimum sizes for different kind of particles. The main reason for inefficient recovery for small particle sizes is unfavorable direct collision between a large bubble and a small particle.

The overall collection efficiency of a bubble (E_K) can be defined as a product of collision and attachment efficiencies, E_c and E_a respectively:

$$E_K = E_c \bullet E_a \quad (4)$$

Reay and Ratcliff [30] suggest that there is a simple relationship for the case that particle size, d_p, is less than 100 μm:

$$E_c \propto \left(\frac{d_p}{d_b}\right)^2 \quad (5)$$

where d_b is bubble size, and $d_b >> d_p$.

This relationship indicates that for a given air flowrate, small bubbles will achieve a better particle separation. This is because small bubbles have long residence time and large

number density in the suspension, which result in an increase in the probability of collision. This relationship also indicates that flotation will be enhanced if a larger particle sizes is used for a given bubble size.

Compared with collision efficiency, attachment efficiency has received less attention in the solid flotation study. For a simple calculation, an ideal assumption is given that there is a fixed attachment rate between bubbles and solid particles. Therefore, E_a becomes a constant and is included in overall collection efficiecny, E_K.

b. An Alternative Kinetic Model

Although the first order kinetics has been used for most flotation analysis, Lai [31] suggested that flotation process obey the principle of continuity, but not a discrete order of kinetics. He proposed an alternative kinetic model in which the rate of flotation (-dC/dt) is proportional to particle (or oil droplet) concentration, C, and inversely proportional to time, t.

$$-\frac{dC}{dt} = K\frac{C - C_\infty}{t} \qquad (6)$$

where the C_∞ is the asymptote of particle (or oil droplet) concentration, which is an empirical constant derived from experiments.

This kinetic model was successfully applied to fine coal cleaning [18] and oily water treatment in the MSTLFLO column [6, 32, 33].

2.2.8 Adsorption of Chemicals on PAC

Industrial and commercial wastewater contains dissolved chemicals which are often difficult to be degraded by biological methods, or by conventional treatments, such as

coagulation, sedimentation, filtration and ozonation. Because of activated carbon's large surface area and strong affinity to organic contaminants, such as phenols, it has been recognized as one of the most effective adsorbents for removing organic substances from wastewater.

To study the amount of activated carbon required for a given volume of wastewater, the adsorption of chemical contaminant in water must first be measured. Freundlich isotherm [34] is suggested for equilibrium study, as shown in the following:

$$q = K_{ads} C_{eq}^{1/n} \qquad (7)$$

where, q is chemical (such as phenol) concentration in adsorbent, and C_{eq} is equilibrium concentration of chemical in aqueous phase, K_{ads} and n are the Freundlich parameters. The value of n is generally greater than 1.

Freundlich isotherm is based on two important assumptions. First, adsorption occurs on adsorbent surface is not monomolecular layer. Second, energy distribution for adsorption site is not uniform. As a specific example, Freundlich parameters for phenol adsorbed on Filtrasorb 300 activated carbon (provided by Calgon Carbon Corp.) at different pH are shown in Table 3 [35]. The data indicate that there is no strong pH dependence on phenol adsorption on activated carbon.

Table 3 Freundlich Parameters for Phenol on Filtrasorb 300

pH	K_{ads}	*1/n*
3.0, 7.0, 9.0	21	0.54

2.3 DEVELOPMENTS OF MSTLFLO FLOTATION COLUMN

As mentioned earlier, a new flotation column design in term of a multistage bubble column (MSTLFLO flotation column) was recently developed in our laboratory. Gu[6] reported that such a column design has the advantages of less surfactant requirement, longer residence time, higher separation efficiency and preventing back mixing.

MSTLFLO column can be viewed as an integration of multistage flotation process and bubble column with draft tubes. It introduces proper hydrodynamic behaviors in the column. A loop flow, caused by pressure difference between inside and outside regions of draft tubes, can keep most of small air bubbles within the contact region in each stage. Therefore, MSTLFLO column provides more contact areas for particle capture than conventional column. Furthermore, long residence time for small bubbles provides better contact between bubbles and suspended particles (including oil droplets) as well as between adsorbent particles (if present) and dissolved chemicals within the contact region. It comprises all the advantages from both multistage operation and bubble column. Consequently, it exhibits high gas holdup, narrow bubble size distribution, and thorough mixing between bubbles and particles. These unique features promote enhanced separation efficiency of the flotation process. A summary discussion of these special attributes of the MSTLFLO column is given below (See Appendix A for detailed experimental results of gas holdup, bubble size and column performance in a 4-in MSTLFLO flotation column).

2.3.1 Gas Holdup

Gas holdup is the ratio of gas volume to liquid phase in a bubble device. The increase of gas holdup will increase the opportunities of contact and attachment between particles and gas bubbles. Gas holdups increase with the dosage of frother and superficial gas velocity. MSTLFLO column has a significantly higher gas holdup (up to 45%) than that of conventional column (no more than 30%)[36]. It is desirable in flotation column to have high gas holdup, because it provides large interfacial area, which favors bubble-particle to form aggregates.

2.3.2 Bubble Size

Gas bubbles generated in MSTLFLO column are relatively small and spherical with a typical bubble Sauter mean diameter as small as 1 mm[37], when frother concentration is 15 ppm, and superficial gas velocity is greater than 2.0 cm/s. This compares with an average bubble size of 2~4 mm in conventional flotation devices under similar operation conditions. Small bubbles not only give high gas holdup, but also provide more opportunities for collisions between particles and bubbles.

2.3.3 Column Performance

MSTLFLO process has demonstrated its superior oil removal efficiency at short contact time for treating oily wastewater[6]. Residue oil concentration as low as 10 ppm in treated water can be achieved with 500 ppm initial emulsified oil. This is much lower than results obtained by other flotation methods. In addition, MSTLFLO column has also been successfully applied to fine coal beneficiation[18] and metal oxide precipitates removal[17].

2.4 A CHALLENGE IN WASTEWATER TREATMENT

In industrial wastewater, not only suspended solid particles and dispersed oil, but also dissolved chemicals are usually present. Thus, the challenge before us is to develop new technologies to deal with wastewater containing mixed contaminants.

In light of its effectiveness in dealing with wastewater containing emulsified oil and fine solid particles, MSTLFLO flotation column is considered to be capable of meeting this challenge. Specifically, the concept of one-step separation or simultaneous removal of emulsified oil, dissolved chemical (phenol) and suspended fine particles (PAC used as an adsorbent for phenol) from wastewater in the MSTLFLO flotation column will be investigated in this study.

3.0 OBJECTIVES

The overall objective of this study is to explore the potential applications of MSTLFLO process for simultaneous removal of suspended solids, dissolved chemicals and emulsified oil mixtures from industrial wastewater. The study is divided into three major parts.

First, conduct experiments to measure the removal efficiency of individual or mixed emulsified oil, phenol and solid particles, including Powdered Activated Carbon (PAC) and glass beads, from simulated wastewater using both 4-in and 12-in MSTLFLO flotation columns. The experimental data thus obtained will be used in subsequent kinetic correlation and process modeling.

Second, analyze the rates of separation (kinetics) for individual components to yield kinetic constants in terms of experimentally determined hydrodynamic parameters. A generalized correlation for kinetic constants of oil and solid removal will be established for process modeling.

Finally, develop a process model and simulation program for the oil removal and solid separation associated with chemical removal in the MSTLFLO column.

Based on the outcomes of this study, a scale-up criterion for column design together with proper operating conditions of the MSTLFLO process will be identified and recommended. The results are intended to provide an engineering design basis in exploring future applications of the MSTLFLO process for industrial wastewater treatment.

4.0 EXPERIMENTAL

A 4-in* pilot-scale MSTLFLO flotation column has been successfully used for oil removal in the earlier work [6, 32 33]. In order to establish scale-up criteria for MSTLFLO process for industrial applications, further experimental study has been conducted in a 12-in MSTLFLO column.

4.1 EXPERIMENTAL EQUIPMENT

In addition to the existing 4-in column [38], a 12-in outside diameter, 21-ft high (including structure supports) MSTLFLO flotation column has been constructed to verify a process model and determine scale-up parameters. The design of this large column is the same as the 4-in column. It contains three draft tubes and cone baffles. The accessories of column consist of an air supply line, air sparger, mixing/feed tanks with recycling loop equipped with a static mixer, concentrated frother feeding line, and all necessary measuring instruments. Detailed descriptions of experimental equipments are given below.

* All dimensions of equipments are given in English Units, 1 in = 2.54 cm, 1 ft =30.4 cm and 1 gal =3.8 Liters.

4.1.1 New MSTLFLO Column

A new MSTLFLO flotation column is made of 12-in outside diameter acrylic tubing with 3/16-in wall thickness. Column is divided into three sections. Both top and bottom sections are 5-ft in length, and middle section is 4-ft long. The height of column body is 16-ft, and the effective column volume is about 11.0 ft^3 (see Figure 5). A 3-ft long draft tube, which is made of a piece of 8¼-in outside diameter and 1/8-in wall thickness acrylics tubing, is installed concentrically in each section. These draft tubes are serving as stages. Between two adjacent draft-tubes, there is a cone baffle. Distance between the bottom edge of draft tube and the topside of cone baffle is either 2-in or 4-in, depending on the shape of cone baffles. Clearance between the inside wall of column and the lower edge of cone baffle is 0.1 in, which facilitates a net downward flow of liquid while prevents gas by-pass to the outside of draft tube in the upper stage. A pair of flanges, which are machined from 2-in thick acrylic flat sheets, connect two adjacent sections. Two different cone baffle designs are used and will be discussed later in this chapter.

4.1.2 Draft Tube

Previous work [38] suggests that a desired hydrodynamic condition can be achieved when the ratio of the cross-section area of riser to downcomer is close to unity. Therefore, an 8-in O.D. tubing is used as a draft tube in the 12-in O.D. column to yield an area ratio of riser to downcomer at 0.95.

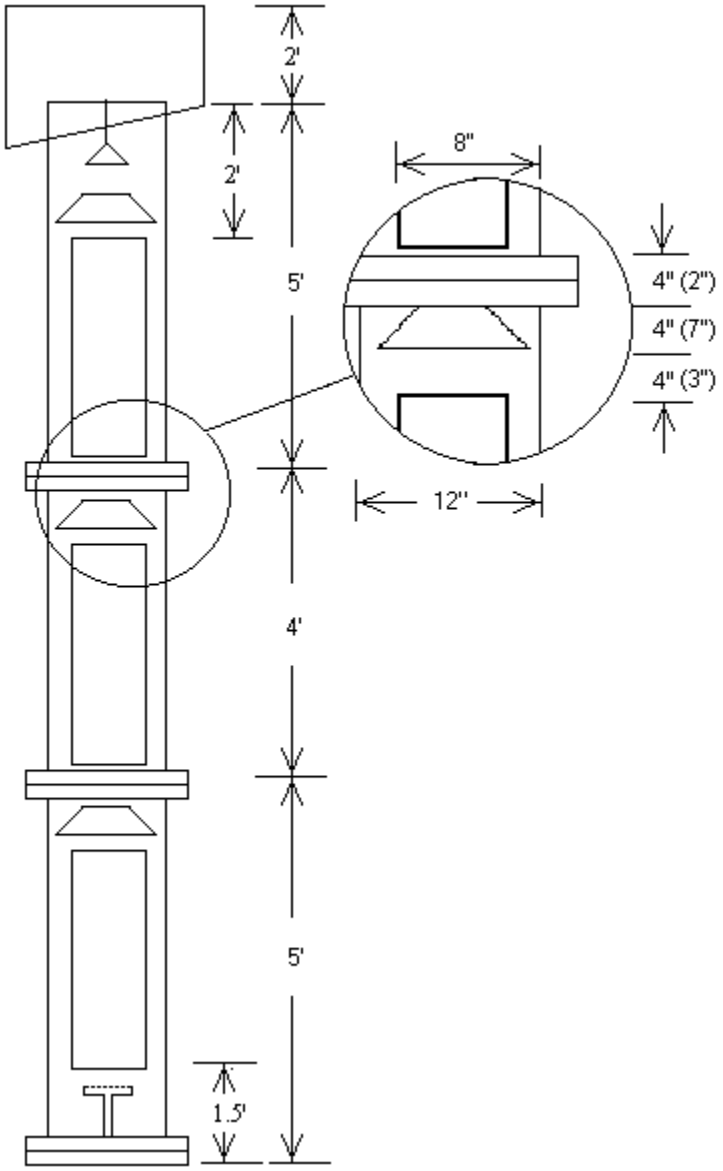

Figure 5 The Geometry of a 12-in MSTLFLO Column

Each draft tube divides column into two distinct regions: central region (riser) and annular region (downcomer), respectively. There is a difference in gas holdups between inside and outside of tube. In turn, it induces a pressure drop and therefore a liquid circulation (or loop-flow) from the outside (annular region) to the inside (central region) of each draft tube.

4.1.3 Sparger

A porous device, a pipe or a disk, used in flotation process to generate small gas bubbles is called sparger. Two different types of gas spargers are used in 12-in column: a sintered metal disk and plastic porous multi-stick module. The average pore size of both types of spargers is 10 microns. The metal disk sparger, supplied by Mott Industry Corporation, is ½-in in thickness and 6.5-in in diameter, which provides 28.3 in^2 surface area. The plastic stick sparger, provided by Porous Products Group, Porex Company, consists of four sticks. Each stick is 6-in long, 1.5-in O.D., ¼-in in wall thickness, and a surface area of 28.3 in^2. Therefore, total surface area of stick sparger is 113.2 in^2. Two specially designed sparger holders are fabricated for supporting these spargers, as shown in Figure 6. These sparger holders are installed in the center of bottom flange, through which gas is fed.

4.1.4 Cone Baffle

Cone baffle plays an important role on flow pattern and mixing conditions in MSTLFLO process. The function of cone baffle is to prevent inter-stage mixing. It allows a net liquid flow downward through the small clearance (~0.1-in gap) between the lower edge of cone and the inner wall of column, while gas by-pass can be prevented. In the meantime, each cone baffle

directs rising bubbly stream from lower stage into the riser region of upper stage and minimize backmixing between two adjacent stages.

In this study, two types of cone baffles are used, a “short” one and a “long” one. A view of cone baffles is depicted in Figure 7. The diameters of base of “short” and “long” cone baffles are both 11 in. The top diameters of two cone baffles are 7-in and 6-in, respectively. And the heights of two cone baffles are 4 in and 7 in, respectively. Their relative positions are shown in Figure 5.

4.1.5 Flange

Because of a lack of commercial flanges matching the 12-in column, all flanges are fabricated by school’s machine shop using 2-in thick flat plastic sheets. All flanges are 14” × 14” square. The dimensions of connecting flanges and bottom flange are shown in Figure 8.

4.1.6 Measuring Accessories

In every stage, two ¼-in NPT holes are tapped through column wall, through which a pair of conductivity probes for liquid velocity measurement is installed. And four 1/8-in NPT holes are tapped to insert pressure taps for measuring gas holdups. All these holes are 30-in apart. In addition, a 1/2-in hole is tapped in the bottom flange as a sampling outlet, as shown in Figure 8.

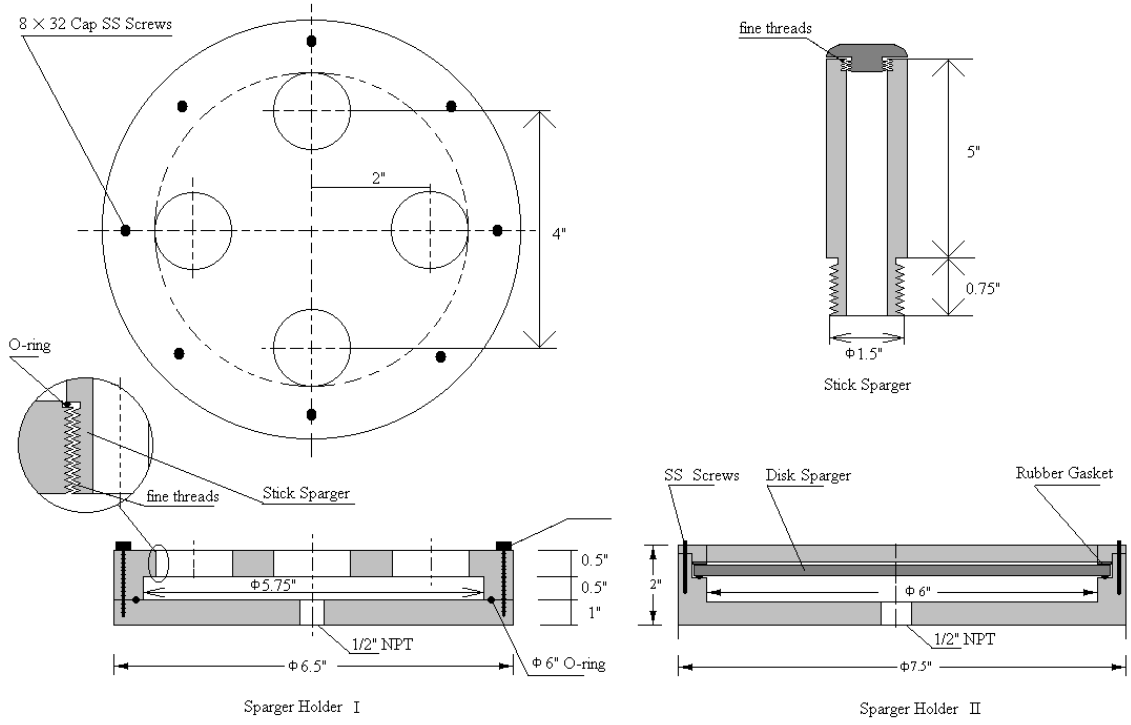

Figure 6 Sparger Holders

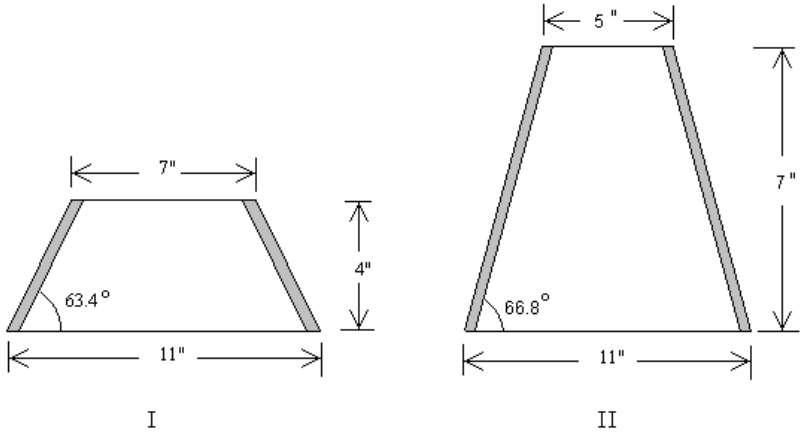

Figure 7 Cone Baffle

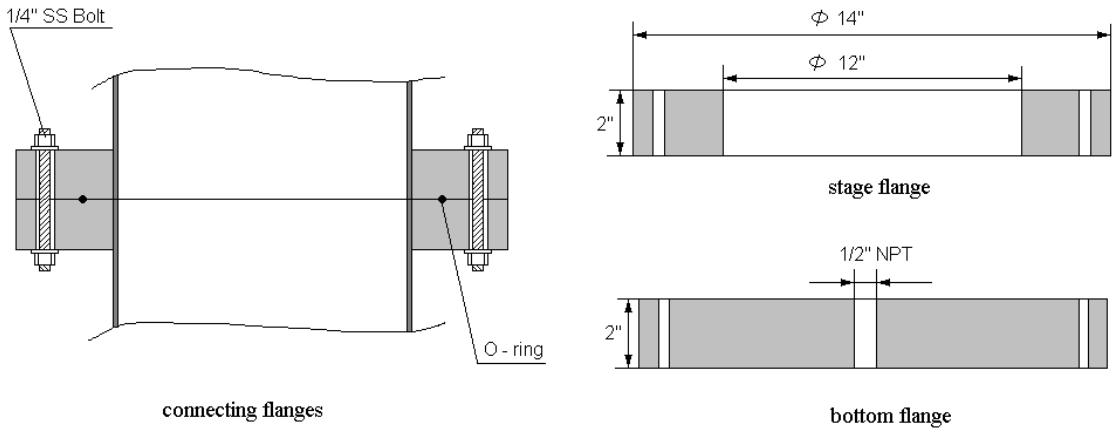

Figure 8 Stage and Bottom Flanges

4.1.7 Other Accessories

There is a 530-gal feeding tank for the 12-in MSTLFLO column. Two 2-ft long static mixers are used for preparing oil-water feed mixture. A 20-gal tank with a mechanic stirrer is applied as fine particle slurry feed tank. A 3-gal bottle is used as feeding tank of concentrated frother solution, when a separated frother feed line is required.

4.2 MATERIALS

To explore the feasibility of removing multi-pollutant from water, simulants have been chosen to represent common contaminants: oil, fine solid particles and dissolved chemicals in wastewater. The simulants used in this study are described separately below.

4.2.1 Oil Simulant

Discarded oil wastes generally consist of mixtures of hydrocarbons discharged from diverse industrial plants. Bentham [39] indicated oil from grease trap waste was a complex mix of fuel oil and lube oil fraction. Sato [40] used heavy oil-A to study the removal of dilute emulsified oil water. Takahashi [41] used kerosene, liquid paraffins as an oil simulant in wastewater treatment. In this study, following the previous study in our laboratory[38], a light mineral oil (liquid paraffin), provided by Fisher Scientific, is chosen as the oil simulant.

4.2.2 Dissolved Chemical

Dissolved chemicals pose a major challenge in industrial wastewater clean-up. Phenol and its derivatives, long been recognized as toxic pollutants, are common dissolved chemicals found in wastewater discharged from many industrial plants, including petroleum refineries, coke plant, resin plants and others[42]. They are relatively soluble in water. The specification of phenol by U.S. Pharmacopeia indicates the clear solubility of 1 part of phenol in 15 parts of water [43]. Concentrations reported in the oil & petrochemical industrial wastewater and other industrial wastewater range from 50 to 600 mg/L and 3 to 12000 mg/L, respectively [43].

Adsorption method and chemical method are commonly used to remove phenol from water. However, in case of removing small amount of phenol from dilute systems, chemical method is not as cost effective as adsorption method.

As a typical dissolved chemical in water, phenol is chosen as a simulant of dissolved chemical in this multi-pollutant removal study with MSTLFLO column. Adsorption method is suggested for phenol removal. Thus, an adsorptive MSTLFLO flotation process is introduced and PAC is selected as the adsorbent for removing dissolved phenol from water. The concentration of phenol to be studied is 40 mg/L.

4.2.3 Adsorbent and Inert Solid Particles

One of the unique features of this study is the addition of adsorbent particles (fine solid particles) into the MSTLFLO flotation process. Solid adsorbent particles (PAC particles) can play a dual role as an adsorbent for removing dissolved chemical (phenol) and as a simulant of suspended fine solid. Hence, the addition of PAC (as a solid adsorbent) offers an opportunity to

test MSTLFLO flotation process's ability to simultaneously remove dissolved phenol, suspended solid as well as emulsified oil from water.

Inert solid particles, such as sand, soil, dirt and metal oxide, are commonly found in wastewater. Conventional mechanical separation methods (filtration, centrifugation and sedimentation) are usually used for separating solid particles, especially for those particles larger than 1 mm. However, ultra fine particles (less than 50 microns) cannot be easily removed by traditional methods at high throughput. To further explore the ability of removing small particles from water using MSTLFLO process, fine glass beads are also tested.

4.2.4 Frother

PAC, used as adsorbent in MSTLFLO process, is able to adsorb not only dissolved phenol but also other chemicals in water, including surfactants used in flotation process. Therefore, it is important to select a proper frother for this adsorptive MSTLFLO process. Two major frothers were tested in the presence of PAC. They are 2-EH (2-ethyle hexane, provided by Fisher Sci.) and MIBC (4-methyl-2-pentanonal, provided by Aldrich). Both frothers show their effectiveness even in the presence of PAC. In order to compare with the previous data [36, 38], frother 2-EH is chosen as the frother for this study, unless otherwise specified.

4.3 EXPERIMENTAL PROCEDURES AND METHODS

In this section, the experimental procedures, including the preparation of solutions, the measurement of hydrodynamic parameters and analytical methods, are discussed.

4.3.1 Preparation of Solutions

a. Oily Water Solution

To obtain a large volume of stable oily water solution (emulsified oil in water), a properly designed mixing procedure must be employed. A three-step pre-mixing procedure is followed to prepare 1400 liters stable 500 ppm (by wt.) emulsified oil solution. Total volume of 840-ml light mineral oil is needed. First, 300-ml oil is added into 600 liters fresh water and then pumped through two parallel static mixers and recycled back to feed tank until a stable solution is made. This step takes about 60 minutes. Then, another 340-ml mineral oil is added and more water is added up to a total of 1200 liters. This oily water is also pumped through static mixers and recycled back to feed tank for another 60 minutes to obtain a stable oily water solution. Finally, the remaining 200-ml oil is added and oil/water mixture is diluted to 1400 liters. The last mixing step takes at least 90 minutes to achieve a stable 1400 liters 500 ppm (by wt.) emulsified oil solution. This prepared oily water solution shows no visible oil film agglomerates and it remains stable more than 12 hours.

b. Phenol-Water Solution

Phenol is a white crystal powder and can be easily dissolved in water. Its solubility in water at room temperature is greater than 100 mg/ml. Its specific gravity is 1.058. In this study, a standard 1% (by wt.%) phenol aqueous solution is prepared. Then, depending on the required quantity of phenol-water solution, the 1% phenol solution is diluted to 40 ppm (by wt.), as the simulated wastewater.

c. PAC-Water Suspension

PAC is fed separately into MSTLFLO column from oil-water solution or phenol-oil-water solution. A 1% (by wt.) PAC slurry is prepared in a stirred tank. To achieve a 300- 500

ppm PAC environment in MSTLFLO column, a fixed ratio of PAC slurry flowrate to phenol solution flowrate is chosen. For example, to obtain a bulk 500 ppm PAC, the feeding rates of PAC slurry and phenol solution are set at 50 ml/min and 950 ml/min, respectively. Before each experiment, the flowrate of PAC slurry is calibrated.

4.3.2 Analytical Methods

A summary of analytical methods used for the present study is discussed in this section.

a. Interfacial property Measurements

Interfacial properties of particles/water under current study are determined by measuring following two key variables: zeta potential (ZP) and surface tension.

(1) Zeta Potential

Zeta Potential meter detects the effect of surface charge on the movement of suspended particles in an electrical field. Zeta Potential measurements are made using a procedure called "microelectrophoresis" with ZETA-METER ZM-80 in our study [25]. The mobility of charged particles is measured by timing their rate of movement in a DC voltage field. The details of electrophoresis cell are shown in Figure 9.

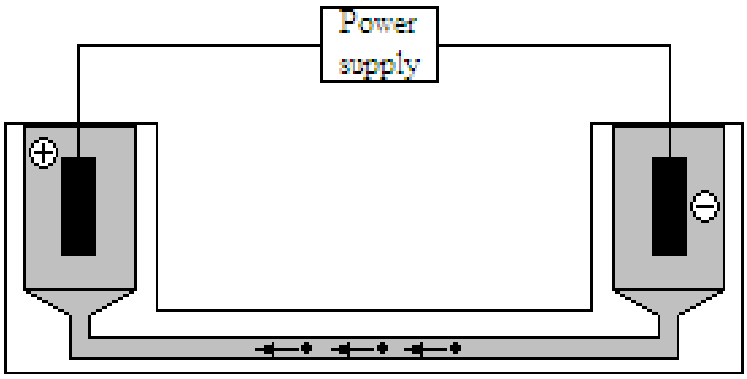

Figure 9 Details of Electrophoresis Cell

(2) Surface Tension

The maximum pull force method [44] is used to measure the surface tensions. In this technique, a thin ring (probe) is lowered into the liquid sample and then drawn out of it, as shown in Figure 10. The maximum pull force is recorded as the surface tension. A standard Surface Tensiometer, by Fisher Scientific, is used to measure surface tension of water in the presence of frother and other chemical additives.

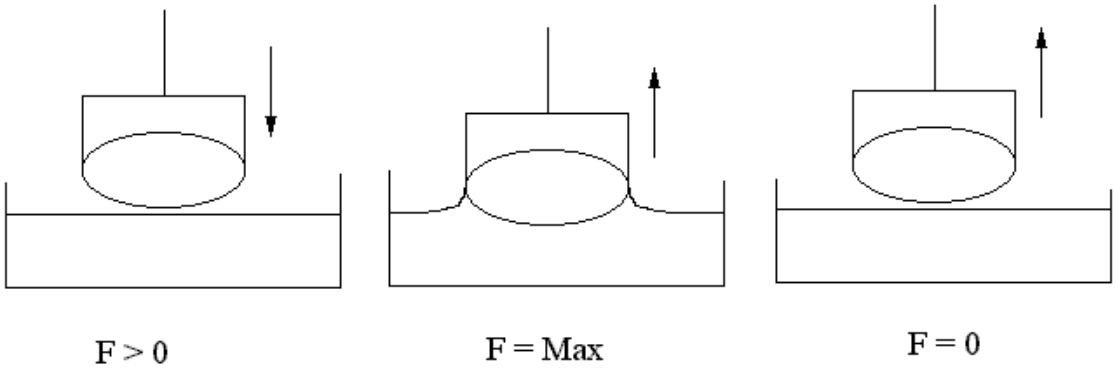

Figure 10 Maximum Pull Force Method to Measure the Surface Tension

b. Hydrodynamic Behaviors

To study hydrodynamic behaviors in MSTLFLO column, two important parameters are measured: gas holdup and liquid circulation velocity.

(1) Gas Holdup

Gas holdup is defined as the volumetric fraction of gas in liquid dispersion. In this study, gas holdup (ε_g) is measured by using hydrostatic pressure method, as shown in Equation (8).

$$\varepsilon_g = \frac{H_m}{H_L} \qquad (8)$$

where, H_L is hydrostatic pressure of water and H_m is pressure difference between two probes. Pressure difference is measured using an inverted U-tube. A detailed discussion of gas holdups measurement is presented in Appendix B.

(2) Liquid Circulation Velocity

Liquid circulation velocity is measured using tracer response technique [45]. Saturated Potassium Chloride (KCl) solution at room temperature is used as a tracer because of its high solubility and conductivity. After the injection of tracer, conductivity changes are detected at a location down stream from the point of tracer injection using conductivity meters. Time difference t_d between peaks on two conductivity meters is taken as average linear time. Average liquid linear velocity (u_L) can be calculated using following equation:

$$u_L = \frac{d_e}{t_d} \tag{9}$$

where d_e is a distance between two electrode probes. Superficial liquid velocity U_L can be obtained using following expression:

$$U_L = u_L(1-\varepsilon) \tag{10}$$

A detailed discussion of the measurement of liquid circulation is described in Appendix C.

c. Physical Properties

The measurements of system's physical properties, including particle/bubble size distributions, oil/solid concentrations and phenol concentration, are summarized below.

(1) Bubble size distribution

As indicated before, bubble sizes directly affect gas holdups, and therefore the efficiency of flotation process. Bubble size is measured using "digital photography method". A Sony DSR PD100A digital camcorder with a Sony × 0.7 wide conversion lens is employed to take digital images of moving bubbles.

In order to "freeze" moving bubbles, shutter speed is set at 1/2000 second. Exposure is set at F4.8. Two 120 V, 300 W Radias tungsten halogen lamps provide a background light

source. Individual digital video image of gas bubbles is analyzed using Adobe Photographic Software [46] and Public Image Analysis Software ImageJ 1.20s [47], developed by National Institutes of Health, USA. Bubbles can be assumed to be spherical, because bubble sizes are very small (less than 2 mm) in the presence of frother. More than 500 individual bubbles are counted for each measurement in order to achieve statistical reliability and to provide a representation of bubble size distribution under investigation.

(2) Particle Size Distribution

Particle size distribution is measured using laser light scattering techniques with MICROTRAC particle size analyzer (Model 7995-11, Leeds & Northrup Co.). A laser beam is projected through a transparent cell in which contained a stream of moving particles suspended in a liquid. When light beam strikes on particles, rays are scattered in different angles, which are inversely proportional to particles size. Standard measurement range is from 0.9 to 176 microns [48]. Optical filter transmits light at a number of pre-determined angles and directs it to a photodetector. Electrical signals are proportional to transmitted light flux values, from which particle size distribution is recorded by the analyzer.

(3) Oil Concentration

A nondispersive infrared (NDIR) technique-based oil content analyzer, Horiba OCMA-220, is applied to measure oil concentration in water. The principle operation [49] is explained as follows.

Hydrocarbon compound contain CH radicals, which exhibit a distinct energy absorption band in the range of 3.4 to 3.5 microns in an infrared spectrum. Consequently, when infrared absorption of an oil sample is measured in this band, the amount of absorbance varies in direct proportion to the concentration of oil in the sample if the absorbance of solvent is negligible.

Halogenated solvents is used as a solvent for OCMA-220 analyzer because: (1) these solvents are insoluble in water, (2) they have a specific gravity heavier than water, (3) they readily dissolve all volatile or nonvolatile organic compounds, and (4) they do not absorb infrared energy in the 2 to 4.5 micron band. This method provides a number of advantages over other methods used for the analysis of oil and grease in water, including the preservation of volatile specificity to hydrocarbons, the lack of interference from suspended solids and colored substances, and good precision.

(4) Solid Concentration

Solid concentration is measured by gravimetric method. A given volume slurry is filtered and filter paper is dried and weighed. Knowing the weight of solid and the volume of slurry, then the concentration of solid by weight can be calculated.

(5) Dissolved Chemical Concentration

For low concentration of phenol, direct photometric method is used to detect the concentration of phenol in water with a DU-600 UV/Vis spectrophotometer, by Beckman Coulter Inc. Standard methods for phenol concentration measurement have been described by Lenore[50]. A wavelength of 500 nm is applied for detection of phenol. The detectable range [51] is from 0.01 up to 50 ppm.

5.0 PROPERTIES OF MATERIALS

Interfacial properties, including contact angles, zeta potential and surface tension, can directly or indirectly influence the hydrophobicity of particles, which in turn affect the removal efficiency of particles. The other properties of particles, including particle size distribution, solid density and PAC adsorption capacity of phenol, are also necessary in the study of fluid/fluid and particle/fluid separations. In this study, key interfacial properties and properties of particles have been measured or obtained from literatures.

5.1 INTERFACIAL PROPERTY

Major interfacial properties in the study of fine particle flotation include contact angle of solid, zeta potential of fine particles and surface tension of liquid. These properties are discussed below.

5.1.1 Contact Angles

In pure water, the value of contact angle can be used to evaluate the hydrophobicity of solid surface. As shown in Figure 11, in a three-phase, gas-liquid-solid surface, contact angle, θ (the angle between liquid/gas and solid/liquid interfaces), which provides a quantitative

measurement of the wettability of solid surface[52]. Solid surface (solid particles) with contact angle greater than 90 degree are said strongly hydrophobic, which are easy to be removed in a flotation process. While hydrophilic particles exhibit small contact angles, which are difficult to be separated using flotation. In a general, only particles with contact angle larger than 30 degree can be separated efficiently by using flotation[27]. The value of contact angle is affected by many factors, i. e. temperature, the type of gas/liquid [53], surface tension [54], the smoothness of solid surface [55], pH value and so on[56]. A summary of contact angles of different solids in aqueous system is shown in Table 4.

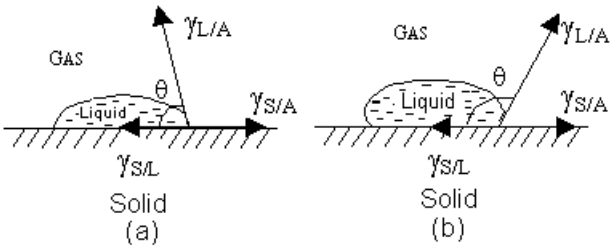

Figure 11 Contact Angle of Solid

Table 4 Contact Angles of Solids in Water

Solid Particles	Contact angle, degree
Paraffin	>109 [55]
HDPE	87[57]
Coal	84[58]
Carbon particle	68[59]
Glass	30 - 115[60, 61]

From above, particles can be grouped into three major categories:

- **Strongly hydrophobic particles**: contact angle is greater than 90 degrees: including paraffin wax (oil), and treated glass.

- **Comparatively hydrophobic particles**: contact angle is in between 40 degrees and 90 degrees: including HDPE, coal, carbon particle and commercial glass.
- **Strongly hydrophilic particles**: contact angle is less than 30 degrees. These particles can not be treated by conventional flotation methods, unless surface modifiers (surfactants) are added.

In our study, emulsified paraffin oil droplet (similar to paraffin particle), which is strongly hydrophobic, can be readily removed by flotation. On the other hand, glass beads (made of commercial grade glass) and PAC particles (similar to coal particles) are of comparatively hydrophobic, and they can also be separated by flotation method. While both of them can be separated by flotation, PAC particles are more naturally hydrophobic than the glass beads because they have relatively larger contact angles (> 80 degree).

5.1.2 Surface Tension

Liquid/air interfacial tension, or surface tension, is one of the most important interfacial properties in flotation study. Frother is used to reduce surface tension in facilitating gas bubble generation. Based on previous work, two different frothers, 2-EH and MIBC, are selected for this study. The surface tension of water is measured at different frother concentrations at 25 ^{0}C, as shown in Table 5.

The results confirm that an increase in frother concentration reduces surface tension. Furthermore, there is no significant difference in surface tension when the experimental data obtained at the same frother concentration for these two frothers are compared. Thus, both 2-EH and MIBC are effective in promoting gas bubble generation for flotation purpose.

Table 5 Surface Tensions at Different Frother Concentrations at 25 ^{0}C

Frother concentration, ppm	Surface tension, dyn/cm	
	2-EH	MIBC
0 (Pure water)	72.8	
5	72.2	72.4
10	71.9	72.0
20	70.6	70.9
40	67.6	68.1
200	55.3	56.2

5.1.3 Zeta Potential

Zeta Potential (ZP) is a measurement of surface charge of fine particles, which in turn controls interactions among particles. Particles with the absolute value of ZP less than 10 mV are easy to aggregate, while particles with ZP larger than 40 mV remain stable in suspension. In this study, ZP of two different particles, i. e. glass beads and PAC, in water have been measured at 20 ^{0}C, as shown in Table 6.

Table 6 Zeta Potential of Fine Particles in Aqueous System at 20 ^{0}C

Solid particle	Average size, μm	Zeta potential, mv	pH
Glass bead	35	-7.2	6.8
PAC	17	-5.5	6.7

The absolute values of ZP of glass beads and PAC are no greater than 10 mV in water, which means that they tend to form aggregates easily in water. Consequently, aggregated particles are much easier to be removed by flotation.

5.2 PROPERTIES OF SOLID PARTICLE

The properties of solid particles include particle size and distribution, bulk and particle density, and the adsorption capacity of chemicals by adsorbent particles.

5.2.1 Particle Size Distribution

Sizes of two different solid particles, i. e. glass beads and PAC, are measured in this study. The number distributions of particle size are shown in Figure 12. The median value of particle diameter, d_{50}, is used to represent particle size. Glass beads have a d_{50} at 35 μm. Two different PAC samples are used. Sample A is prepared in a mortar grinder (by Fritsch) for one hour and sample B has been grinded for 24 hours in a ball mill with 1 cm diameter ceramic balls. The d_{50} of sample A and sample B are 17.2 μm and 4.7 μm, respectively.

5.2.2 Density of Particles

Bulk density and particle density are two major physical properties to describe solid particle. Bulk and particle densities of glass beads and PAC are listed in Table 7.

Table 7 Bulk and Particle Density of Particles

Particles	Bulk density, kg/m^3	Particle density, kg/m^3
Glass beads	949	2497
PAC[35]	400-640	2082

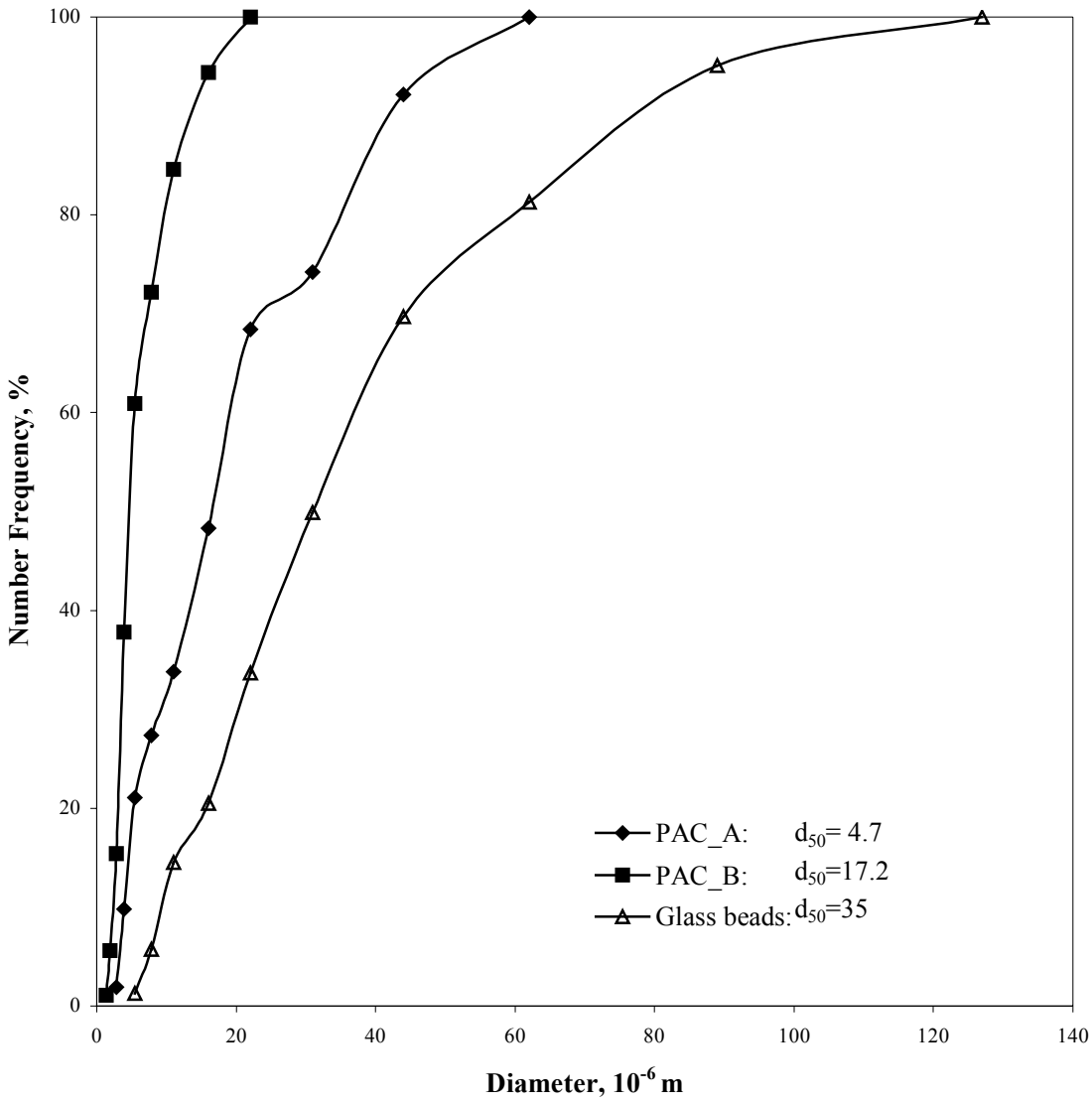

Figure 12 PAC and Glass Beads Particle Size Distributions

5.2.3 Phenol Adsorption Isotherm

The adsorption isotherm of phenol on PAC in aqueous system is determined. As indicated earlier, Freundlich model is recommended for the study of phenol adsorption on PAC, which is given in the following equation:

$$Q = K_{ads} C_{eq}^{\frac{1}{n}} \qquad (11)$$

where, Q is adsorption amount of phenol per gram of PAC. K_{ads} is adsorption constant, or Freundlich constant; C_{eq} is phenol concentration in water; and n is a constant related to temperature, usually greater than 1.

The adsorption isotherms of phenol on two types of PAC, React-A and F-300, are measured in a stirred beaker at 20 ^{0}C in the presence of 500 ppm PAC. Solid symbols representing experimental data points are shown in Figure 13. The solid curves are adsorption isotherms based on the Freundlich model. The calculated constants are K_{ads} = 24.78 and n = 2.768 for React-A PAC, and K_{ads} = 12.57 and n = 2.149 for F-300, respectively. These data show that the value of K_{ads} of PAC React-A is nearly double that of F-300, indicating React-A has a greater adsorption capacity than F-300. Therefore, React-A is recommended for the subsequent study on phenol removal.

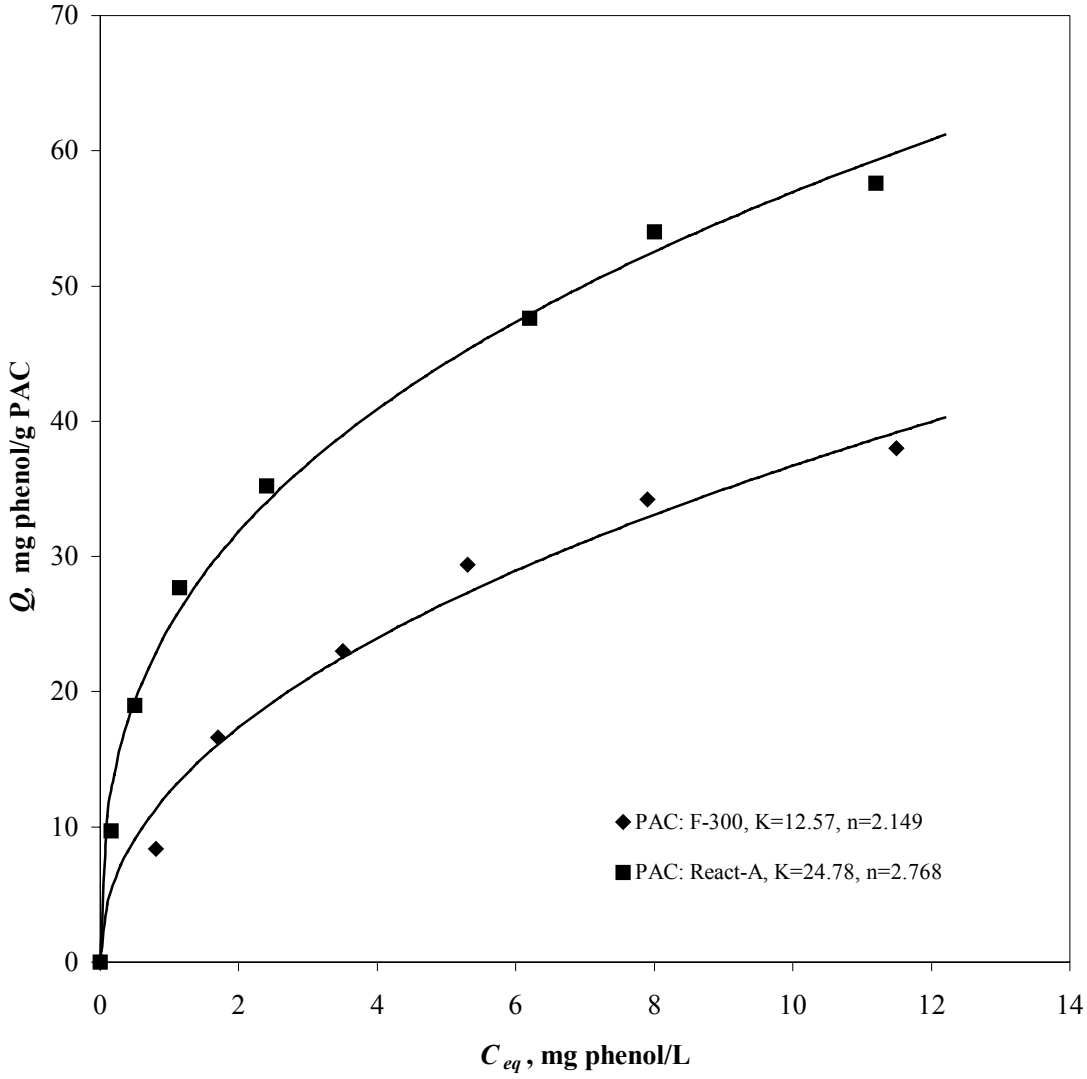

Figure 13 Freundlich Isotherm of Phenol Adsorbed on PAC at 20 ^{0}C

In flotation experiments, the adsorption equilibrium is not achievable due to short contact time, or residence time. Therefore, a study of adsorption as a function of time is necessary. The transient adsorption study has been carried out in a one-liter stirred beaker at initial phenol concentration of 40 mg/L with 100 ppm or 500 ppm PAC at 20 ^{0}C. The removal efficiency of phenol by PAC expressed in terms of the amount of phenol removed (C-C_0) divided by initial concentration (C_0) as a function of adsorption time is shown in Figure 14. The results show that the phenol removal efficiency highly depends on PAC concentration. With 500 ppm PAC, 66% of initial phenol (26.4 mg phenol) is adsorbed during the first 10 minutes and approaches 70% (31.3 mg phenol) at 30 minutes. On the other hand, with 100 ppm PAC, the phenol removal efficiency at 10 minutes and 30 minutes are 39% and 54%, respectively.

Based on the volume of MSTLFLO column and operating conditions, the maximum residence time of PAC particles in the MSTLFLO column is estimated to be less than 30 minutes. Therefore, transient adsorption is only carried out up to 30 minutes, when the amount of phenol removed by 500 ppm of PAC (in an one liter container) is 31.3 mg, which is equivalent to (62.5 mg of phenol)/(g of PAC). This value provides a reference point for the evaluation of phenol removal efficiency in flotation experiments.

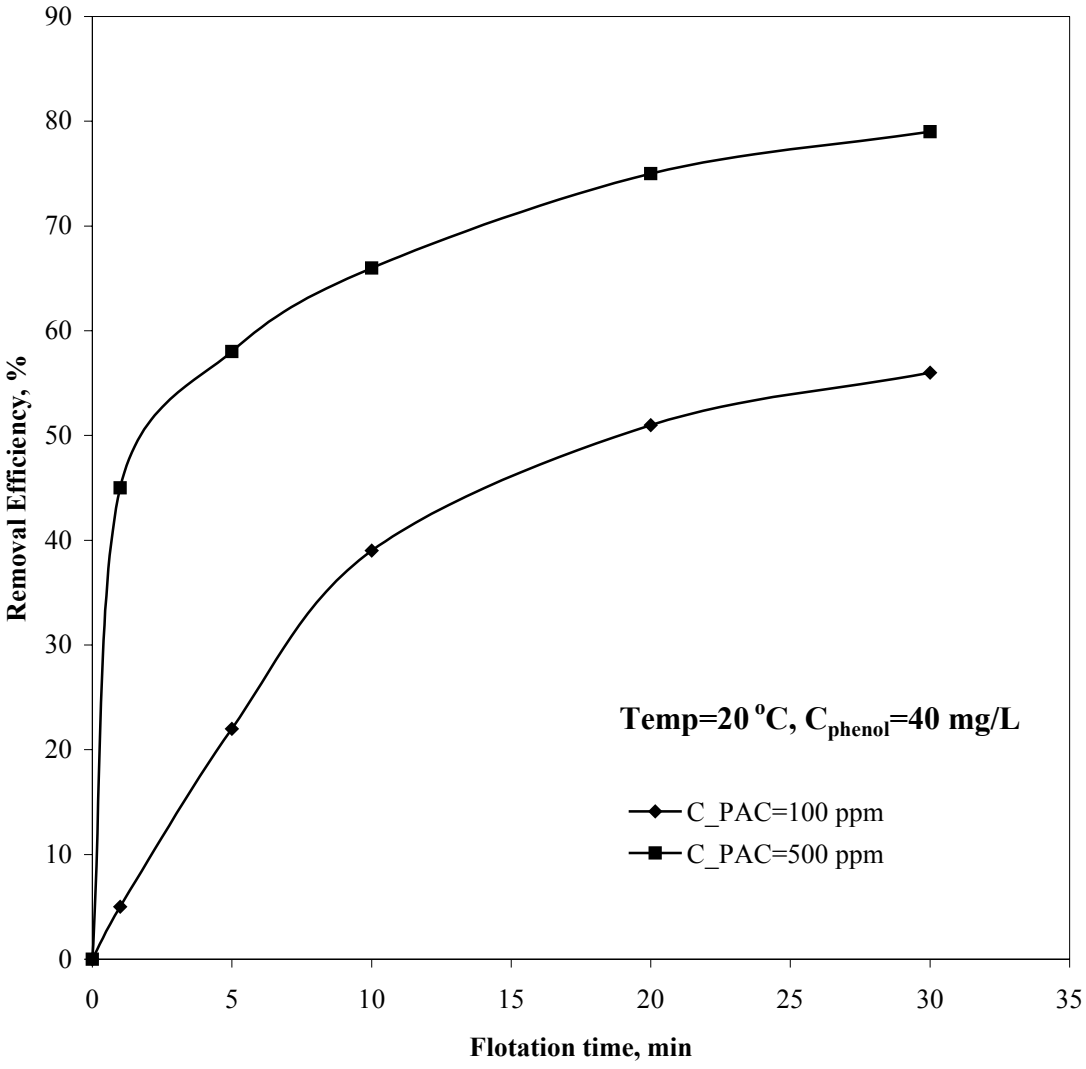

Figure 14 Phenol Adsorption Kinetics on PAC at 20 ^{0}C

6.0 STUDY OF HYDRODYNAMIC PROPERTIES

In this study, following hydrodynamic parameters have been investigated in both 4-in and 12-in column:

1. In the 4-in column, since the hydrodynamic properties in the absence of solids have been previously determined, only gas holdups in the presence of fine particles, such as glass beads, will be measured.
2. In 12-in column, following parameters will be measured in the absence of solid particles:
    - Gas holdups;
    - Bubble size distributions;
    - Liquid circulation velocities (linear and superficial)

6.1 GAS HOLDUPS WITH FINE PARTICLES IN THE 4-IN COLUMN

To investigate the influence of small amount of fine solid particles on gas holdup, glass beads are tested as a simulant of solid phase in the 4-in MSTLFLO column. The concentration of glass beads applied in experiments is 500 ppm, while frother concentrations vary from 10 to 30 ppm.

The results of gas holdups with and without solid particles are compared in Table 8. The data show that the gas holdups in the presence of 500 ppm solid particles are very close to those

in the absence of solids. Under certain operations, gas holdups with solids are slightly larger than those without solid particles. In all cases, differences are less than ±5%. It is clear there is no significant effect on gas holdup when a small amount (≤ 500 ppm) of fine solids is added. Therefore, it can be assumed that gas holdups with small amount solids are the same as gas holdups without solids.

Table 8 Gas Holdups in 4-in Flotation Column

Frother ppm	SGV cm/s	Gas holdup, % (W/ solids)			Gas holdup, % (W/O solids)		
		B	M	T	B	M	T
10	1	10	11.3	11.9	10.6	10.6	11.6
	2	26	25.3	25.8	23.8	23.1	23.1
	3	31.8	30.8	31.9	31.3	30	30
20	1	8.8	10	10	10	10	10.5
	2	26.3	26.3	26.3	23.8	23.8	24.4
	3	33.8	33.8	31.9	32.5	32.5	32.5
30	1	10.6	10	11.3	11	10.8	11
	2	55	57.5	57.5	56.3	54.4	57.5

6.2 Hydrodynamic Study in 12-in Column

Extensive experimental studies on the measurement of gas holdup, bubble size and distribution, and liquid circulation velocity have been carried out in 12-in column.

6.2.1 Gas Holdup Measurements

As reported in previous study in the 4-in column[6], the favorable gas holdup is between 20-50% while unfavorable or unstable operations prevail at too low (< 10%) or too high (>50%) gas holdups. This information serves as guideline for gas holdup study in current study. In order to investigate influences of the geometry and operating factors on gas holdups, a series of experiments have been carried out in the 12-in column. Two column design factors, air sparger as well as cone baffle, and three operating parameters, frother type, frother concentration, and feeding position, are examined. At the end of this section, gas holdups with single stage operation in the 12-in column have been measured and are compared with those data in the 4-in column.

a. Effect of Sparger

As discussed earlier (see chapter 4), two different types of spargers have been tested in 12-in column: a sintered metal disk sparger and a multi-stick sparger. From previous discussion, a 4-stick sparger can provide sparging surface area four times larger than a disk sparger. As a result, under a given air pressure, a multi-stick sparger with larger surface area yields greater gas flow rate and higher gas holdup.

In Table 9 the experimental results show that gas holdups increase with SGV, as expected. However, due to insufficient sparging surface area, gas holdups with disk sparger are much smaller than those using stick spargers, especially when frother and high SGV are applied. For example, at 2.6 cm/s SGV and no frother, gas holdup in the middle stage is only 5% and 6% with disk sparger and stick sparger, respectively. Differences become more pronounced with

frother at high SGV. With 10 ppm frother at 3.9 cm/s SGV, gas holdup with stick sparger is 27% higher than that with disk sparger.

Table 9 Gas Holdups in the Middle Stage Using Two Types of Spargers

Sparger type	Frother ppm	SGV, cm/s		
		1.3	2.6	3.9
Stick	0	5 %	6 %	8 %
Disk		4 %	5 %	6 %
Stick	10	6 %	10 %	15 %
Disk		5 %	8 %	11 %

Though disk sparger is mechanically simple in design, its disadvantage of poor bubble generation is obvious. Therefore, in order to obtain high gas holdup, stick-type sparger is chosen for subsequent experiments.

b. Effect of Cone Baffles

Cone baffles are used to direct rising bubbly stream into the riser of upper stage and to minimize backmixing between two adjacent stages. Properly designed cone baffle is very important to keep high gas holdup within each stage. As mentioned earlier (see chapter 4), two different designs of cone baffles, “short” cone and “long” cone, have been tested.

The measurements of gas holdups have been obtained with two types of cone baffles at 10 ppm frother are shown in Figure 15. The results indicate that the “long” cone baffle yields higher gas holdups than the “short” under the same operating conditions. Gas holdup reaches 34% in the top stage at 3.9 cm/s SGV with a “long” baffle, while gas holdups are less than the desired range (<25%) under all operating conditions when a “short” cone baffle is used. This implies that insufficient small gas bubbles are retained in contact region (the riser) and loop flows are weak. The possible reason may be the gap between draft tube and upper open of cone is too large for a short cone baffle. Hence, a fraction of small bubbles escape into the downcomer

instead of the riser, which would lead to poor mixing between liquid and gas phases and therefore poor column performance. Thus, in order to obtain sufficient gas holdups, the installation of "long" cone baffle is recommended.

c. Effect of Frothers and Usage

As mentioned earlier, two major commercial frothers, MIBC and 2-EH, have been tested. Gas holdups in 12-in column and 4-in column [36] with 5, 10 and 20 ppm frother are compared in Figure 16-18, respectively. As expected, gas holdups increase with SGV and frother dosage. Although both MIBC and 2-EH can effectively generate adequate gas holdups (>20%) with properly selected operating conditions, to provide a direct comparison with previous experimental data [38], 2-EH is used in subsequent experiments.

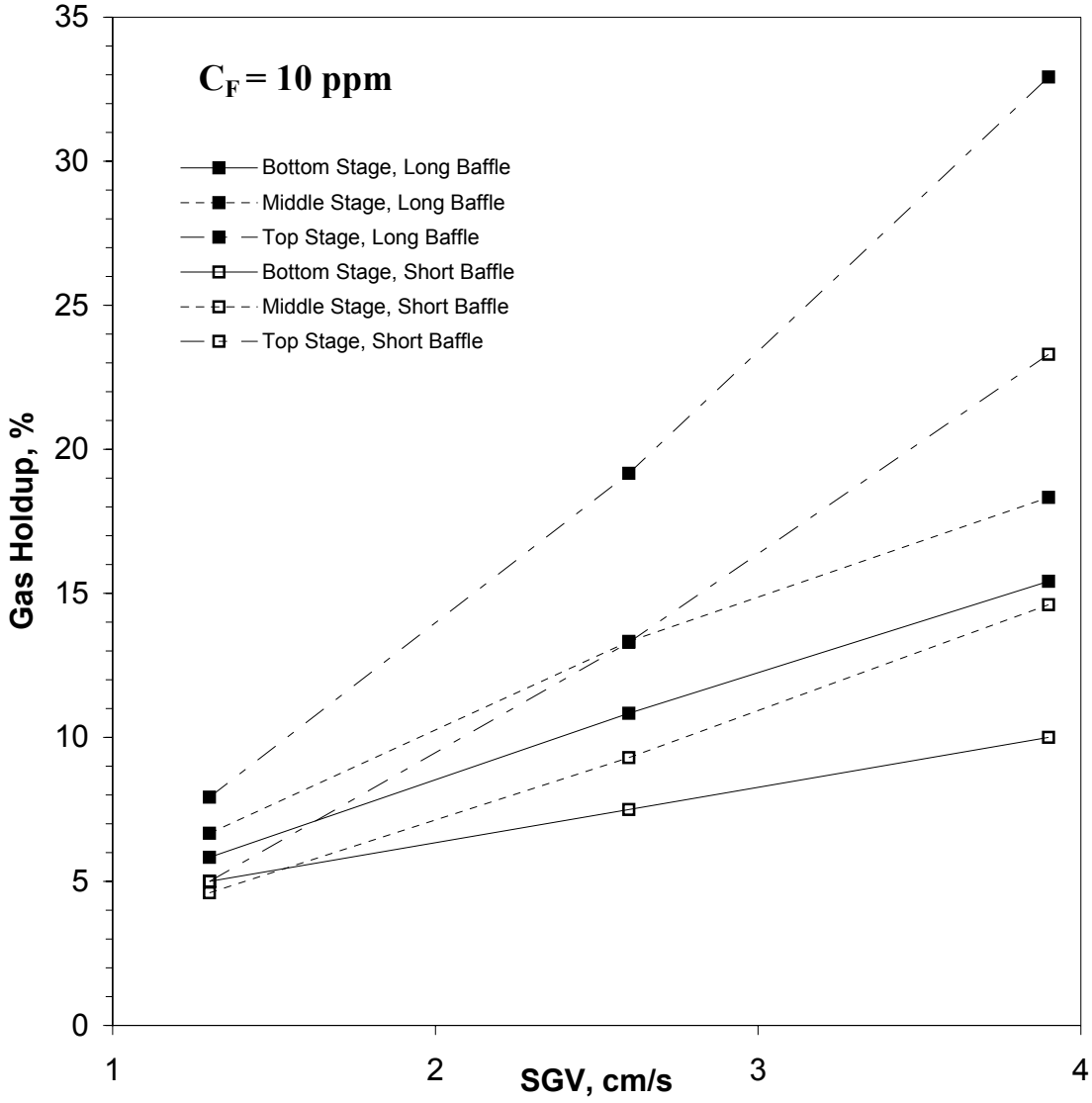

Figure 15 Gas Holdups with Different Cone Baffles in 12” Column

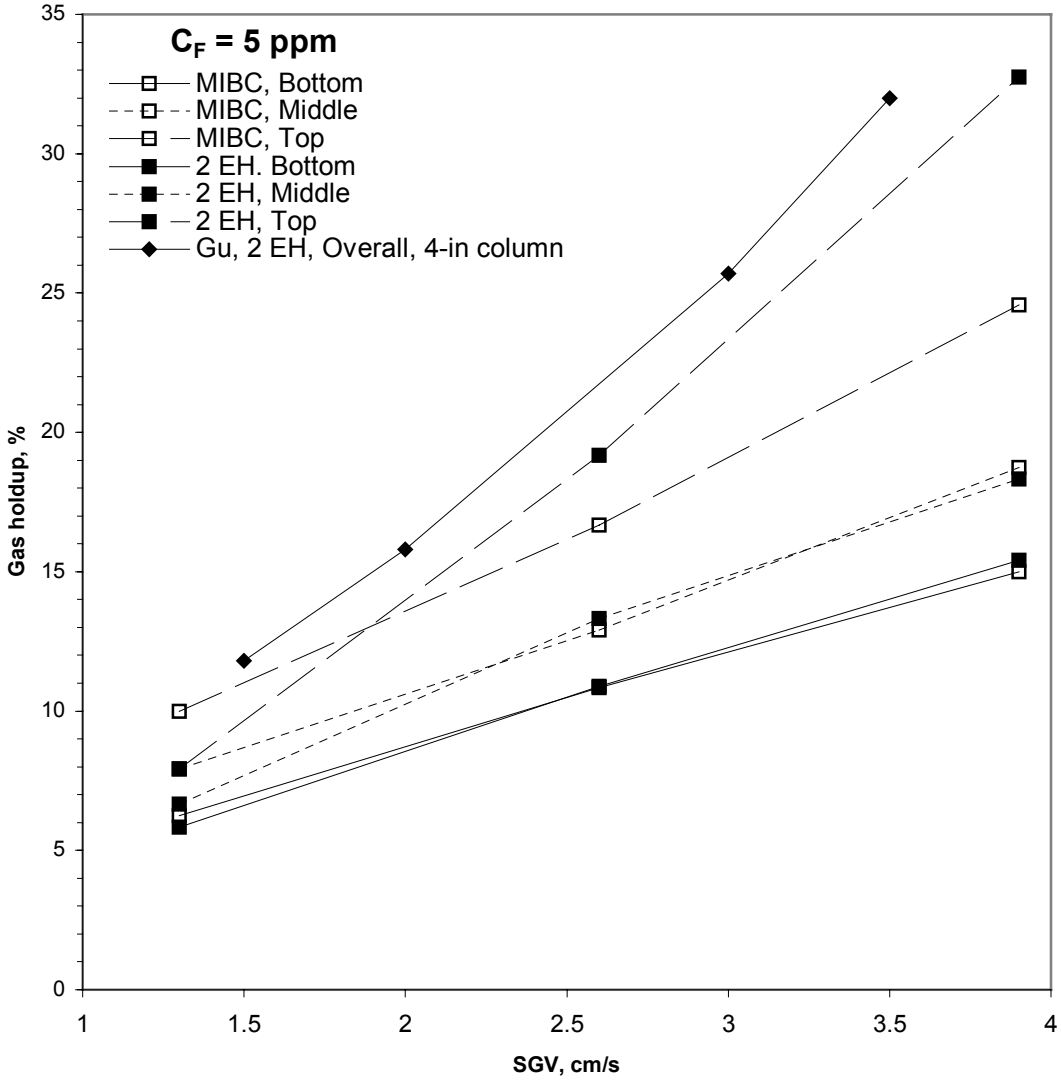

Figure 16 Gas Holdups with Frother Concentration at 5 ppm (in 12" and 4" Columns)

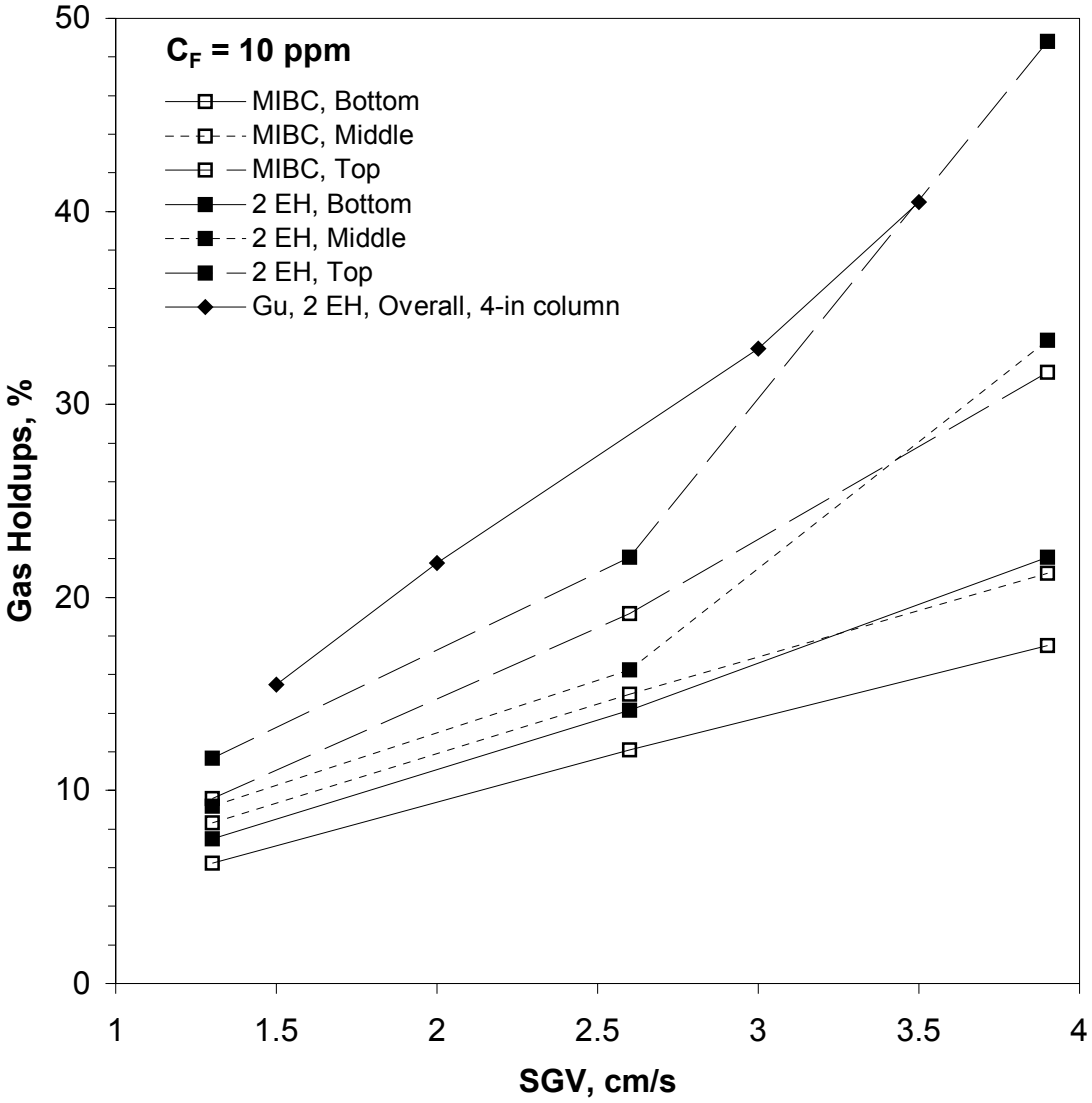

Figure 17 Gas Holdups with Frother Concentration at 10 ppm (in 12" and 4" Columns)

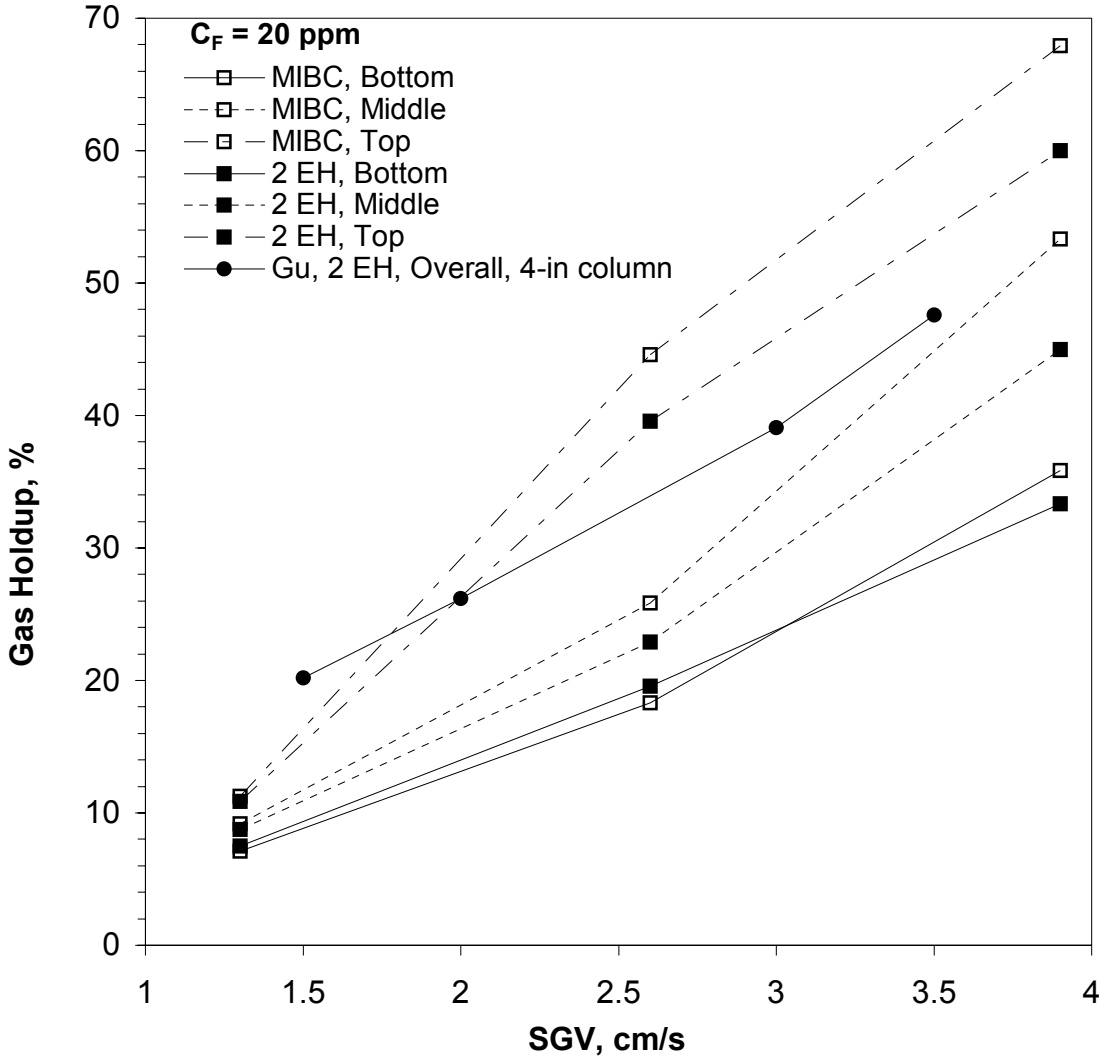

Figure 18 Gas Holdups with Frother Concentration at 20 ppm (in 12" and 4" Columns)

In Figures 16 to 18, it is seen that the gas holdups in 12-in column are generally lower than that in the 4-in column at comparable frother concentrations. Also, the distribution of the gas holdups in the 120-in column is uneven. In order to seek remedy to this situation, experiments of different frother feeding positions are investigated.

d. Effect of Frother Feeding Positions

In this section, influences of frother feeding positions on gas holdup are discussed. Three feeding positions, top, middle and bottom along column are tested. To obtain consistent data, 20 ppm frother is applied.

As shown in Figure 19, gas holdups can be grouped into three different zones: unstable operation condition (ε_g > 50%), favorable operation condition (20%<ε_g<50%) and unfavorable operating condition (ε_g<20%). With a few exceptions, most gas holdups are found within the operable range (between 20-50%) in the 12-in MSTLFLO column and therefore enable proper column operations. In experiments of frother feeding into the top stage, most gas holdups are in the range of 20-50% when proper operating conditions are applied. However, when SGV is greater than 3.0 cm/s, gas holdup in the top stage reaches beyond 50%. At such a high gas holdup, unstable loop flow occurs because of insufficient quantity of liquid phase and it results in a decrease in separation efficiency. In the cases of frother feeding into the middle stage or through the sparger to the bottom stage, gas holdups are mostly found in the operable range. Only a few exceptional experiments are observed, where the gas holdup in the top stage exceeds 50% when SGV is greater than 3.9 cm/s. Thus, in order to avoid unstable operating conditions, feeding frother into the middle stage or through sparger is recommended for subsequent experiments.

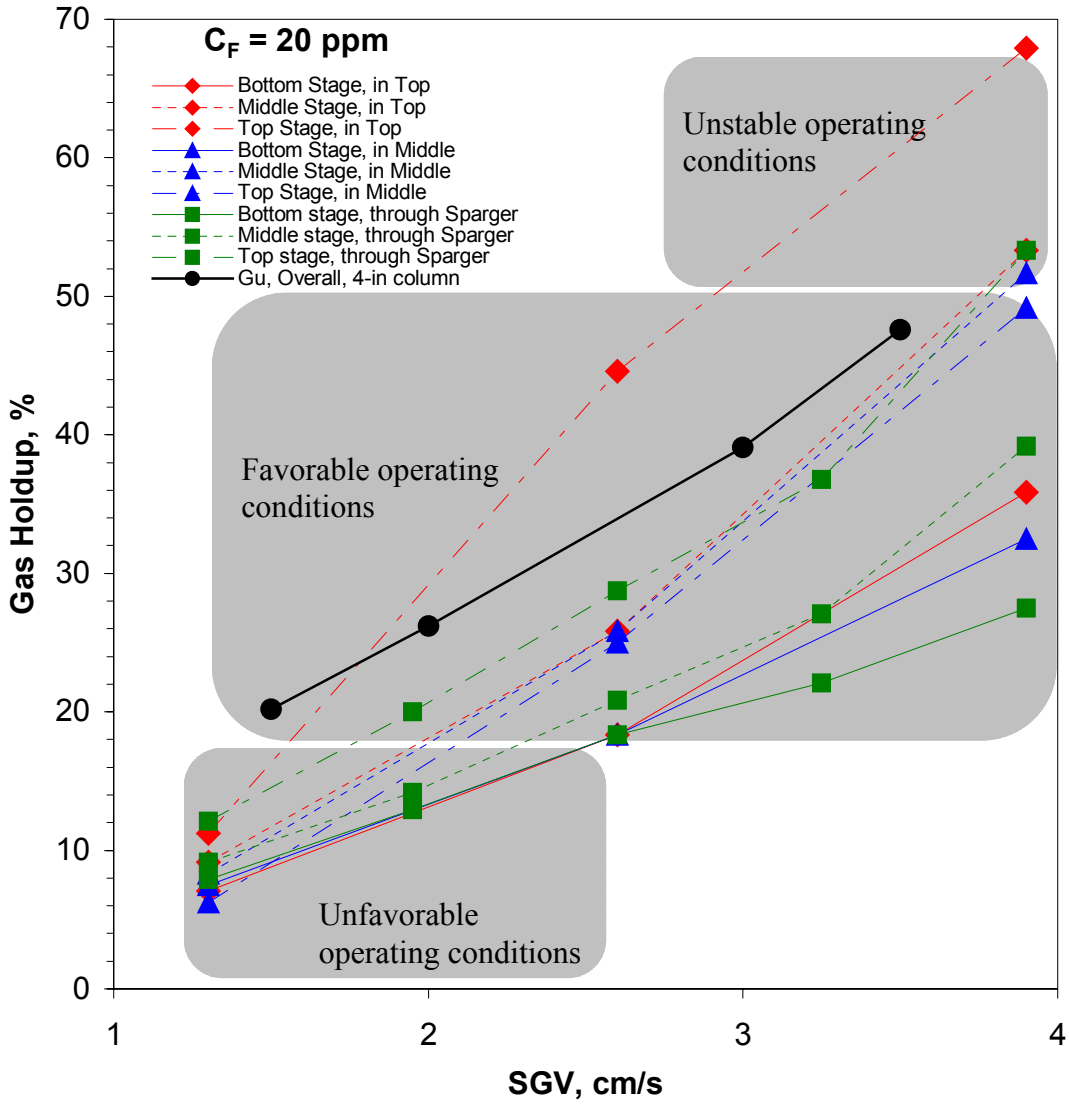

Figure 19 Gas Holdup of All Stages at Different Frother Feed Positions (in the 12" Column)

e. Measurements of Gas Holdups in the Riser and Downcomer

The unique loop flow around each draft tube (or stage) in MSTLFLO column is induced by pressure difference between annular space (downcomer) and central space (riser), which is due to a difference in gas holdups. In order to gain a better understanding of liquid circulation in MSTLFLO column, gas holdups in both riser and downcomer are determined based on hydrostatic pressure differences measured by using a U-tube manometer positioned between the two ends of each draft tube. From these measurements the pressure drop between the downcomer and riser also can be determined. Equipment setups for these measurements are shown in Appendix B.

Gas holdups in riser and downcomer at different operating conditions are presented in Table 10. Experimental results indicate that gas holdups in riser are always greater than those in downcomer, which induce a pressure drop and generate a loop flow. It is also shown that pressure drop between riser and downcomer increases with SGV at a give frother concentration. When gas holdups are greater than 50%, pressure drops cannot be accurately measured due to pressure fluctuations in riser and downcomer. As discussed in the previous section, favorable gas holdups for a high separation efficiency are in the range of 20-50%. As shown in Table 10, although there are a few exceptions of unstable conditions (when ε_g>50%) or unfavorable conditions (when ε_g<20%), favorable gas holdups prevail when proper operating conditions are chosen.

Table 10 Gas Holdups in Riser and Downcomer in 12-in Column

Frother ppm	SGV cm/s	Stage	Pressure difference kPa	Gas Holdup (riser), %	Gas Holdup (downcomer) %
0	1.3	B	0.03	6.3	5.2
		M	0.03	7.2	6.0
		T	0.05	9.5	8.1
	2.6	B	0.06	11.7	11.3
		M	0.06	14.2	13.3
		T	0.08	17.6	16.0
	3.9	B	0.06	16.7	15.8
		M	0.06	19.4	18.3
		T	0.09	23.1	21.3
10	1.3	B	0.05	8.3	6.7
		M	0.05	10.8	9.2
		T	0.06	13.5	11.7
	2.6	B	0.09	15.8	13.8
		M	0.12	18.5	16.3
		T	0.16	24.0	22.1
	3.9	B	0.17	23.8	21.7
		M	0.22	35.5	33.3
		T	U/A	>60	58.3
20	1.3	B	0.03	9.2	7.1
		M	0.05	10.7	8.8
		T	0.06	13.1	10.9
	2.6	B	0.07	16.3	14.6
		M	0.10	24.8	22.9
		T	U/A	42.0	39.6
	3.9	B	0.09	30.0	27.9
		M	U/A	47.5	45
		T	U/A	>60	60

*B, M, and T stand for the bottom, middle and top stage respectively.

6.2.2 Liquid Circulation Velocities

It has been reported [62, 63, 64, 65, 66] that liquid circulation velocity is a function of superficial gas velocity and linear liquid circulation velocities. Linear liquid circulation velocities have been measured in the 12-in column using "tracer method". Measurements have been carried out at 10 L/min liquid feeding rate with different frother concentration and SGV. Superficial liquid velocity is then calculated.

Figure 20 presents calculated superficial liquid circulation velocities at different frother concentrations and SGV. Similar to gas holdup, the liquid circulation velocities can be divided into in three regions: unstable circulation (U_L> 0.3 m/s); sufficient circulation (0.3 m/s > U_L> 0.1 m/s); and insufficient circulation (0.1 m/s > U_L). It is seen that most liquid circulation velocities are in the sufficient circulation zone. As shown in the Figure 20, there are no obvious changes in superficial liquid velocity in the absent of frother. The superficial liquid velocity increases with SGV only when frother is presented. With 10 to 15 ppm frother, superficial liquid velocities in all three stages are nearly the same. However, when frother is increases to 20 ppm, superficial liquid velocity in individual stage varies significantly. Especially at 3.0 cm/s SGV, liquid circulation velocity in top stage is far greater than that in the bottom and middle stages. This confirms the earlier observations in gas holdups experiments, where unstable operating conditions occur in the top stage. However, these exceptional cases may be avoided if proper ratio of draft tube length to diameter and operating conditions are applied.

These experimental results provide preliminary guidelines for the design of large scale operation of MSTLFLO column. However, in order to achieve the best separation efficiency of MSTLFLO column, further study on the modification of sparger, cone baffles and the ratio of draft tube length to diameter may be necessary.

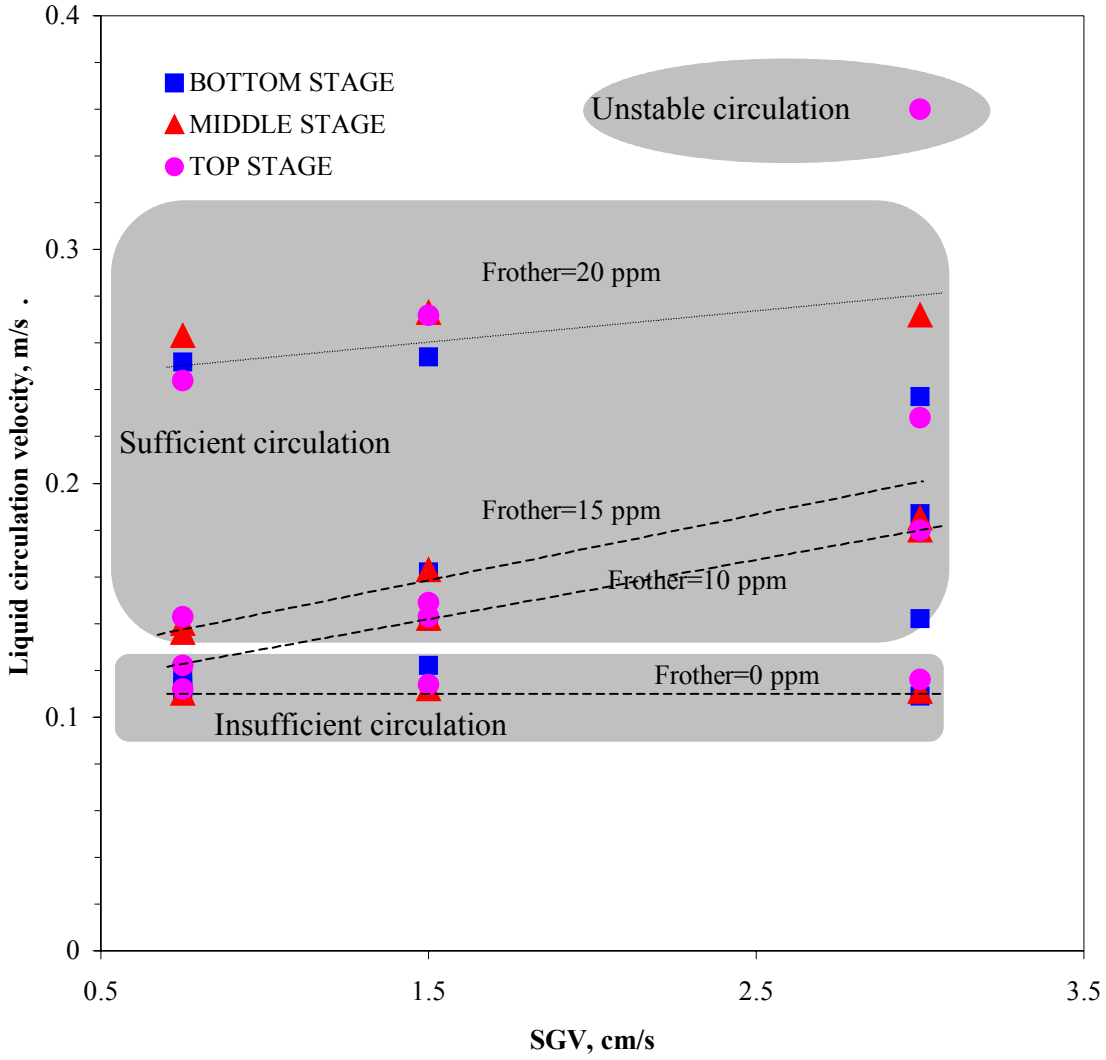

Figure 20 Liquid Circulation Profiles in Three Stages at Different Frother Concentrations

6.2.3 Bubble Size Distribution

The size of bubbles is critical in maintaining high level of gas holdup. Small bubbles can provide high gas holdup as well as large specific interfacial area and effective collisions between bubbles and particles. Therefore, it is important in hydrodynamic study to measure bubble size and size distribution.

A digital photographic technology is used to capture pictures of rising bubbles in the 12-in column. Each picture covers a projected area of 20 mm × 26 mm in each of stage. The resolution of the picture is 1200 × 1600 dpi. Software Photoshop is used to convert images into 8-bit grayscale format. Then clearly shaped bubbles in each picture are highlighted manually in black dots. The number and sizes of black dots are automatically counted by using software ImageJ. More than 500 bubbles are counted for each operating condition. A summary of Sauter diameter of bubbles under different operating conditions is shown in Table 11. As expected, bubble size increases with SGV but decease with frother concentration. Bubbles in upper stages are slightly bigger than bubbles in lower stages. Compared with results in the 4-in column[38], Sauter bubble sizes in 12-in column are slightly larger than those in 4-in column. Such a difference is primarily due to the hydraulic head in the 12-in column is much larger than in the 4-in column. Other different hydrodynamic behaviors, as discussed above, are also considered.

A typical bubble size distribution curve when the column is operated with 2.6 cm/s SGV and 20 ppm frother is shown in Figure 21. Bubble size ranges from 0.4 mm to 2.4 mm. It can be seen that most bubble sizes are in between 0.5 mm and 1.0 mm. Only a small number of bubbles

Table 11 Sauter Mean Bubble Size at Different Operating Conditions

Frother Ppm	Stage	SGV cm/s	Average bubble size, mm
0	B	1.3	3.87
		2.5	4.27
		3.9	4.30
	M	1.3	3.78
		2.5	4.22
		3.9	4.39
	T	1.3	3.82
		2.5	4.37
		3.9	4.51
5	B	1.3	1.32
		2.5	1.79
		3.9	1.90
	M	1.3	1.26
		2.5	1.83
		3.9	1.92
	T	1.3	1.30
		2.5	1.76
		3.9	1.98
10	B	1.3	1.17
		2.5	1.46
		3.9	1.73
	M	1.3	1.18
		2.5	1.46
		3.9	1.80
	T	1.3	1.17
		2.5	1.48
		3.9	1.82
20	B	1.3	0.92
		2.5	1.18
		3.9	1.23
	M	1.3	0.99
		2.5	1.21
		3.9	1.30
	T	1.3	0.98
		2.5	1.16
		3.9	1.29

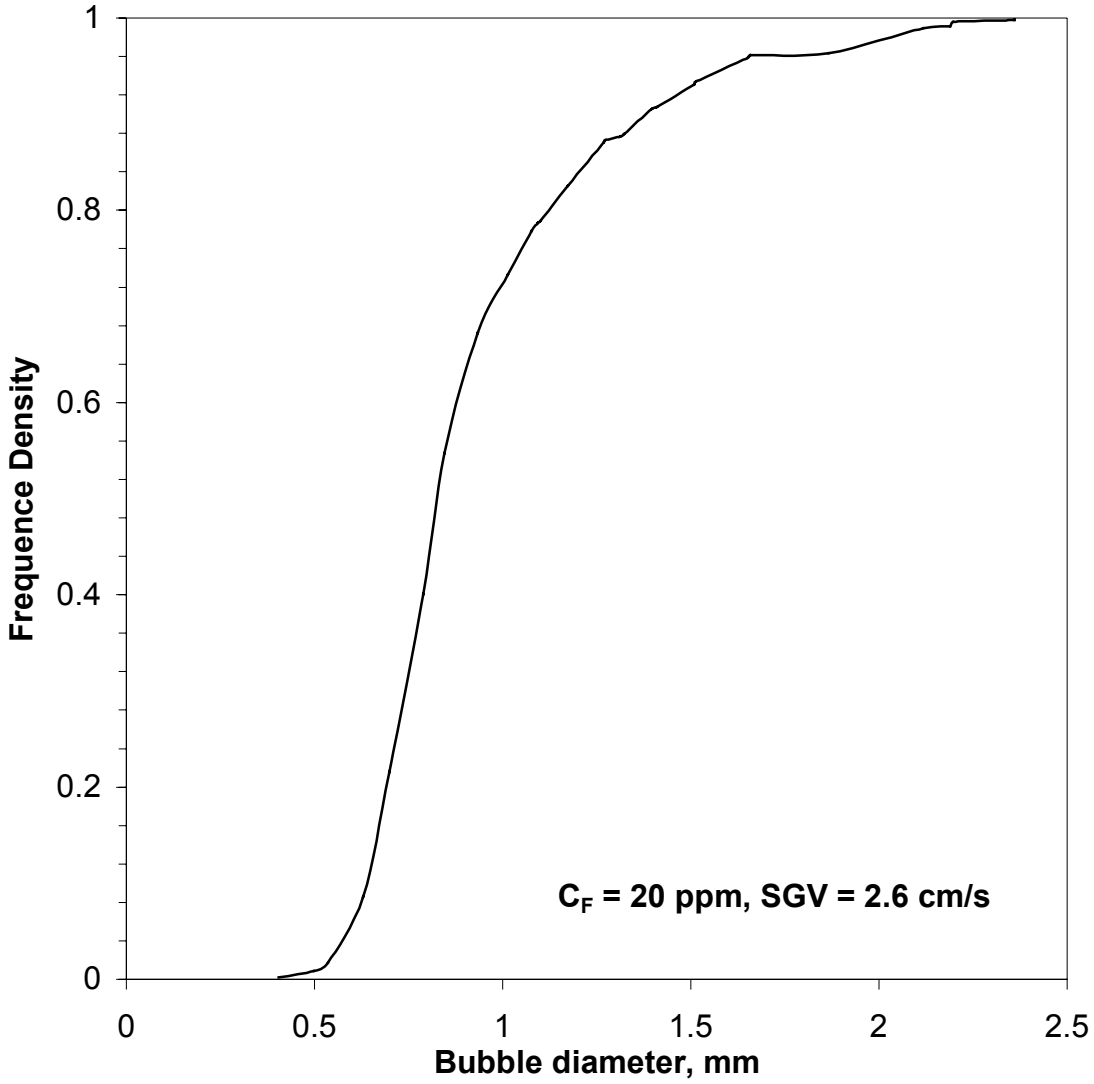

Figure 21 A Typical Bubble Size Distribution at 20 ppm Frother

6.2.4 Experimental Errors

Experimental Errors can be determined by measurement deviations and/or statistic error analysis. In this section, the measurement deviations of hydrodynamic properties, including gas holdup, liquid circulation velocity and bubble size, and statistic error analysis for particles/oil/phenol removals are discussed.

a. Gas Holdup

Gas holdups are measured by hydrostatic pressure method using a manometer. Absolute measurement deviations is determined as the smallest scale on manometer reading, which is 1 mm, or in term of 0.13% (equals 1 mm of 30 × 25.4 mm) gas holdup. Relative measurement deviations are calculated by dividing absolute error by experimental values. Estimated relative measurement deviations range from 1.2% to 8.07%. However, in most experiments, relative measurement deviations are less than 5%.

b. Liquid Circulation Velocity

Liquid circulation velocity is calculated with liquid linear velocity and gas hold up, as discussed in Appendix C. Linear velocity of liquid is obtained by dividing the distance between two conductivity probes by time lag between an individual peak value appeared on two conductivity meters. Measurement deviation associated with stop-watch is estimated to be 0.1 second. Typical time lags are between 2 and 7 seconds. Therefore, relative measurement deviations are ranging from 1.4% to 5.0%.

c. Bubble Size

In order to obtain statistically reliable data, more than 500 bubbles are measured under each operating condition. Because the diameter of column is large (305 mm), the magnification effect due to curvature of column wall can be neglected. Images of bubbles are nearly perfect

circles in the digital recording when frother is present. Only when frother is not present, bubbles show greater deviation from circles. In such a case, equivalent area diameter is applied. Therefore, absolute measurement deviation is associated with the smallest scale in the graphic software Photoshop, which is 1 pixel. In all cases, the diameters of smallest bubbles are larger than 25 pixels. Therefore, relative measurement deviations are less 4.0%.

d. Experimental Errors

Experimental errors are determined statistically in terms of the standard deviations [67], σ, for multiple experiments at a given operating condition:

$$\sigma = \sqrt{\frac{n\sum d_i^2 - \left(\sum d_i\right)^2}{n(n-1)}} \qquad (12)$$

where, d_i is the value of the i^{th} measurement and n is number of measurements.

Experimental errors associated with different operating conditions are summarized in Table 12. Smaller standard deviation represents a higher reproducibility. For all six parameters, the experimental errors are considered to be statistically acceptable in view of the fact that only a relatively small number of experiments were performed in each case.

Table 12 Experimental Errors At Given Operating Conditions

	SGV cm/s	Frother Conc. ppm	# of Runs	Experimental data	Experimental errors, σ
Gas Holdup, %	1.3	20	4	8.8	0.6
	2.6	20	4	22.9	0.6
	3.9	20	4	45	1.7
Bubble Size, mm	1.3	20	4	0.99	0.01
	2.6	20	4	1.20	0.01
	3.9	20	4	1.31	0.01
Oil Residual, ppm	1.3	20	3	54	4.7
	2.1	20	3	49	5.3
	2.6	20	3	40	5.9
PAC Residual, ppm	3	30	3	15	3.2
	4	30	3	9	2.3
	3	40	3	10	2.1
	4	40	3	7	1.5
Glass beads Residual, ppm	2	10	3	27	3.5
	3	10	3	19	3.0
	2	20	3	11	2.3
	3	20	3	3	1.0
Phenol Residual, ppm	1	20	3	14.8	1.3
	2	20	3	19.6	1.0
	1	30	3	12.4	0.9
	2	30	3	12.8	0.9

6.3 GAS HOLDUPS WITH SINGLE STAGE OPERATION

As indicated in previous discussions, unevenly distributed gas holdups along the column have been found in the 12-in MSTLFLO column, which introduces lower overall gas holdups as well as unstable liquid circulations in the top stage. To verify scale-up effects on hydrodynamics in individual operating stages, gas holdup measurements have been carried out in the 12-in column with single-stage (the bottom stage only) operation.

Results are compared with gas holdups of the bottom stage in the 4-in MSTLFLO column at similar operating conditions, as shown in Figure 22. The gas holdups obtained in single stage operation for the 12" column are comparable to those in the bottom stage of the 4-in column. This finding shows that the excellent hydrodynamic conditions can be achieved in the 12-inch column. It also confirms the previous discussions (see section 6.2) that unfavorable hydrodynamics along the 12-in column, especially in the upper stages, can be greatly improved by applying properly chosen baffles and air sparger as well as a correct choice of the draft tube length to diameter ratio. Furthermore, it implies that the current geometric design of the 4-in and 12-in column can be used as a basis for future scale-up to larger size MSTLFLO columns for commercial applications.

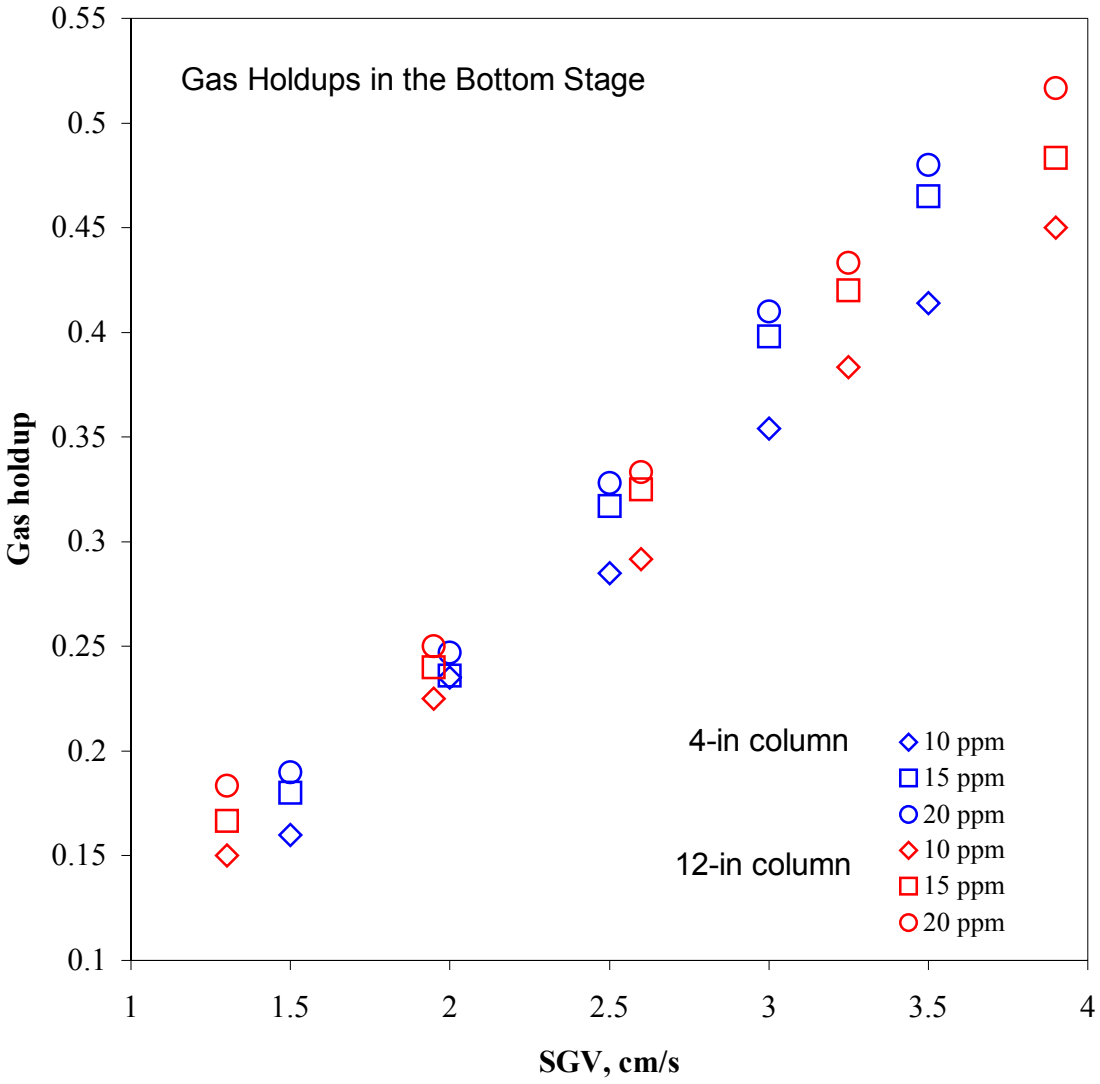

Figure 22 Gas Holdups in the Bottom Stage with Single Stage Operations

7.0 SEPARATION RESULTS

A series of experiments of removing mixed types of pollutants from wastewater have been carried out in the 4-in column. In addition, oil removal experiments have been performed in the 12-in column. The results of oil removal in 12-in and 4-in columns are compared to establish a basis for the scale-up of the MSTLFLO column design.

7.1 EXPERIMENTAL RESULTS IN 4-IN COLUMN

Three different types of experiments are performed: (1) suspended fine particles, (2) fine PAC particles/phenol mixture, and (3) fine PAC particle/oil/phenol mixture. Removal efficiency, defined as the amount of component removed divided by the initial concentration in the feed, and its relation to operating conditions will be discussed.

7.1.1 Fine Particle Removal

Based on particle's surface property, two major types of fine particles have been tested in 4-in MSTLFLO column. These include naturally hydrophobic PAC particles and comparatively hydrophobic glass beads.

a. PAC Particles Removal

Due to its hydrophobic nature, PAC is easy to attach to air bubbles. To explore the effect of particle size to remove efficiency, two different PAC samples, size-A and size-B (17.2 and 4.7 μm, respectively, see **Section 5.2.1**) are used in experiments. Water/particle slurry is fed into the top stage at a concentration equivalent to 100 ppm in bulk stream. A fixed 20 ppm of frother is applied. Treated water samples are taken at the bottom outlet of column when steady state operating condition is achieved. Results are shown in Figure 23.

MSTLFLO is an effective process for PAC particles removal. As high as 90% of the PAC particles are removed at 4.0 cm/s SGV, for particles range from 1.0 μm to 20 μm. It is seen that the removal efficiencies for both sample A and B increase with SGV. At low SGV, the removal efficiency of sample A is slightly lower than that of sample B, while at 4.0 cm/s SGV, the results are reversed. However, the differences in removal efficiency between two PAC samples is likely to be random and within experimental uncertainty. In both cases, the removal efficiency reaches 90% at 4.0 cm/s SGV.

The effects of frother concentration and PAC feeding positions on PAC removal have been investigated using sample A. Figure 24 shows PAC removal efficiency increases with frother dosage, which provides large gas holdup and therefore increase collisions frequency between bubbles and particles. PAC feeding position also plays an important role in the removal of particle. To generate a counter-current flow between liquid and rising bubbles, only middle and top stage are selected as feeding sites. Generally, feeding in the top stage yields higher PAC removal efficiency. In the top stage, PAC can be fed into riser or downcomer. In the case of feeding to the riser, the flow of PAC and rising bubbles are counter-current, while they are co-current in the case of downcomer feed. Higher removal efficiency is found in the case of feeding

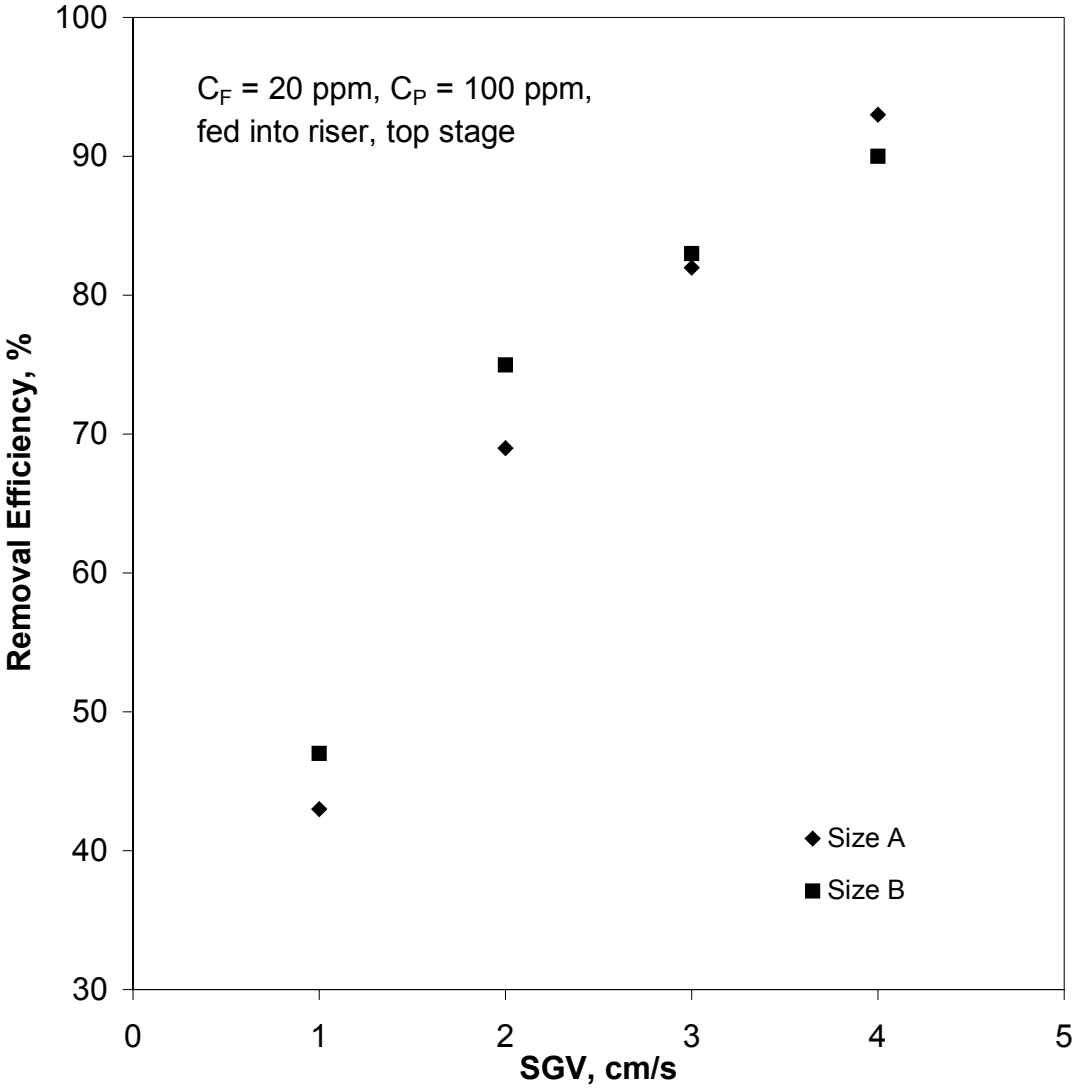

Figure 23 Removal of PAC in 4-in Column

to the riser than that to the downcomer. However, in both cases, particle removal efficiencies excess 95% when 4.0 cm/s SGV and 40 ppm frother are applied.

b. Removal of Glass Beads

In order to investigate comparatively hydrophobic particles, experiments have been carried out with glass beads. Results are shown in Figure 25. Similar to the results of PAC, the removal efficiency of glass beads increase with SGV and frother concentration, as anticipated. As much as 97% glass beads are removed when favorable hydrodynamic conditions prevail.

Despite of its comparative hydrophobic nature, the results of glass beads compare favorablely with that of PAC. In fact, at the same frother concentration and SGV, removal efficiency of glass beads is better than that of PAC. The probably reason is that PAC is a strong absorbent and it can reduce effective local frother concentration in the column. Consequently, more frother is needed for PAC to achieve the same separation efficiency as glass beads.

These results clearly show that fine particles (less than 35 μm), even not naturally hydrophilic, can be removed effectively by the MSTLFLO process. Thus, it is fair to conclude that MSTLFLO column is very effective in removing suspended fine solid particles from water.

7.1.2 Phenol Removal

Based on the concept of adsorptive flotation, suspended adsorbent particles can be used to remove dissolved substances. The system chosen for this study consists of a dilute solution of phenol (40 mg/L) in the presence of 500 ppm PAC, which serve as the adsorbent for phenol removal. Experimental results of PAC and phenol removals are shown in Table 13.

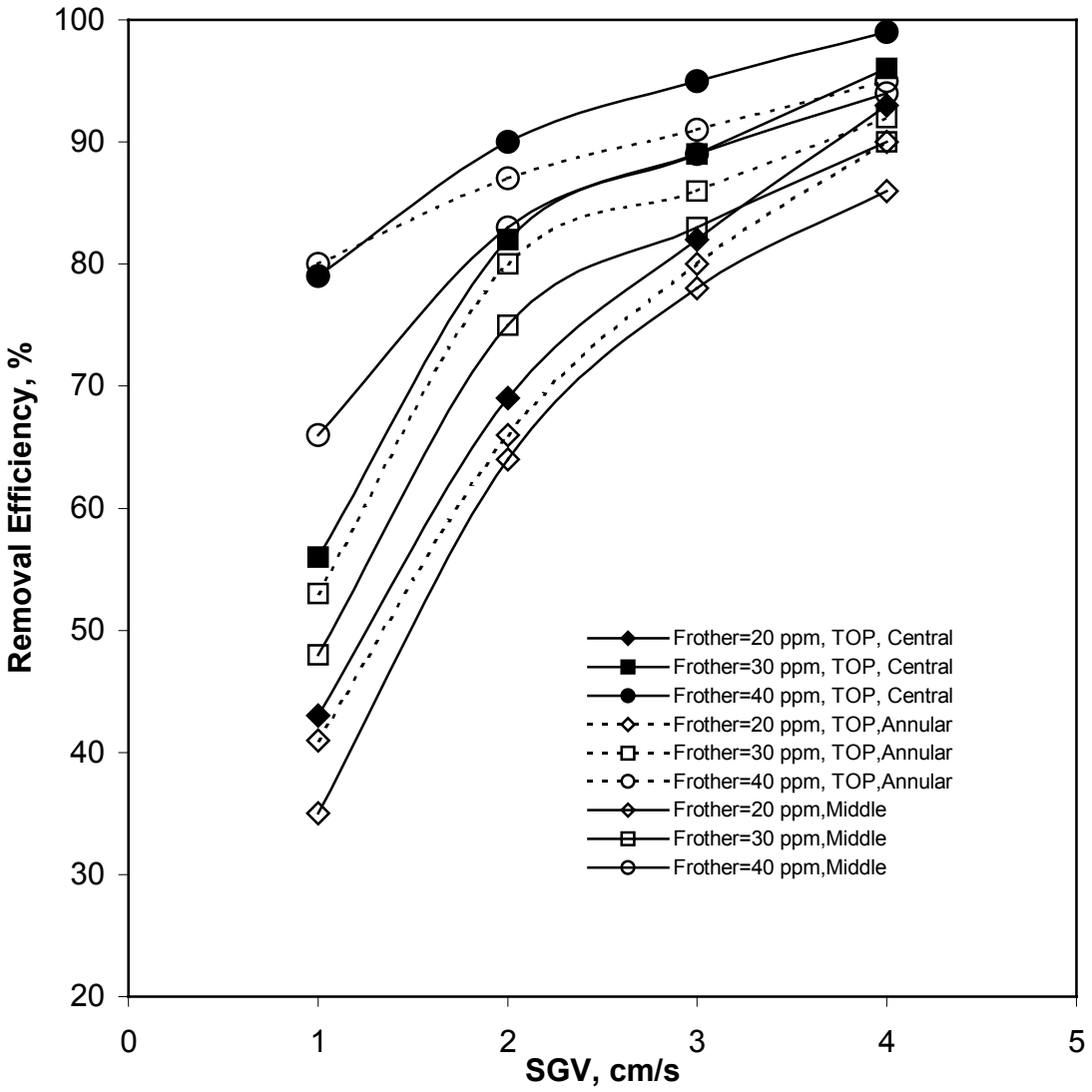

Figure 24 PAC Particles Removal Efficiency at Different Operating Conditions in 4-in Column

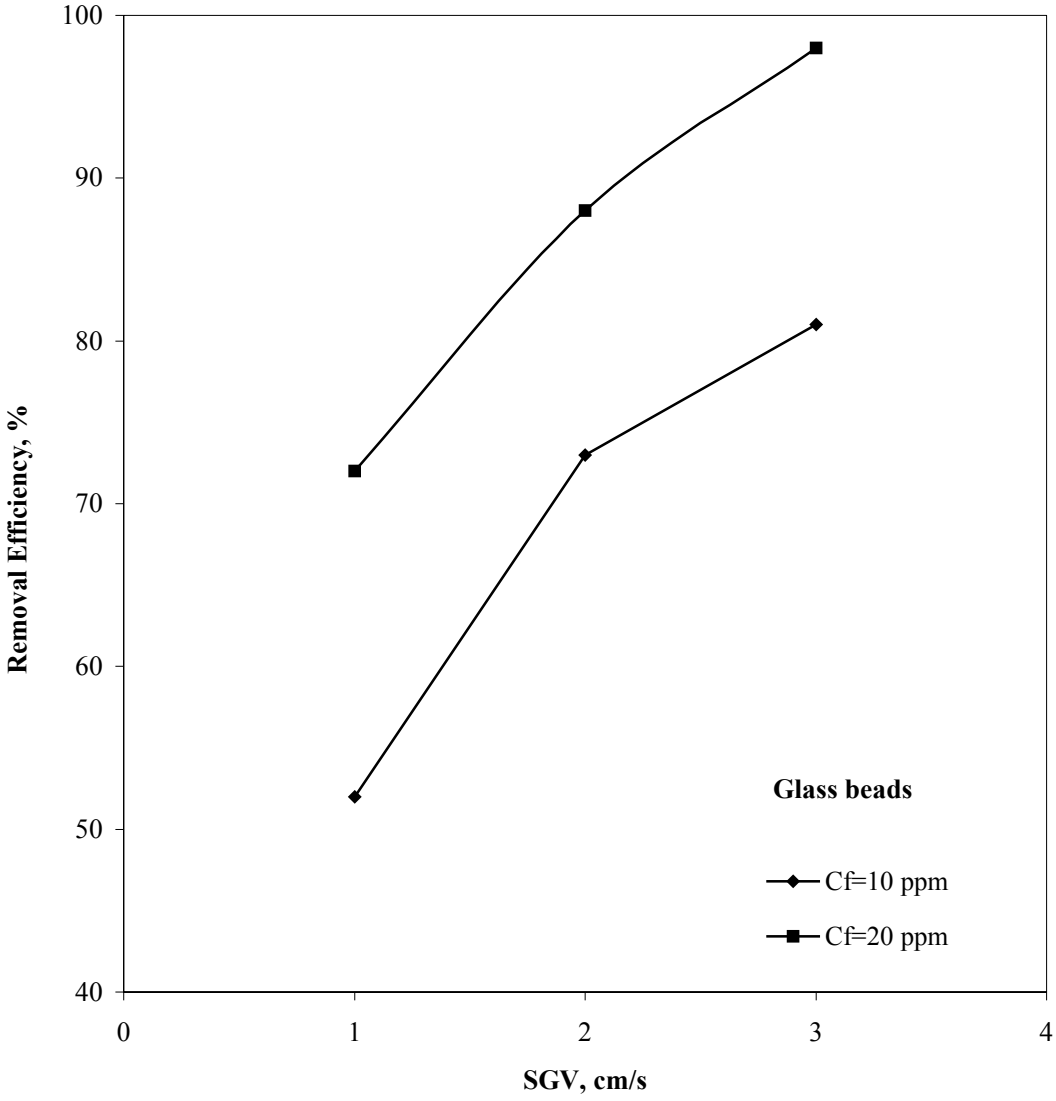

Figure 25 Removal of Glass Beads in 4-in Column

Table 13 Simultaneous Removal of PAC and Phenol

Frother, ppm	20		30	
SGV, cm/s	1.0	2.0	1.0	2.0
PAC removal efficiency, %	91	94	92	95
Phenol residue conc., mg/L	14.8	19.6	12.4	12.8
Relative phenol removal efficiency, %	80.6	65.3	88.3	87.0

The data show that PAC removal efficiencies are greater than 90%, while the residual concentrations of phenol are all less than 20 mg/L. Although the apparent removal of phenol is less than 50%, it should be noted that "relative" separation efficiency of phenol must be evaluated by considering the transient adsorption capacity of PAC. As indicated in Section 5.2.3, PAC adsorption capacity is only (62.5 mg phenol)/(g PAC) at a contact time of 30 minutes. Based on this value, "relative" removal efficiency of phenol can be calculated in terms of the ratio of adsorbed amount and PAC adsorption capacity in a 500 ppm suspension. Therefore, the "relative" removal efficiency of phenol is as high as 88%. Furthermore, consideration should also be given to the fact that the distribution of PAC is not uniform along the column. The very efficient removal of PAC implies that PAC particles tends to concentrate near the top of column while relatively small amount of PAC is present in the lower portion of column. This extremely uneven distribution of adsorbent particles can significantly reduce overall contact time between phenol and PAC particles. Therefore, the "relative" local adsorption efficiency would be much greater than overall efficiency indicated here. With a proper choice of operating conditions, the prospect of using an adsorptive flotation scheme for removing dissolved chemicals together with fine adsorbent particles from water is very promising.

7.1.3 Simultaneous Removal of Oil/Phenol/PAC

The excellent performance for suspended fine particles and PAC/phenol mixtures separations suggest the possibility of extending MSTLFLO applications to multi-component systems. To determine the effects of operating conditions on the overall removal efficiencies of oil, phenol and PAC, based on previous discussions, four key operating conditions are investigated. These include PAC feeding position, PAC concentration, SGV and frother concentration. The Box-Behnken design, a response surface method, provided by software MINITAB [68], is used to construct a set of non-sequential experiments for simultaneous removal of phenol/oil/PAC particles from wastewater. The design of experiments is shown in Table 14 and the selected operating conditions are listed in Table 15. There are 27 experiment conditions in total. The concentrations of emulsified oil and phenol in the feed are 500 ppm and 40 mg/L, respectively. Simulated wastewater feed rate is set at 1.0 L/min. Results are summarized in Table 16.

Data show that most of oil removal efficiencies are greater than 90%, which is primarily due to the hydrophobic nature of emulsified oil. Again, this result verifies the superior performance of MSTLFLO process in oil removal, even in the presence of other components.

As discussed earlier, the removal of PAC highly depends on operating conditions. So is the removal of phenol. The removal efficiency of PAC increases with frother concentration and SGV. For example, in Runs # 21 and 23 at 3.0 cm/s SGV, PAC removal efficiency increases from 91% to 96% when frother concentration increases from 20 ppm to 40 ppm. When 20 ppm frother is presented (see Runs # 18 and 20), PAC removal efficiency improves from 90% to 98% as SGV increases from 2.0 cm/s to 4.0 cm/s. The feed position of PAC also affects its removal significantly. When PAC is fed into middle stage, the removal efficiencies decrease to less than

80%. As high as 95% and 97% removal efficiency can be achieved when PAC particles are fed into the downcomer or the riser in the top stage, respectively.

Experiment results of simultaneous removal of emulsified oil, PAC particles and dissolved phenol are also illustrated in Figure 26 and Figure 27. Based on the concept of adsorptive flotation process discussed earlier, the removal of phenol depends on the local concentration of PAC in MSTLFLO column, which means that the removal of PAC tends to reduce the separation of phenol. As shown in Figure 25, within operating range, as much as 24 mg/L of phenol have been adsorbed by PAC with PAC removal efficiency up to 90%. When PAC removal efficiency increases beyond 92%, adsorbed phenol decreases to 21.4 mg/L of phenol is adsorbed. Similar results are also observed in Figure 26 for a frother concentration at

Table 14 Design of Experimental

		A1			A2			A3		
		C1	C2	C3	C1	C2	C3	C1	C2	C3
B1	D1					13				
	D2		1		21		23		2	
	D3					15				
B2	D1		17		5		6		18	
	D2	9		11		25,26,27		10		12
	D3		19		7		8		20	
B3	D1					14				
	D2		3		22		24		4	
	D3					16				

Table 15 Values of Operating Parameters

PAC feeding position		PAC conc., ppm		Frother conc., ppm		SGV, cm/s	
A1	Middle stage	B1	300	C1	20	D1	2.0
A2	Top stage, downcomer	B2	400	C2	30	D2	3.0
A3	Top stage, riser	B3	500	C3	40	D3	4.0

Table 16 Simultaneously Removal Efficiencies of Oil, PAC particles and Phenol

Run No.	Oil removal, %	PAC particles removal, %	Relative Phenol removal, %
1	90.9	78	49.3
2	93.1	92	48.6
3	90.2	85	80.9
4	93.7	90	64.5
5	90.0	82	75.4
6	91.3	84	76.1
7	90.1	89	61.6
8	94.4	95	57.9
9	86.7	76	52.3
10	92.3	92	54.3
11	92.1	80	53.7
12	93.3	96	54.0
13	90.6	89	50.1
14	91.4	81	85.3
15	93.5	94	51.0
16	93.2	92	77.1
17	90.1	76	54.3
18	91.1	90	55.1
19	93.5	80	53.6
20	94.5	97	55.5
21	90.3	91	53.0
22	91.2	80	78.9
23	94.1	95	51.9
24	94.5	90	80.5
25	92.6	83	73.5
26	92.0	83	74.2
27	91.1	84	74.3

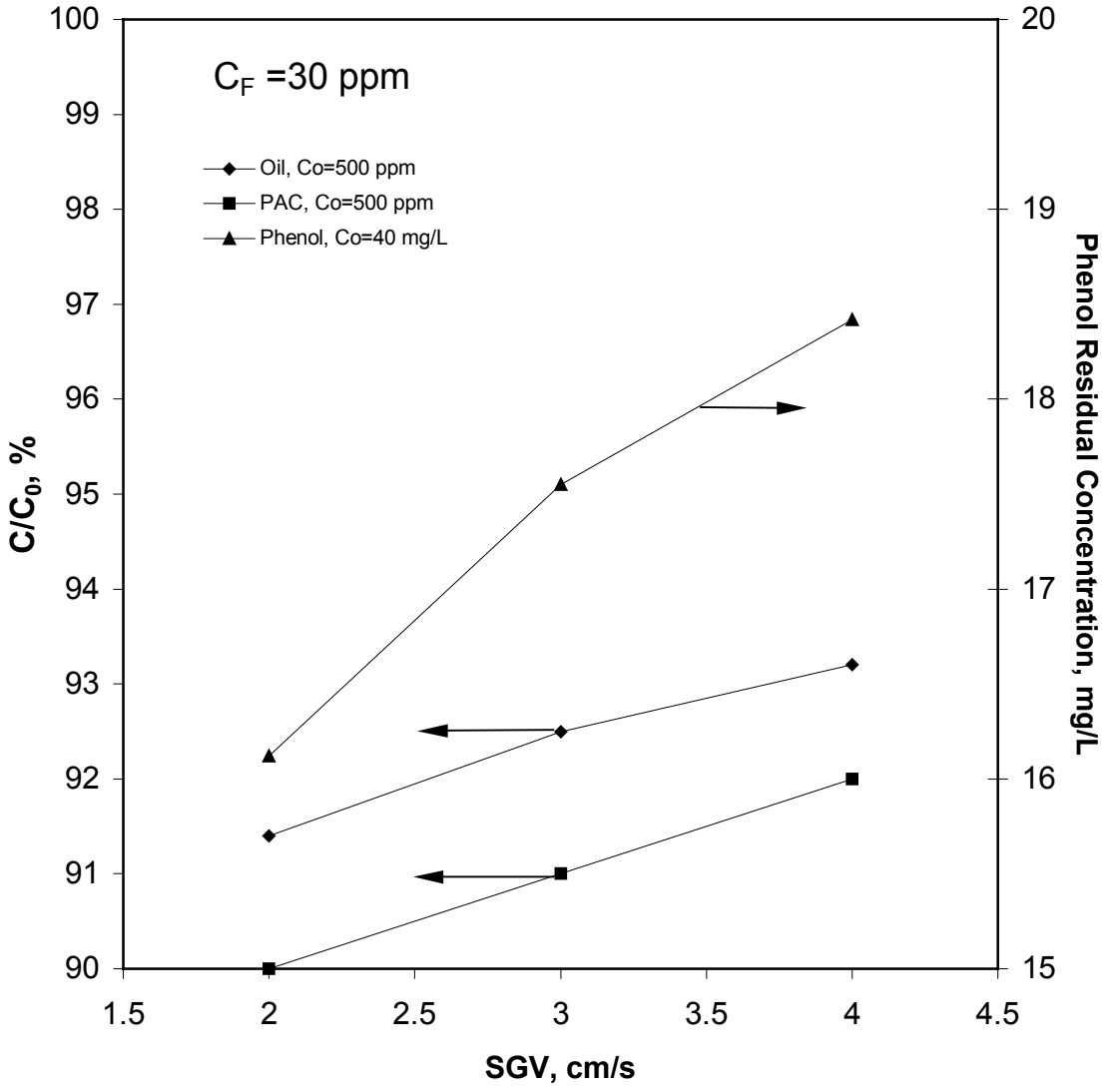

Figure 26 Oil/PAC/Phenol Removal in a 4-in Column at 30 ppm Frother

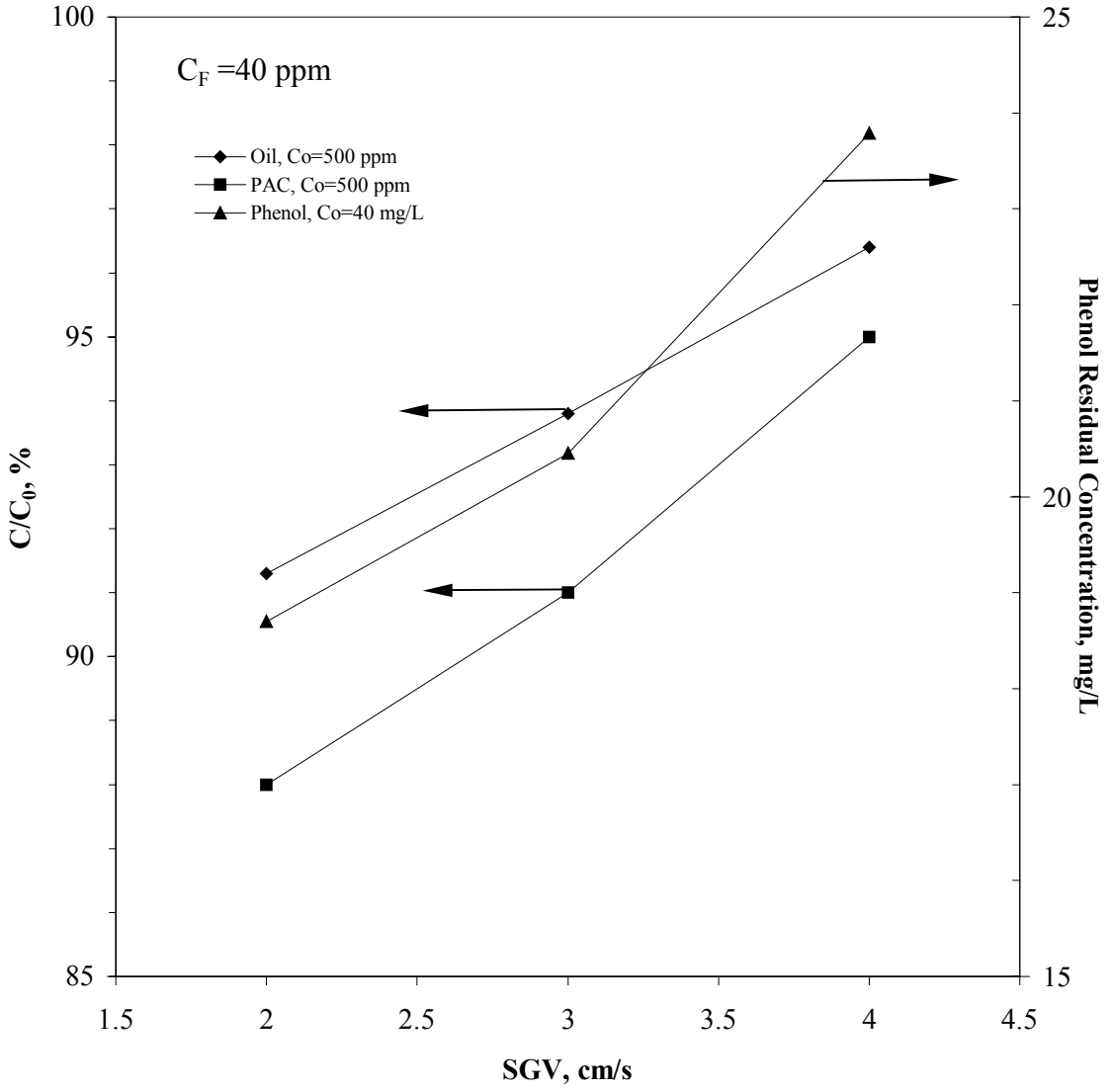

Figure 27 Oil/PAC/Phenol Removal in a 4-in Column at 40 ppm Frother

40 ppm. Comparing these results with that of PAC / phenol mixtures separation, much lower phenol removing efficiency is found. The primary reason is because the presence of oil decreased the PAC's absorptivity of phenol from water. Based on the value of PAC adsorption capacity, the highest relative phenol removal efficiency within the operating range is 77%. In addition, the unevenly distribution of PAC along the column could cause a reduction in overall removal efficiency for phenol, while the "relative" local adsorption efficiency would be much greater than the observed overall efficiency.

As shown in Figures 26 and 27, removal efficiencies of both oil and PAC are greater than 90% and increase with SGV as predicted. These findings are essentially the same as those discussed in the previous sections for single component separation. Both oil and PAC separations appear to be not effected by the presence of other components. Therefore, with properly chosen operating conditions as well as the type and quantity of adsorbent particles, the adsorptive flotation scheme for simultaneously removing dissolved chemicals from wastewater together with fine particles and emulsified oil is a viable operation. Consequently, MSTLFLO column is shown to be an effective one-step separation device for the treatment of wastewater containing mixed contaminants.

7.2 OIL REMOVAL USING A 12-IN COLUMN

The effectiveness and versatility of a 4-in MSTLFLO column are clearly demonstrated. To investigate the effectiveness of a scale up, oil removal experiments have been carried out in a 12-in column. The results of oil removal can also be used to indicate the capability of fluid/fluid and solid/fluid separations in a large scale MSTLFLO device.

Earlier hydrodynamics study has shown that the 12-in column can be operated in similar gas holdup ranges as a 4-in column. Based on these results, the following operating parameters are selected.

1) Frother concentrations: 20 and 30 ppm;
2) Initial oil concentration: 500 ppm;
3) SGV: 1.3, 2.1 and 2.6 cm/s. (due to the limitation of air supply in the laboratory)

The oil removal efficiency is plotted against SGV in Figure 28. In most cases, oil removal efficiency exceeds 90%. As discussed in Section 7.1.3, oil removal efficiency is found to increase with SGV and frother concentration. For example, oil removal efficiency exceeds 92% as SGV reaches 2.6 cm/s at 20 ppm frother. When 30 ppm of frother is applied, oil removal efficiency is greater than 93% at 2.6 cm/s SGV.

The rate of oil removal (kinetic) is also studied in 12-in column by conducting flotation experiments in a batch mode. The ratio of residual concentration to initial concentration(C/C_0) against flotation time is plotted in Figure 29. As expected, the values of C/C_0 can be reduced to less than 0.1 in most of experiments, resulting in removal efficiencies greater than 90%. Most oil removal operations can reach steady state condition in less than 15 minutes. The time required to reach steady state conditions depends on SGV and frother concentration. With high SGV and frother concentration, it requires less time to reach steady state. At 30 ppm frother and 2.6 cm/s SGV, it takes less than 10 minutes for the column to achieve steady state. While at 20 ppm frother and 1.3 cm/s SGV, the column does not reach steady state even after 30 minutes operation.

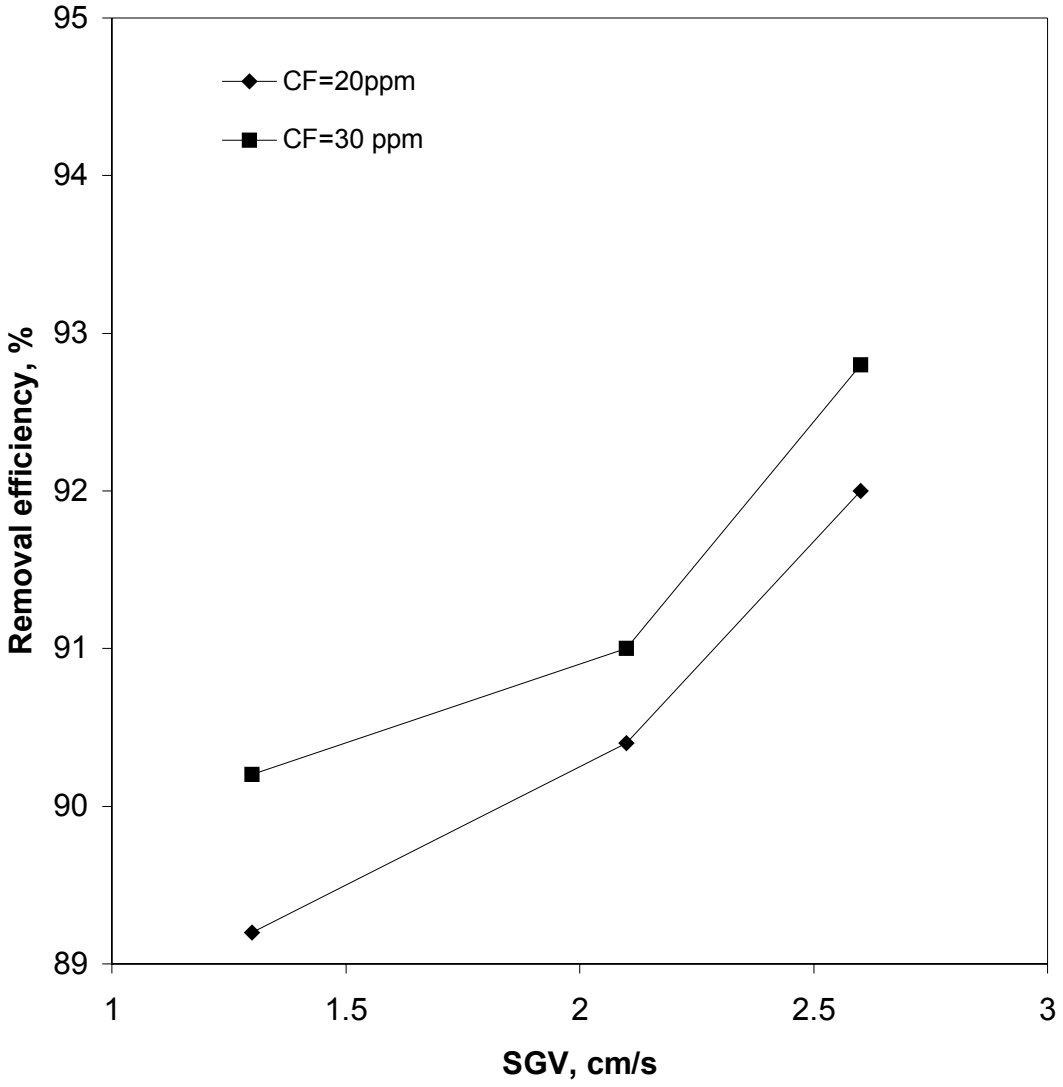

Figure 28 Oil Removal Efficiency in 12-in Column

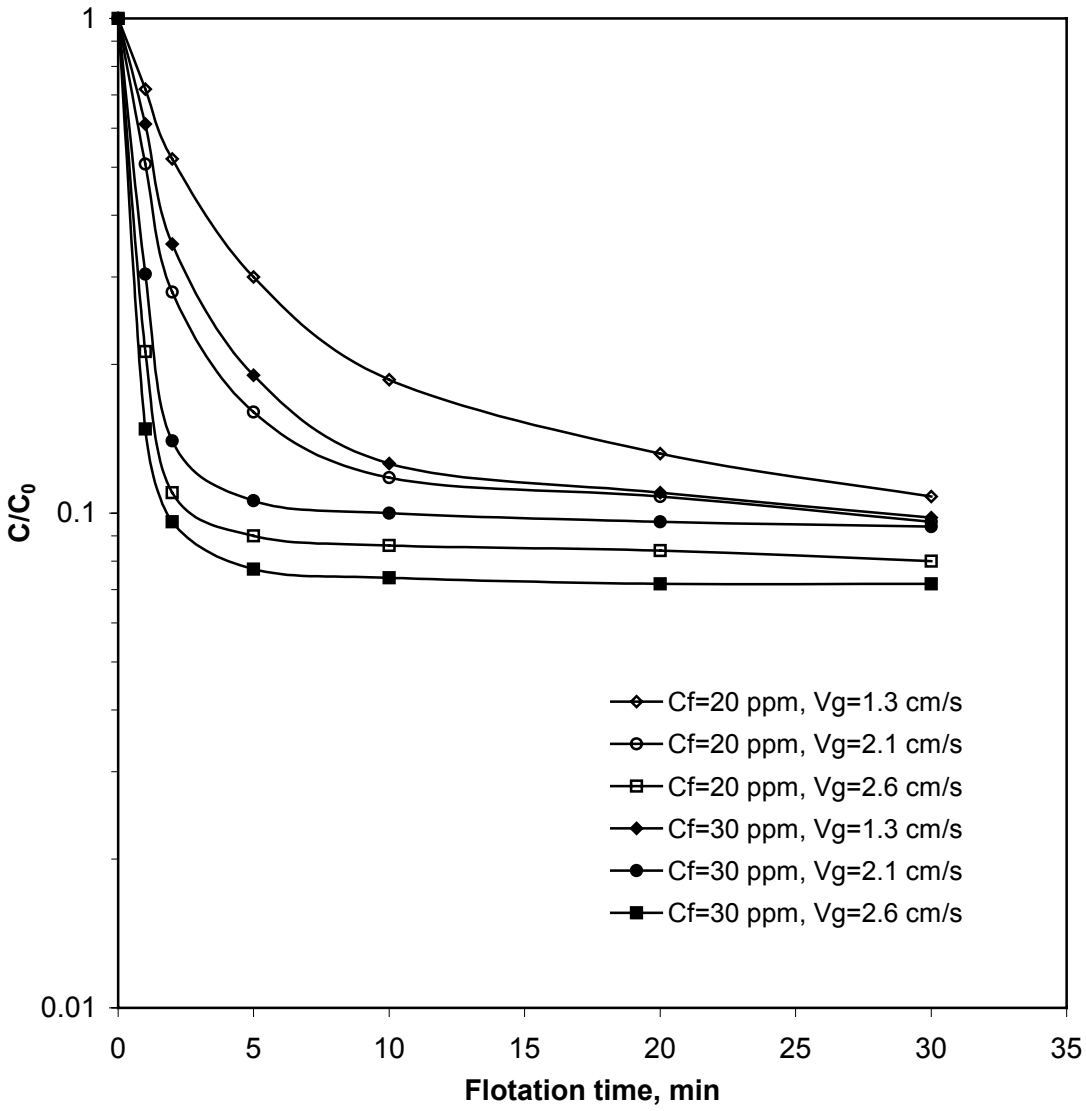

Figure 29 Oil Removal in the 12-in Column

Comparing with results in 4-in column, oil removal efficiency is slightly lower. This is primarily due to the low SGV used because of limitation of gas supply in the laboratory. Overall, the experimental results further confirm the superior oil removal efficiency of the MSTLFLO process as well as the validity of scale-up from 4-in to 12-in column.

8.0 KINETIC MODEL IN MSTLFLO COLUMN

As reported in the previous study[6, 32, 36, 69], a non-linear kinetic model has been successfully applied to the rate of oil removal in the 4-in MSTLFLO column. In this section, the same kinetic model is to be tested for both fine particle removal in the 4-in column and oil removal in the 12-in column. The experimentally determined kinetic constants are analyzed in terms of operating variables. The results are used to establish a generalized kinetic constant correlation for subsequent process modeling.

8.1 NONLINEAR KINETIC MODEL

As discussed earlier, Lai[70] proposed a "proportionality law" to describe the kinetics of column flotation, in which flotation rate is expressed as a function of both concentration and flotation time as follows,

$$-\frac{dC}{dt} = K\frac{C - C_{\infty}}{t} \tag{13}$$

where K is kinetic constant; t is flotation time; and C and C_{∞} are residual and asymptote concentrations in treated water, respectively. C_{∞} can be derived from experiments empirically for different conditions. Upon integration, Equation (14) is obtained:

$$\log \frac{1}{C - C_{\infty}} = K \log t + \log a \qquad (14)$$

where a is an integration constant.

8.1.1 Fine Particles Removal

For the separation of solid particle in the 4-in MSTLFLO column, Equation (14) is expressed as:

$$\log \frac{1}{C_p - C_{p,\infty}} = K_p \log t + const. \qquad (15)$$

where C_p and $C_{p,\infty}$ are concentration and asymptote concentration of fine particles, respectively; K_p is the kinetic constant of particle separation; and t is flotation time.

To obtain kinetic constants for PAC and glass beads separations in the 4-in MSTLFLO column, $1/(C-C_{\infty})$ is plotted against flotation time, t, in logarithmic scale, as shown in Figures 30 and 31. In these figures, solid symbols designate experimental data and straight lines represent the calculated results. Straight lines fit experimental data very well, which validate Equation (13) as the rate expression for fine particle flotation in MSTLFLO column. Kinetic constants are determined from the slope of each line. The determination coefficient, R^2, which quantify the accuracy of regression model, is also calculated for each case. In general, a correlation is regarded as accurate when R^2 is greater than 0.90. A summary of kinetic constants, K_p, and corresponding R^2 are shown in Table 17. The values of R^2 are all greater than 98%, indicating the robustness of the rate expression for fine particle removal.

Table 17 Kinetic Constants for Removal of Fine Particles

Fine particles	Frother conc., ppm	SGV, cm/s	K_p	R^2
PAC	20	1.0	0.649	0.997
		2.0	0.840	0.999
		3.0	0.941	0.999
		4.0	1.103	0.994
Glass Beads	10	1.0	0.882	0.997
		3.0	1.053	0.993
	20	1.0	1.207	0.985
		3.0	1.249	0.982

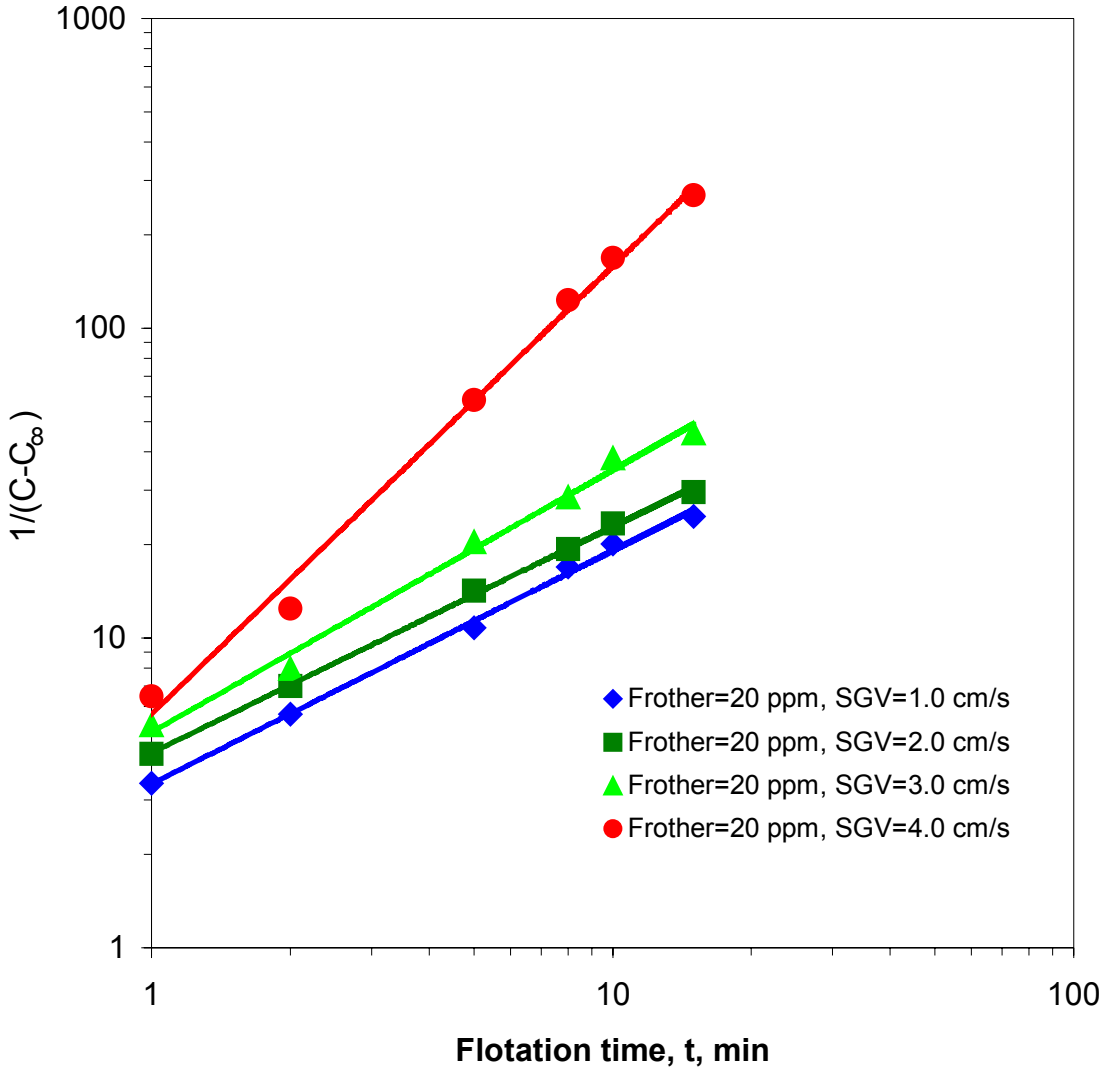

Figure 30 Kinetic Constants for the PAC Removal in 4-in Column

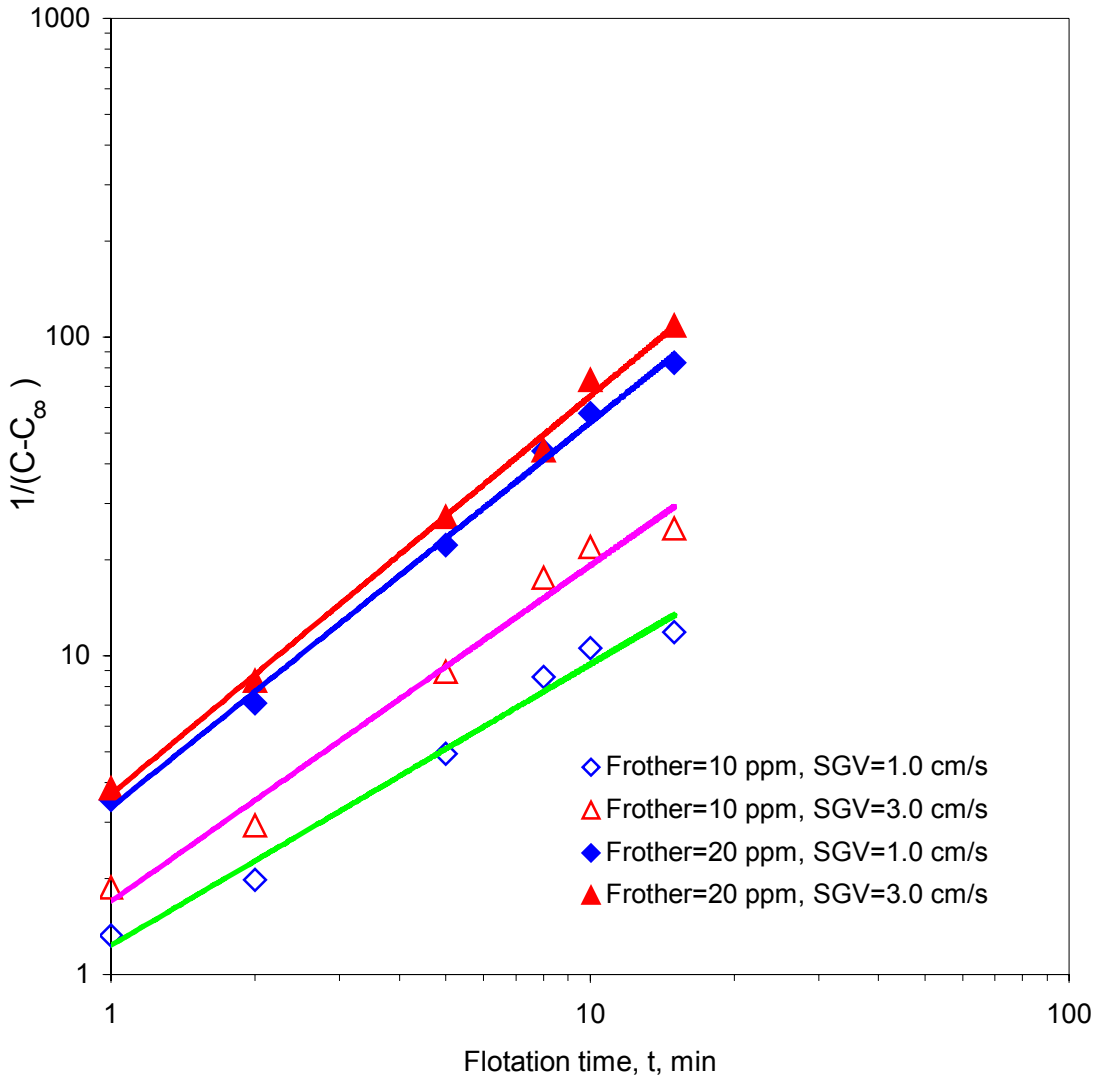

Figure 31 Kinetic Constants for the Glass Beads Removal in 4-in Column

From Table 17, it can be seen that kinetic constants increase with SGV and frother concentration. When SGV increases from 1.0 cm/s to 4.0 cm/s in PAC separations, the values of kinetic constant increases from 0.649 to 1.103, which means that the rates of solid separation are almost doubled. This result indicates that at high SGV, not only a better mixing environment is provided but also a faster separation process is achieved. Same conclusion can be drawn from the experimental data of glass beads separations (see Table 17 and Figure 31).

Due to the adsorption feature of PAC, glass beads are also used to investigate frother's influence on the kinetics of particle separation in MSTLFLO column. As indicated in Table 17, a high frother concentration and large SGV can accelerate fine solids separation.

8.1.2 Oil Removal in 12-in MSTLFLO Column

Similar to particle separations, oil separation kinetics has also been correlated using Equation (13). In Figure 32, $1/(C_{oil}-C_{oil,\infty})$ is plotted versus flotation time in a logarithmic scale. Experiment data (represented by solid symbols) under different operating conditions all fall along straight lines, which confirm the validity of the kinetic expression, Equation (13). As mentioned before, the values of kinetic constants are determined from the slope of each line.

Kinetic constants in 12-in column for oil removal, $K_{oil,12}$, are listed in Table 18. The values of determination coefficient, R^2, are all greater than 98%, which further validate the kinetic expression, Equation (13), for oil removal in the MSTLFLO column.

Table 18 A Summary of Kinetic Constants For Oil Separations in 12-in Column

Frother conc., ppm	SGV, cm/s	$K_{oil,\ 12}$	R^2
20	1.3	0.66	0.997
	2.1	1.25	0.996
	2.6	2.24	0.991
30	1.3	0.91	0.985
	2.1	1.35	0.992
	2.6	2.30	0.987

From Table 18, it can be seen that kinetic constants change with SGV and frother concentration. When SGV is doubled from 1.3 cm/s to 2.6 cm/s at 20 ppm frother, the values of kinetic constants increase from 0.66 to 2.24, which means the rates of oil separation are more than tripled. As discussed earlier, at high SGV, the MSTLFLO column not only provides a better mixing environment but also offers a faster oil separation. The influence of frother on kinetics of oil separation is also investigated. Similar conclusion can be drawn from the experimental data: i.e., a higher frother concentration tends to accelerate the oil separation in a MSTLFLO column.

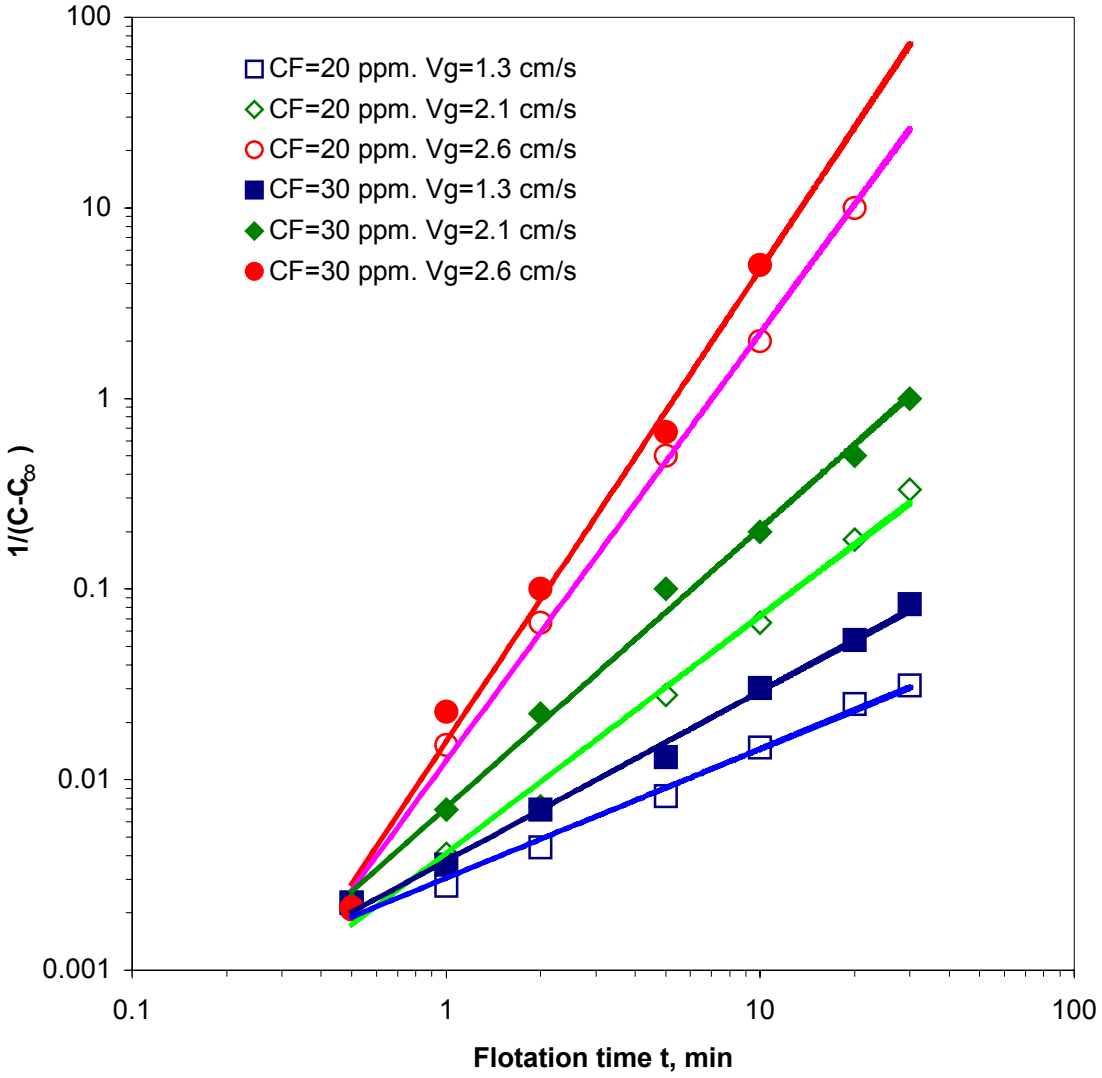

Figure 32 Kinetic Constants of Oil Removal in 12-in Column

8.2 GAS HOLDUP MODEL

As indicated earlier, gas holdup is a critical hydrodynamic parameter in the MSTLFLO process. Couvert reported [62] that in a bubble column with internal baffles, gas holdup in riser, ε_{gr}, was a function of SGV and (A_d/A_r), the area ratio of riser to downcomer. In this study, the value of (A_d/A_r) is fixed close to unity in both 4-in and 12-in columns. Therefore, the effect of column geometry is not considered. On the other hand, frother plays a very important role in maintaining high gas holdup. Hence, frother concentration must be included in the correlation of gas holdup. Consequently, an empirical expression for gas holdups in terms of frother concentration and SGV is suggested as follows:

$$\varepsilon_{gr\ B,M,T} = a \cdot V_{gr}^{\ b} \cdot \left(\frac{1 + C_f}{1 - C_f} \right)^c \qquad (16)$$

where, *a, b, c* are empirical constants; $\varepsilon_{gr\ B,M,T}$ are gas holdup in the bottom, middle and top stages, respectively; V_{gr} is SGV; and C_f is frother concentration.

The STATISTICA software [71] is applied to evaluate the empirical constants, *a, b, c,* respectively. An implicit non-lineal numerical method, Quasi-Newton method, is used as regression method. Initial values and step sizes are automatically allocated by the software. In this regression, second-order (partial) derivatives of the loss function are used to determine iteration steps. Convergence is achieved when the difference between consecutive iteration calculations is less than a preset criterion. The differences between experimental data and corresponding calculated results, or residual value (R), indicate the reliability of correlation. Small and randomly distributed residual values are desired for a valid regression. Therefore, determination coefficient, R^2, is used to quantify the accuracy of regression. As mentioned earlier, in general, a correlation is regarded as accurate when R^2 is greater than 0.90.

Estimated results based on the proposed correlation are plotted at different operating conditions and compared with experimental data, as shown in Figures 33, 35 and 37. Corresponding residual values are illustrated in Figures 34, 36 and 38. In Figure 33, circle solid symbols represent experimental data while lattice stands for regression results. Regression results match experiment data very well. As expected, calculated gas holdups increase with frother concentration and SGV. In addition, Figure 34 shows that residual values are randomly distributed close to zero, within the tolerance of ±0.04. Thus, Equation (15) provides a good correlation for gas holdup in the bottom stage. From Figures 35 and 36, similar conclusion can be drawn for gas holdup in the middle stage: Regressed results match experimental data well. Randomly distributed residual values are found and deviations values are all within ±0.04. However, as shown in Figures 37 and 38, the correlation of gas holdups in the top stage does not fit experimental data well at high SGV, primarily due to unstable pressure drops. Figure 38 shows that residual values are randomly distributed within the tolerance of ±0.12. If the two data points associated with high SGV (SGV = 3.9 cm/s) are excluded, the residual values for all remaining data fall randomly within the tolerance of ±0.05. Therefore, under this circumstance, Equation (15) provides a good correlation for gas holdup in all three stages.

Empirical correlation constants and corresponding determination coefficients (R^2) for gas holdup correlations are summarized in Table 19.

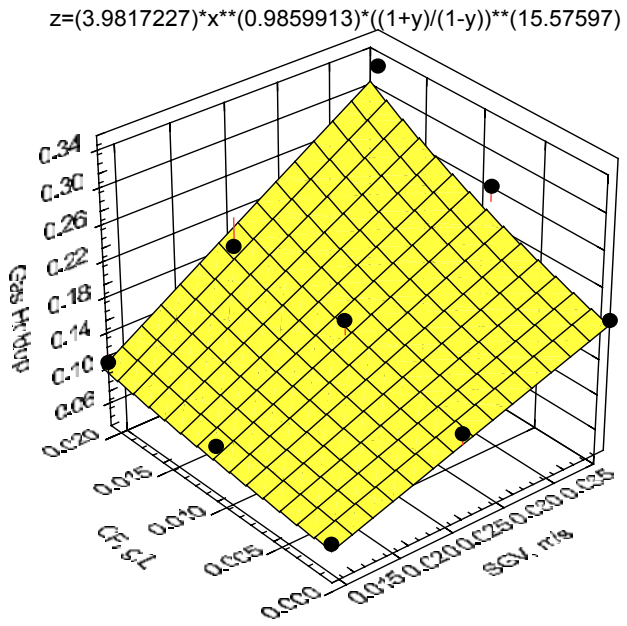

Figure 33 3-D Gas Holdup Profile in the Riser of Bottom Stage (observed vs. estimated)

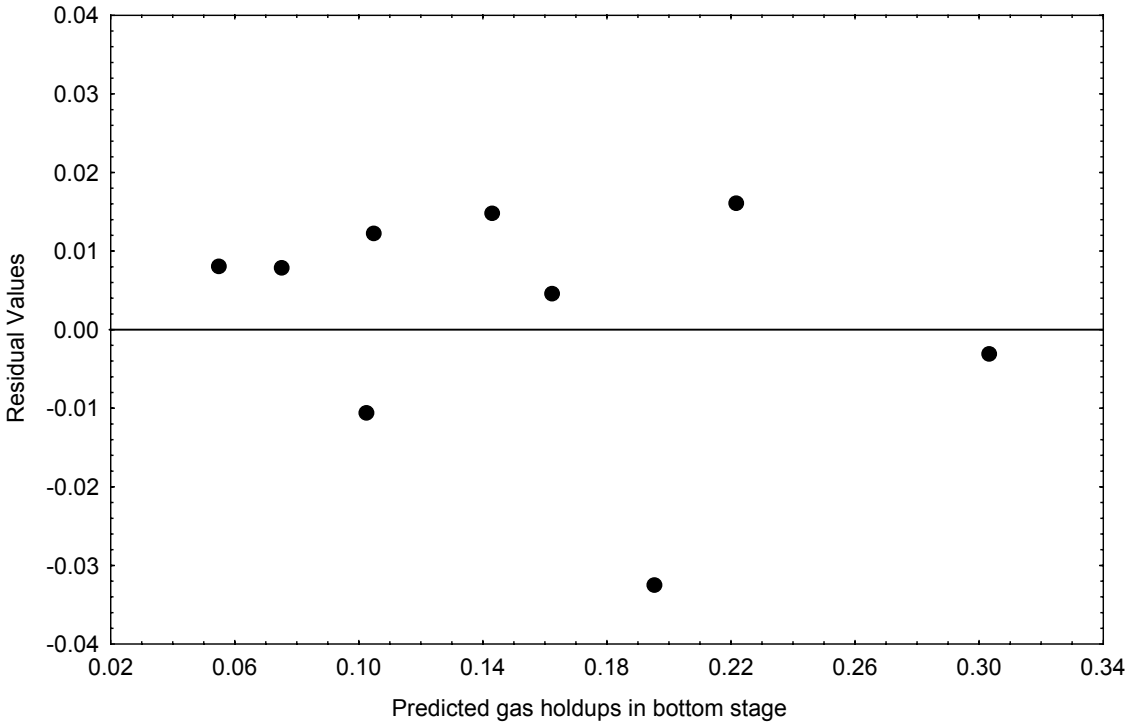

Figure 34 Relationship between Residual Values and Estimated Gas Holdups

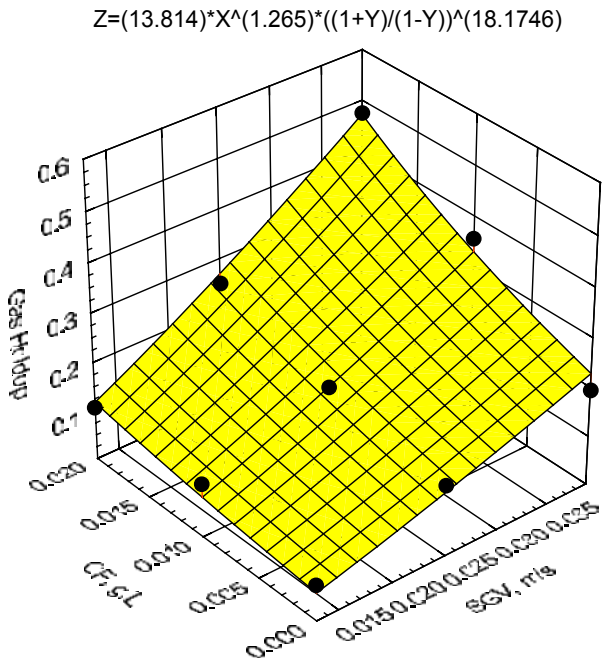

Figure 35 3-D Gas Holdup Profile in the Riser of Middle Stage(observed vs. estimated)

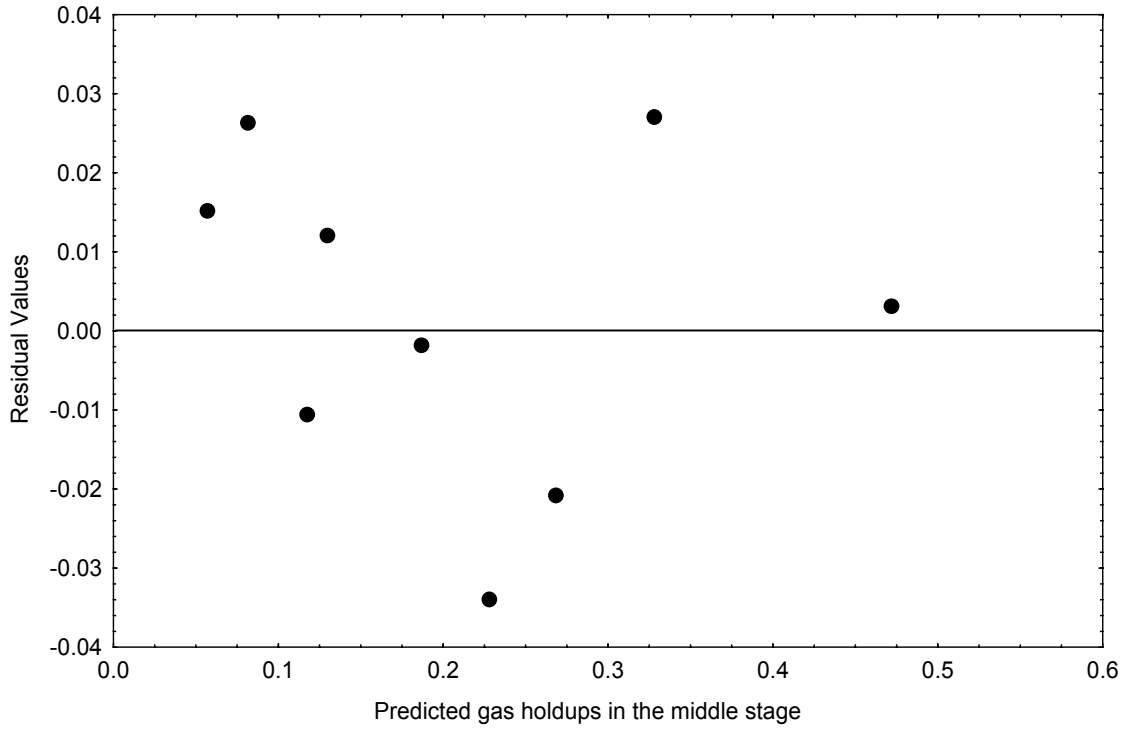

Figure 36 Relationship between Residual Values and Estimated Gas Holdups

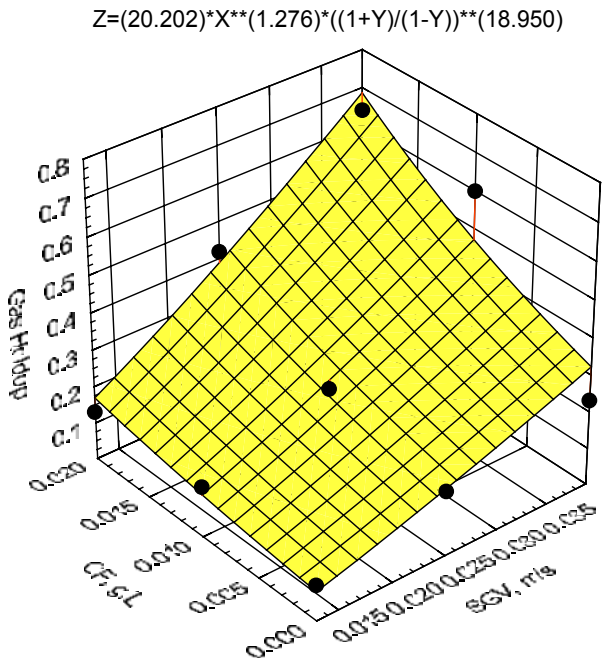

Figure 37 3-D Gas Holdup Profile in the Riser of Top Stage(observed vs. estimated)

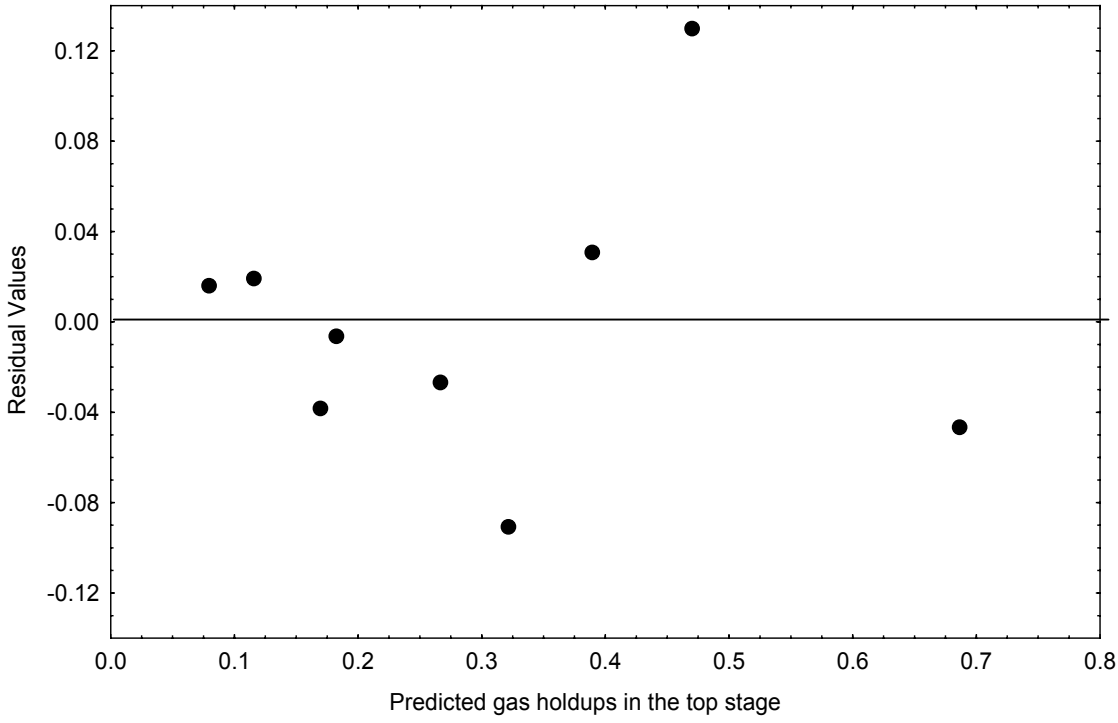

Figure 38 Relationship between Residual Values and Estimated Gas Holdups

Table 19 Empirical Constants for Gas Holdups Correlations in the Riser of Each Stage

Stage	*a*	*b*	*c*	*b/c*	R^2
Bottom	3.98	0.99	15.6	15.7	0.98
Middle	13.8	1.27	18.2	14.3	0.97
Top	20.2	1.28	18.9	14.8	0.91

Table 19 shows that the values of R^2 are all greater than 0.90, which indicates that Equation (15) and experimental data are in good agreements and this correlation of gas holdup has been successfully established. As specified in Equation (15), empirical constants *b* and *c* are associated with the effects of SGV and frother concentration on gas holdups, respectively. Since the numerical value of *c* is much greater than *b*, frother concentration plays a more prominent role than SGV in gas holdup generation. This conclusion has also been mentioned in previous discussions. An examination of the ratio of *b* to *c* shows that the values of (*b/c*) falls in a narrow range between 14 and 16. This indicates that the effects of hydrodynamic conditions to gas holdup in all three stages are approximately equal. In other word, the flow patterns in all three stages are comparable.

8.3 KINETIC CORRELATIONS FOR FINE PARTICLE SEPARATION IN 4-IN MSTLFLO COLUMN

To establish relations between the value of K_p and selected operating variables, five different empirical correlations have been tested for both PAC and glass beads separations (see Appendix D). Two regression methods, quasi-Newton and Hooke-Jeeves pattern methods, are

used to determine empirical constants involved in these correlations. Based on the value of determination coefficient (R^2), the following two correlations are selected

$$K_p = \frac{a\varepsilon_g^b}{d_b^e} \tag{17}$$

$$K_p = \frac{aV_g^d}{d_b^e} \tag{18}$$

where, ε_g is gas holdup; V_g is superficial gas velocity (SGV); d_b is bubble size; and a, b, d and e are empirical constants, associating with the correlation variables in each model. The effects of correlation variables on kinetic constant are discussed below.

Equations (16) and (17) indicate that the kinetic constant is positively correlated to either gas holdup (ε_g) or SGV (V_g), and inversely related to bubble size (d_b). The empirical constants, b, d and e for above expressions are summarized in Table 20 and 21. Their values indicate the relative importance of corresponding variables to kinetic constant, K_p. The results show that the values of these empirical constants follow the order of: $e >> b, d$. Since e (the exponent for bubble size, d_p) is the largest among three constants, bubble size plays a more important role in controlling the rate of fine particle removal than the gas holdup and SGV, which link to b and d, respectively. Gas holdup and SGV have similar degree of influence on K_p since values of b and d are approximately equal to each other. In all cases, the values of R^2 are greater than 0.98, which confirms the accuracy of two proposed correlations. In addition, these empirical constants obtained by two different regression methods are nearly identical, which implies that both correlations are independent of regression methods.

From the above discussions, it is fair to conclude that both correlations fit experiment data very well. However, since in previous kinetic study [69] the gas holdup and bubble size are used for correlating the kinetic constant for oil removal, Equation (17) will be adopted for the

fine particle separation in the 4-in column. This correlation will also be included in the discussions of subsequent kinetics study of oil removal in the 12-in MSTLFLO column.

Table 20 Regressed Empirical Constants of Kinetic Correlations for PAC Particles Removal

Model	Regression method*	PAC				
		a	*b*	*d*	*e*	R^2
$K_p = \frac{a\varepsilon_g^b}{d_b^e}$	H-J	0.808	0.210	--	3.60	0.999
	Q-N	0.810	0.209	--	3.63	0.999
$K_p = \frac{aV_g^d}{d_b^e}$	H-J	1.43	--	0.213	3.79	0.999
	Q-N	1.43	--	0.213	3.79	0.999

* Q-N: quasi-Newton; H-J: Hooke-Jeeves pattern method

Table 21 Regressed Empirical Constants of Kinetic Correlations for Glass Beads Removal

Model	Regression method*	Glass beads				
		a	*b*	*d*	*e*	R^2
$K_p = \frac{a\varepsilon_g^b}{d_b^e}$	H-J	1.10	0.075	--	0.766	0.980
	Q-N	1.11	0.075	--	0.766	0.980
$K_p = \frac{aV_g^d}{d_b^e}$	H-J	1.35	--	0.08	0.79	0.999
	Q-N	1.35	--	0.08	0.79	0.999

* Q-N: quasi-Newton; H-J: Hooke-Jeeves pattern method

8.4 KINETIC CORRELATIONS FOR OIL SEPARATION IN 12-IN MSTLFLO COLUMN

To study the relationship between oil removal kinetic constant, K_{oil}, and correlation variables, two different correlations are suggested. The first correlation is expressed as:

$$K_{oil,i} = \frac{a\varepsilon_g^b Q_L^c}{d_b^d},\ i = 4,\ 12 \qquad (19)$$

where, $K_{oil,\ 4}$ and $K_{oil,\ 12}$ are kinetic constants for oil removal in the 4-in and 12-in column, respectively. The exponents, b, c and d are empirical constants associated with gas holdup (ε_g), bubble diameter (d_b), and liquid flow rate (Q_L), respectively. The second correlation is Equation (17), which has been successfully applied to fine particle separation. In Equation (17), only gas holdup (ε_g) and bubble diameter (d_b) are included.

Again, software STATISTICA is used for the evaluation of empirical constants and the same regression methods as fine particle separation correlations are employed. The correlation results of oil removal in 4-in column, $K_{oil,\ 4}$,[38] are also shown in Table 22 together with that of 12-in column.

Table 22 A Summary of Empirical Constants For Oil Separation Kinetic Constants

Model	Regression method	a	b	c	d	R^2
$K_{oil,12} = \frac{a\varepsilon_g^b Q_L^c}{d_b^d}$	H-J	0.199	0.662	0.390	1.700	0.988
	Q-N	0.191	0.664	0.351	1.601	0.988
$K_{oil,12} = \frac{a\varepsilon_g^b}{d_b^d}$	H-J	0.129	0.659	--	1.043	0.988
	Q-N	0.129	0.659	--	1.043	0.988
$K_{oil,4} = \frac{a\varepsilon_g^b Q_L^c}{d_b^d}$	--	1.003	0.602	0.519	1.150	>0.95
$K_{oil,4} = \frac{a\varepsilon_g^b}{d_b^d}$	Q-N	25.96	1.078	--	7.198	0.987
	H-J	25.95	1.078	--	7.196	0.987

It can be seen in Table 22 that correlations for oil separation in both 12-in and 4-in columns are of high accuracy, with all R^2 values greater than 0.98. The variations between different regression methods are very small, especially when a simple two-variable correlation is applied. Therefore, as expected, correlations for oil removal in 12-in MSTLFLO column are independent from regression methods. It is also found that in the three-variable correlation (Equation (19)), kinetic constant, $K_{oil,\ 12}$, increases with gas holdup and liquid volumetric flow rate but decreases with bubble diameter. Among the three variables, bubble size has much bigger influence on oil removal rate than gas holdup and liquid volumetric flow rate ($d>b>c$). Similarly, the results show that the order of $d >> b$ is the same as in the two-variable correlation (Equation (17)). Again, these findings indicate that bubble size is the most critical operating variable for the oil removal rate in MSTLFLO column.

Same conclusion has been previously reported[69] regarding these two correlations for oil removal in the 4-in column. As shown in Table 22, both two-variable and three-variable correlations are of high accuracy (R^2 >0.95) and are also independent from regression methods. A comparison between two correlations shows that the liquid circulation velocity is the least important factor on oil removal rate. Furthermore, it is not a directly measured operating parameter. With the same regression accuracy, two-variable correlation is simpler and easier to use in practice. Therefore, the two-variable correlation, i.e. Equation (17), is chosen as the kinetic constant correlation for subsequent process modeling.

9.0 PROCESS SIMULATION IN MSTLFLO COLUMN

A classic tank-in-series model has been successfully applied to the oily water treatment in the 4-in MSTLFLO column [6]. This model will be used here for the process simulations of solid particle removal and simultaneous oil/solid particle removal in the 4-in column as well as oil removal in the 12-in column. A detailed description of such a model is given in Appendix E.

When the tank-in-series model combined with a non-linear kinetic model (Equation (12)) is applied to a three-stage MSTLFLO column, a set of non-linear first order differential equations results,

$$\frac{dC_T}{dt} = \frac{F}{V_T(1-\varepsilon_T)}(C_0 - C_T) - K_T \frac{C_T - C_{T,\infty}}{t_t} + K_M \frac{C_M - C_{T,\infty}}{t_M}, \qquad \text{(Top stage)} \quad (20\text{ a})$$

$$\frac{dC_M}{dt} = \frac{F}{V_M(1-\varepsilon_M)}(C_T - C_M) - K_M \frac{C_M - C_{M,\infty}}{t_M} + K_B \frac{C_B - C_{B,\infty}}{t_B}, \qquad \text{(Middle stage)} \quad (20\text{ b})$$

$$\frac{dC_B}{dt} = \frac{F}{V_B(1-\varepsilon_B)}(C_M - C_B) - K_B \frac{C_B - C_{B,\infty}}{t_B}, \qquad \text{(Bottom stage)} \quad (20\text{ c})$$

where V_i, K_i, ε_i and $C_{i,\infty}$ are volume, kinetic constant, gas holdup and asymptotic concentration of stage i (i = T, M, B), respectively; F is feed rate; C_0 is the initial concentration; and t is corresponding flotation time. The subscriptions, T, M and B designate top, middle and bottom stages, respectively. A procedure for solving this set of equations is illustrated in Figure 39, where kinetic constant correlation in terms of hydrodynamic parameters, i.e. ε_i, and d_{32}, and

column operating conditions, as inputs. The numerical solutions of these equations are obtained using a Fortran program (see Appendix F).

9.1 PROCESS MODELING FOR SOLID SEPARATION IN 4-IN MSTLFLO COLUMN

Numerical simulations are carried out for both batch operations and continuous operations of solid particles separations in the three-stage 4-in MSTLFLO column.

For batch operation, in avoiding the computational problem caused by logarithmic value at $t = 0$, the following "shifted" initial and boundary conditions are applied:

$$i.c.: t = \sqrt[k]{\frac{1}{a(C - C_\infty)}},\ C_T = C_M = C_B = 100 \tag{21}$$

$$b.c.: t = \infty,\ \frac{dC_i}{dt} < \lambda, i = T, M, B \tag{22}$$

where a and k are empirical constants. λ is a preset criteria at a very small value. As defined in the *b.c.*, when dC_i/dt is smaller than λ, which means the steady state condition is achieved and the simulation program will be terminated.

At the beginning, column is filled with water containing 100 ppm fine particles (C_0 = 100). Concentration in the bottom stage (C_B) represents solid concentration in treated water. Particle removal efficiency is defined as the value of $(C_0 - C_B)/C_0$. Experimental data show that the operation of solid particle separations in the 4-in column reaches the steady state condition in a relatively short time. Therefore, simulation cuts-off time of batch operations is set at 15 minutes or as the boundary condition, Equation (22) is satisfied.

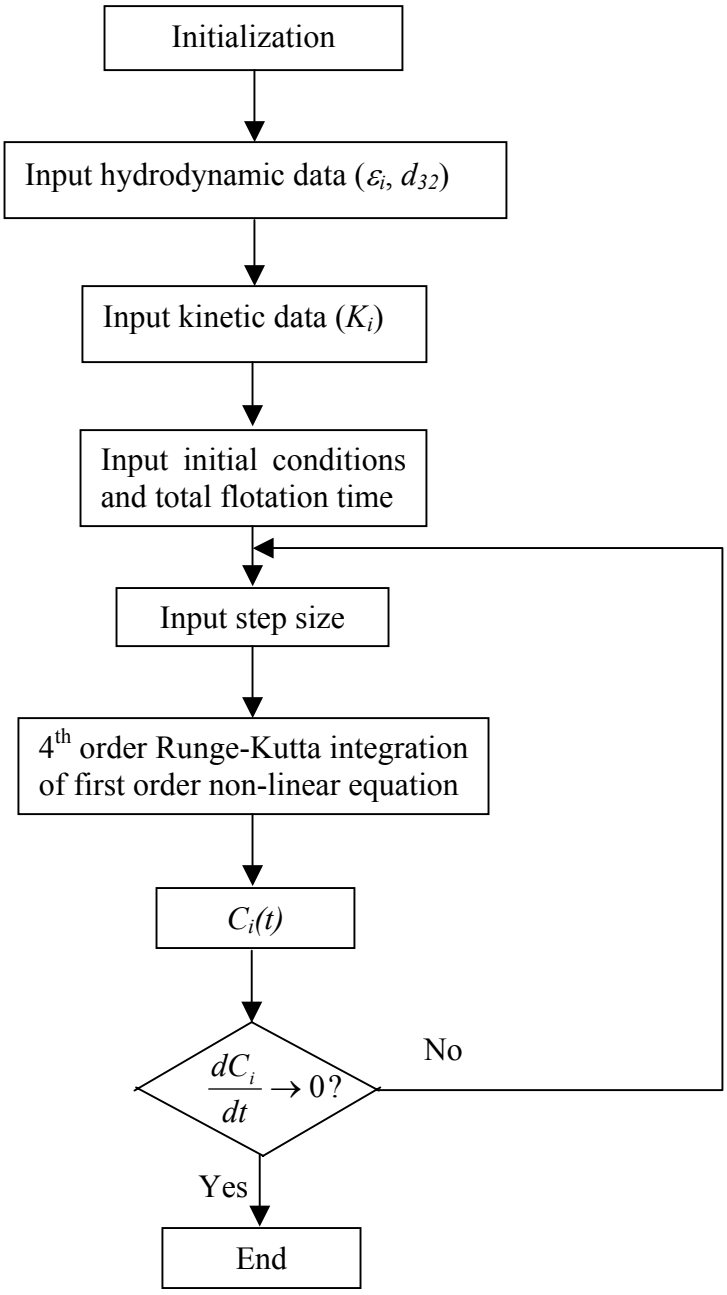

Figure 39 Flowchart of Solving MSTLFLO Process Model

Selected PAC and glass beads removal simulations together with experimental results are plotted in Figures 40 - 42. Solid symbols represent experimental data while curves stand for simulations of particle concentrations vs. time in different stages. The simulated curves agree with experiment measurements very well for both PAC and glass beads. It is shown in these Figures that the particle concentration decreases along with flotation time. At the end of 15 minutes, it approaches closely the steady state condition.

In Figures 41-42, it is found that high SGV not only improves removal efficiency but also enhances separation rate, which has previously been reported by Gu for oily water treatment [6].

For continuous operation simulations, for the same reason as the batch operation simulation at the start point, the "shifted" initial conditions are applied:

$$i.c.: t = \sqrt[k]{\frac{1}{a(C - C_\infty)}},\ C_T = C_M = C_B = 0 \text{ or } 100 \qquad (23)$$

where, a and k are empirical constants. The condition, $c = 0$ or 100, represents the case that the column is initially filled with either pure water or a slurry concentration of 100 ppm particles. The continuous feed rate (F) is 1 L/min.

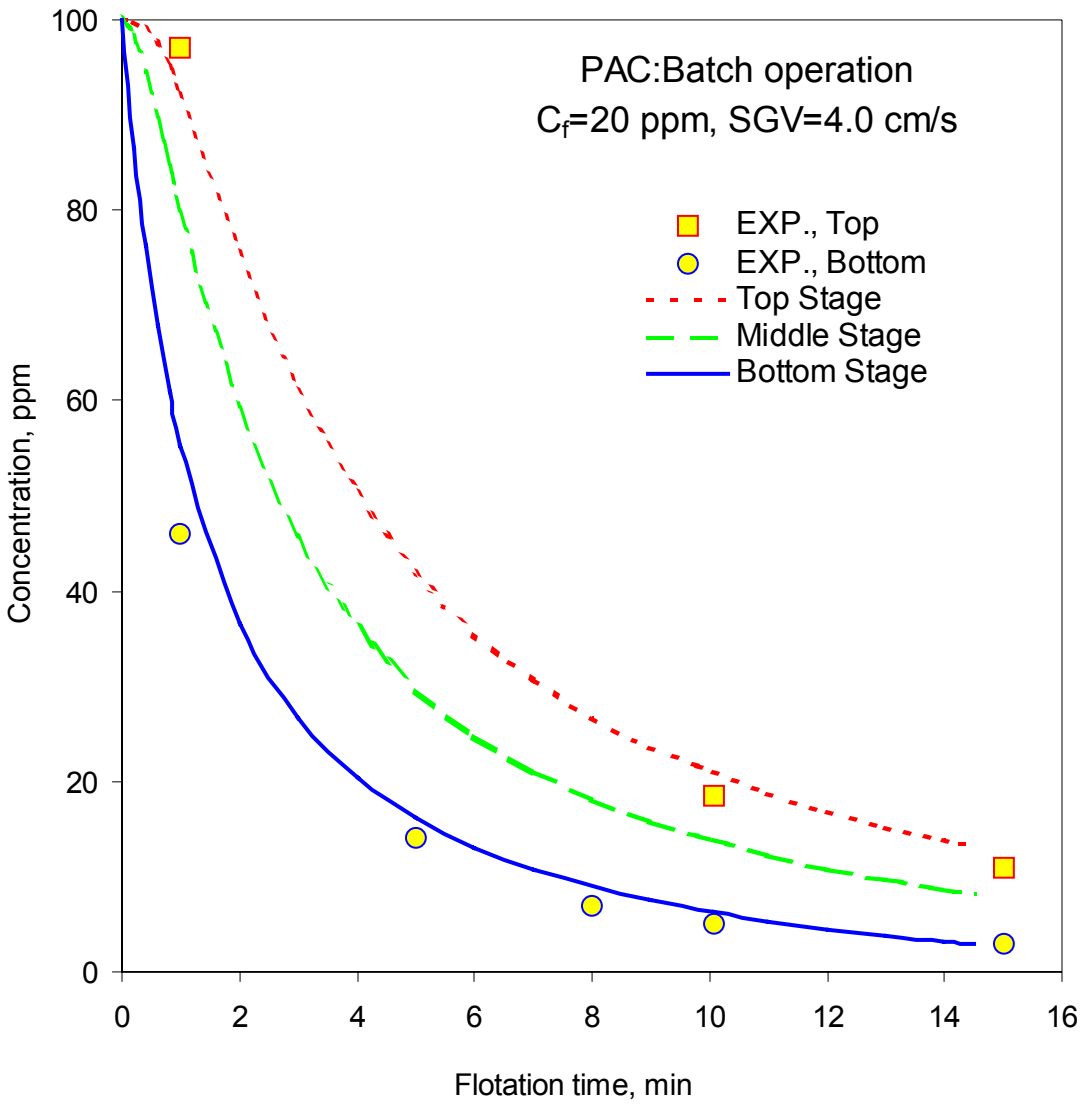

Figure 40 Simulation Results of PAC Removal under Batch Operation in a 4-in Column

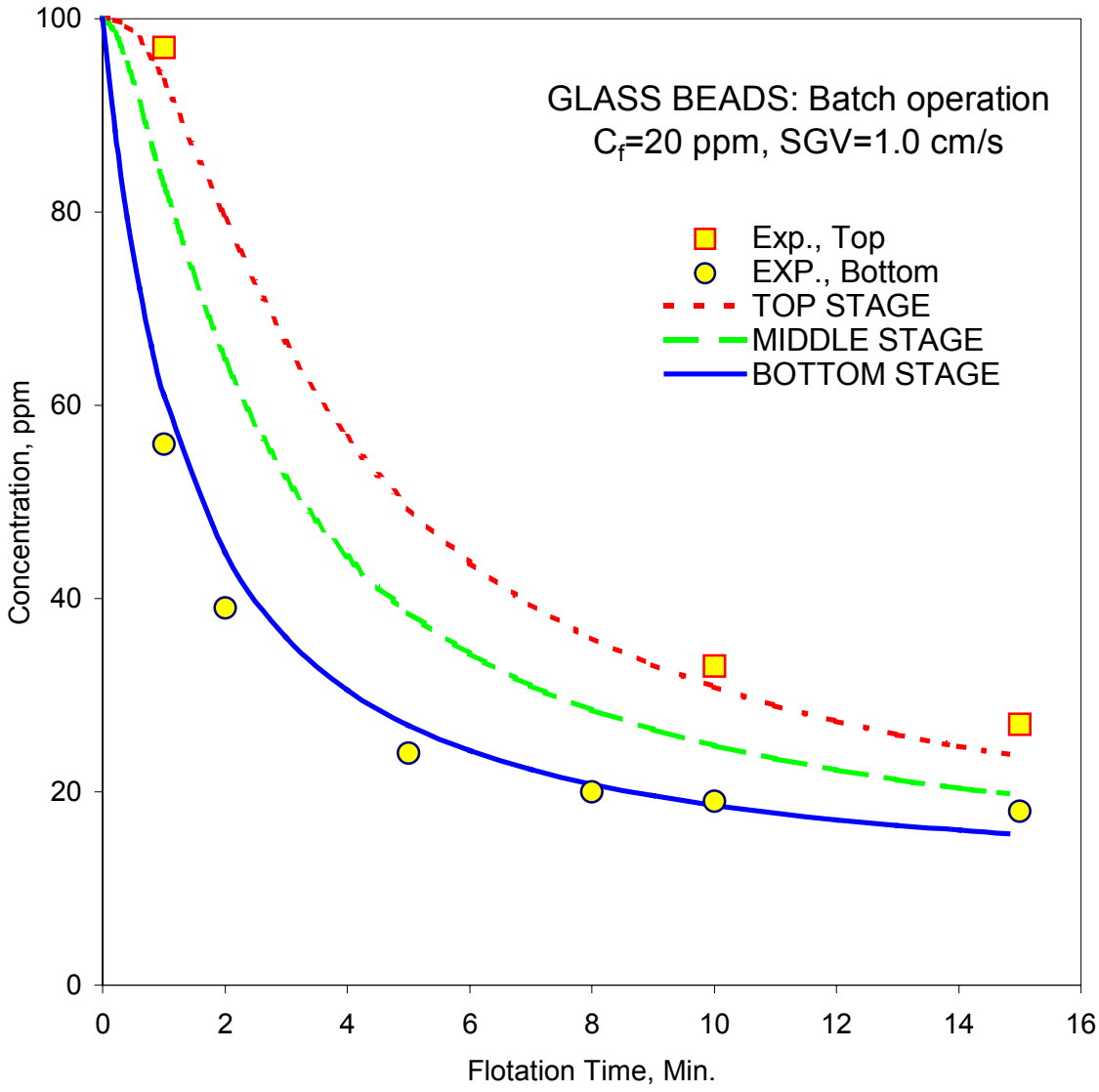

Figure 41 Simulation Results of Glass Beads Removal under Batch Operation in a 4-in Column (SGV=1.0 cm/s)

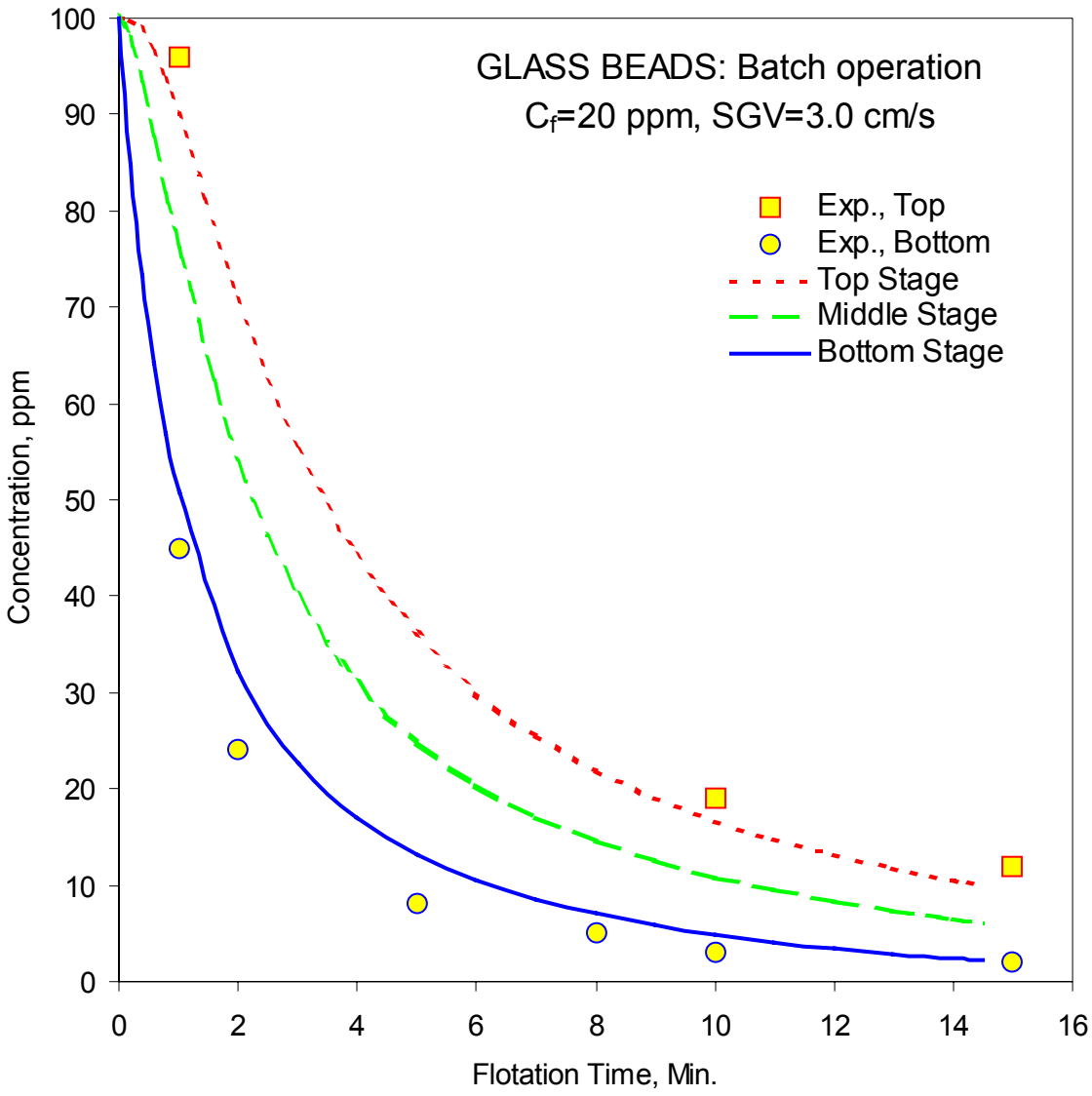

Figure 42 Simulation Results of Glass Beads Removal under Batch Operation in a 4-in Column (SGV=3.0 cm/s)

Simulated concentration profiles for both PAC and glass beads in all three stages are plotted in Figure 43 - 50. Solid symbols represent experimentally measured solid concentrations in the treated water. Curves represent simulated concentration profiles in different stages with initial feeding concentrations at 0 and 100 ppm, respectively.

Good agreements are found between simulation and experimental data for glass beads separations, as shown in Figures 43-46. In all three stages, simulated solid concentration profiles converge in the end, which indicate the steady state operation conditions are achieved, from which particle removal efficiency can be determined.

The separations of PAC particles are simulated at different SGV and frother concentrations. Due to PAC's strong ability of chemical adsorption, variations in frother dosage have limited effect on the hydrodynamics and separation efficiency. Therefore, only simulations obtained at different SGV for PAC removal are shown in Figures 47-50. Again, the results show that the simulated PAC concentration profiles agree with experimental data well. Similar to the findings in cases of glass beads, the concentration profiles of PAC for two different initial conditions converge at the steady state operation. The convergence occurs at the points ranging from 25 minutes to 55 minutes, depending on the values of SGV used. As expected, higher SGV yields shorter time to reach the steady state.

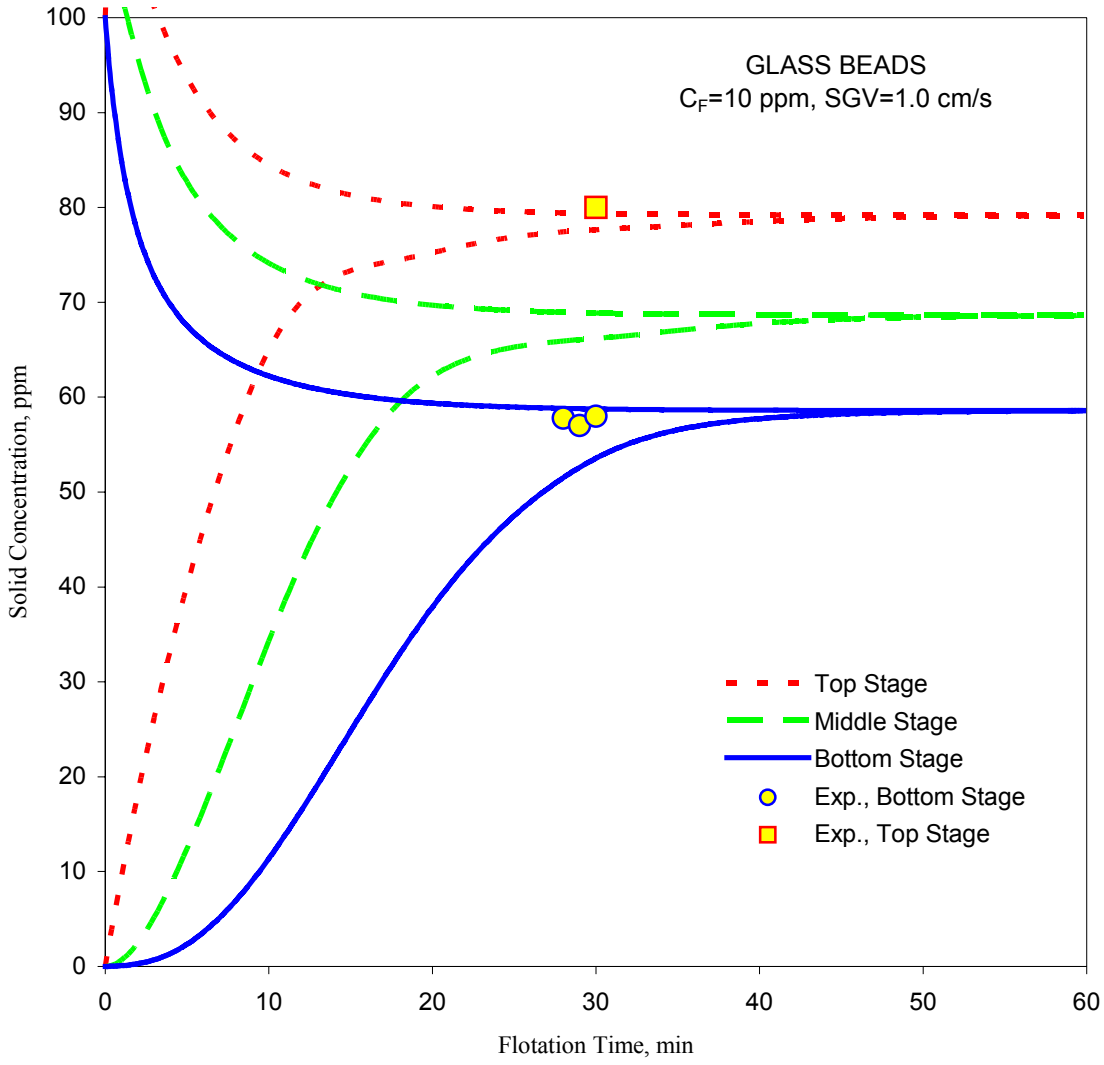

Figure 43 Simulation Results of Glass Beads Removal under Continuous Operation in a 4-in Column (SGV=1.0 cm/s, C_f=10 ppm)

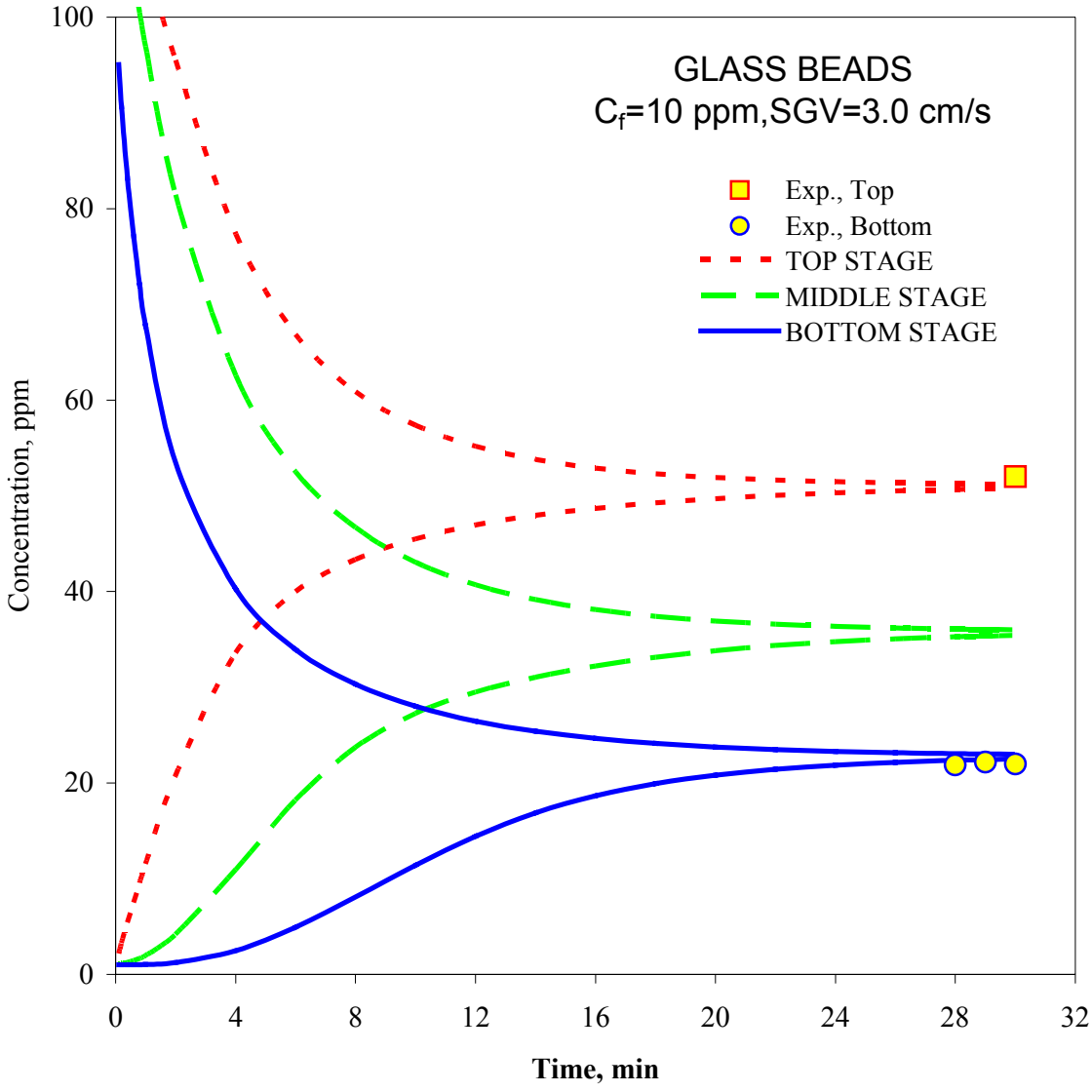

Figure 44 Simulation Results of Glass Beads Removal under Continuous Operation in a 4-in Column (SGV=3.0 cm/s, C_f=10 ppm)

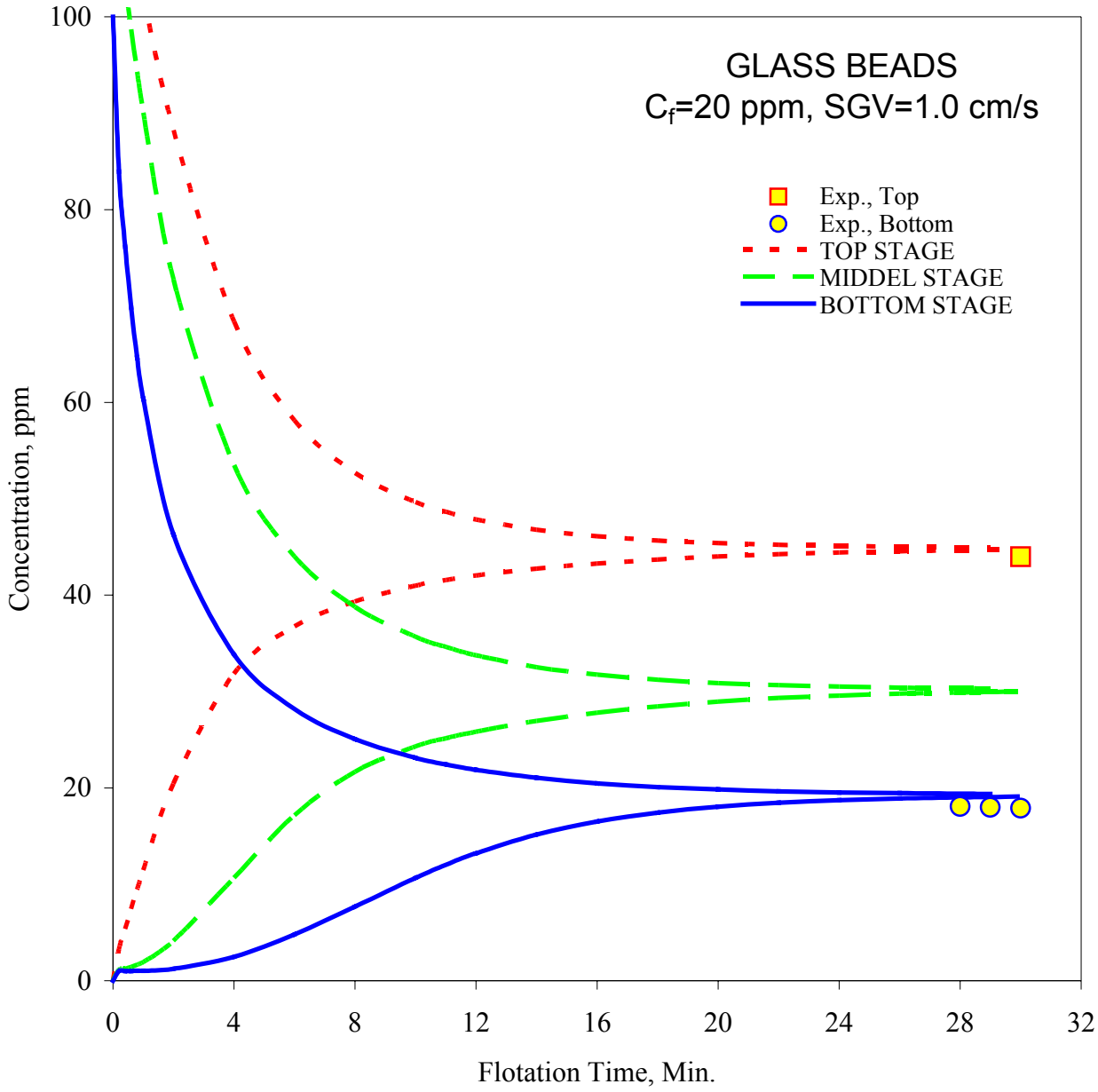

Figure 45 Simulation Results of Glass Beads Removal under Continuous Operation in a 4-in Column (SGV=1.0 cm/s, C_f= 20 ppm)

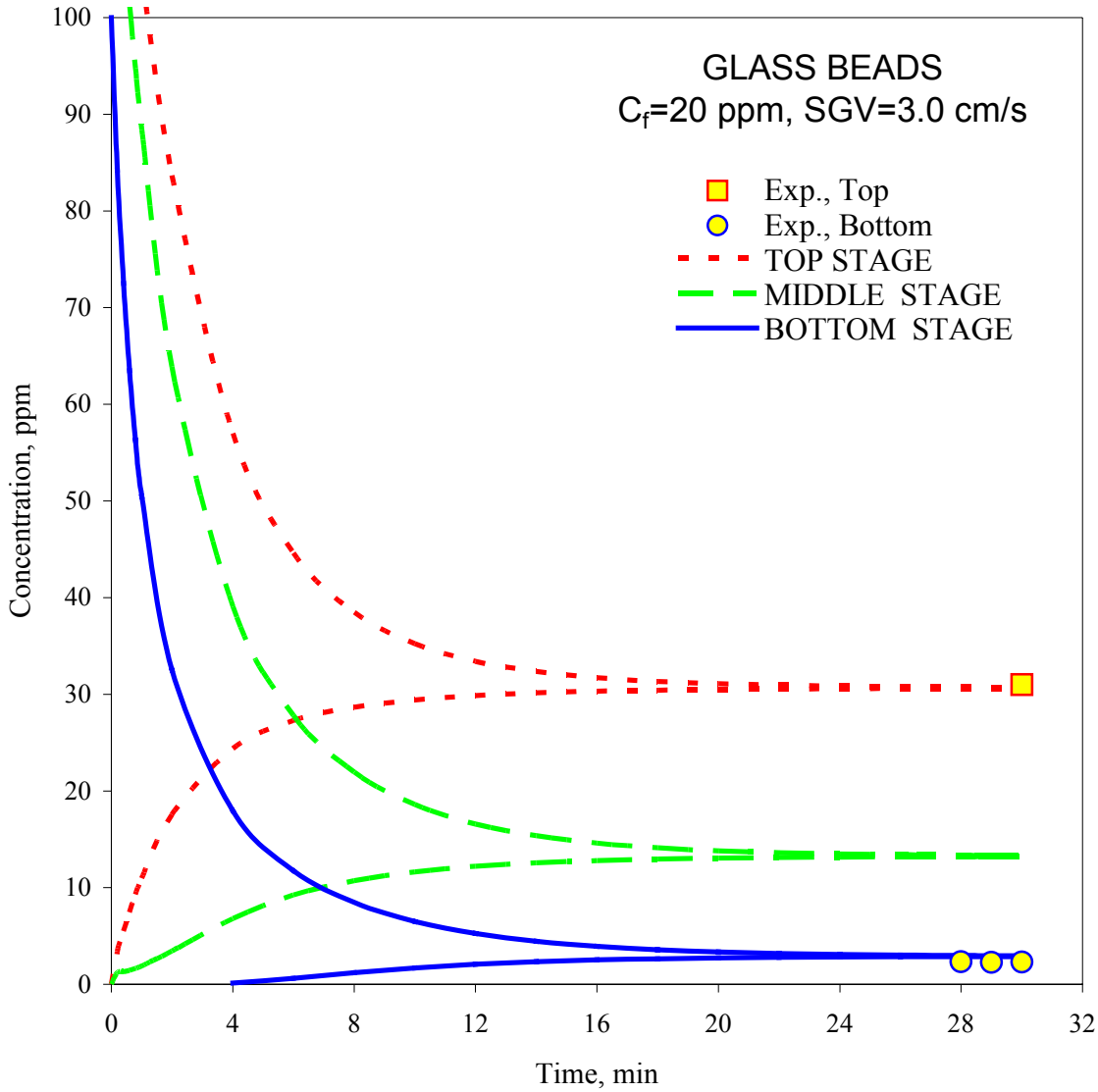

Figure 46 Simulation Results of Glass Beads Removal under Continuous Operation in a 4-in Column (SGV=3.0 cm/s, C_f= 20 ppm)

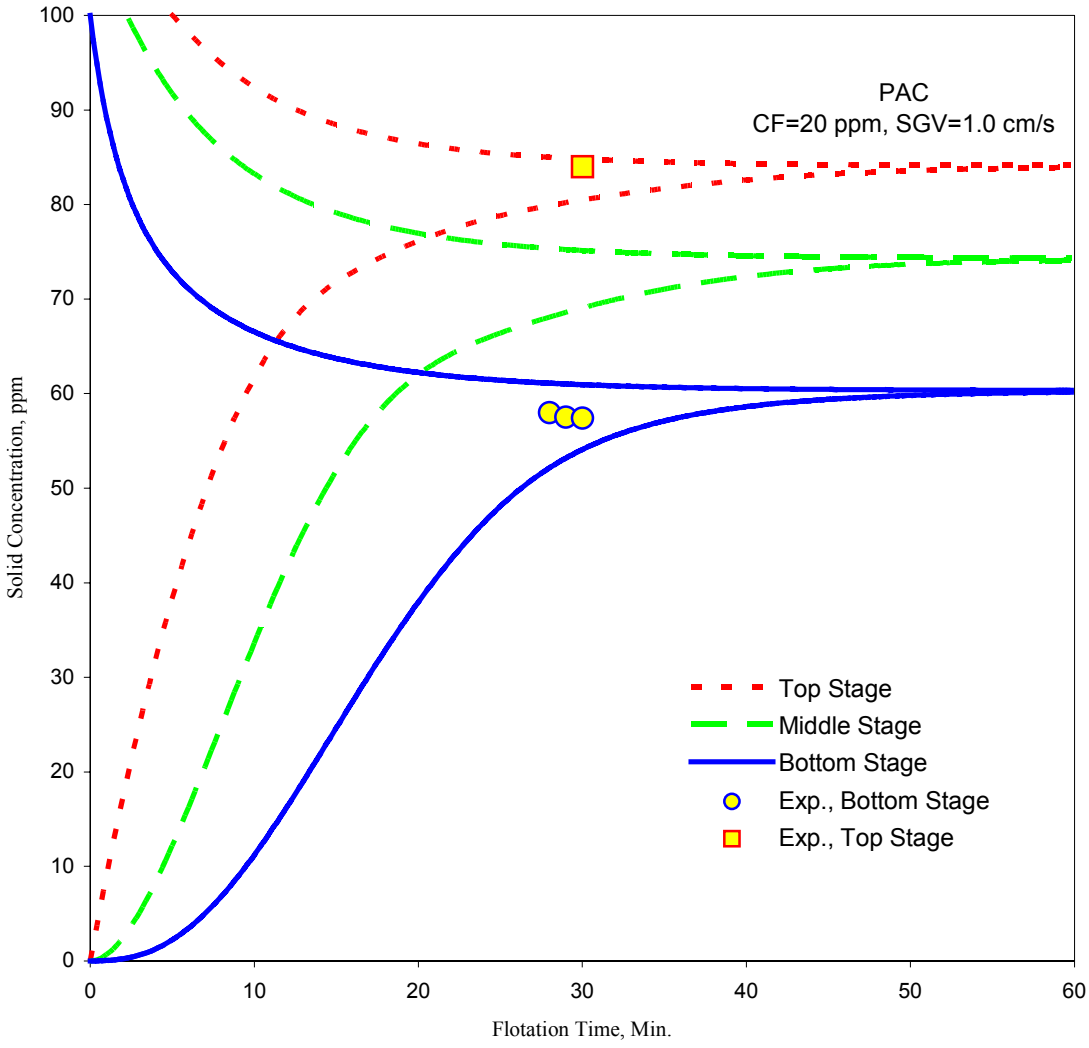

Figure 47 Simulation Results of PAC Removal under Continuous Operation in a 4-in Column (SGV=1.0 cm/s, C_f=20 ppm)

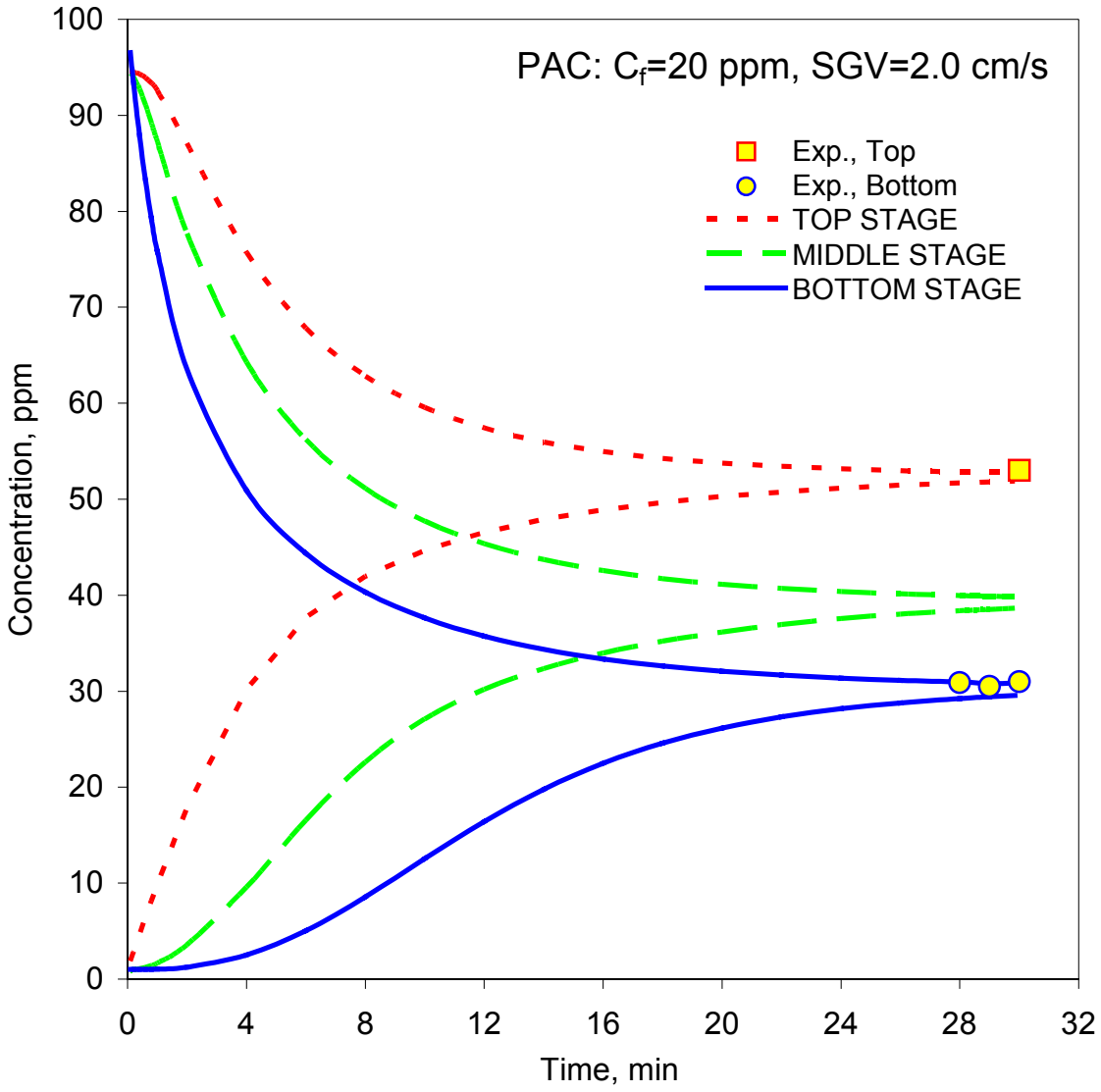

Figure 48 Simulation Results of PAC Removal under Continuous Operation in a 4-in Column (SGV=2.0 cm/s, C_f=20 ppm)

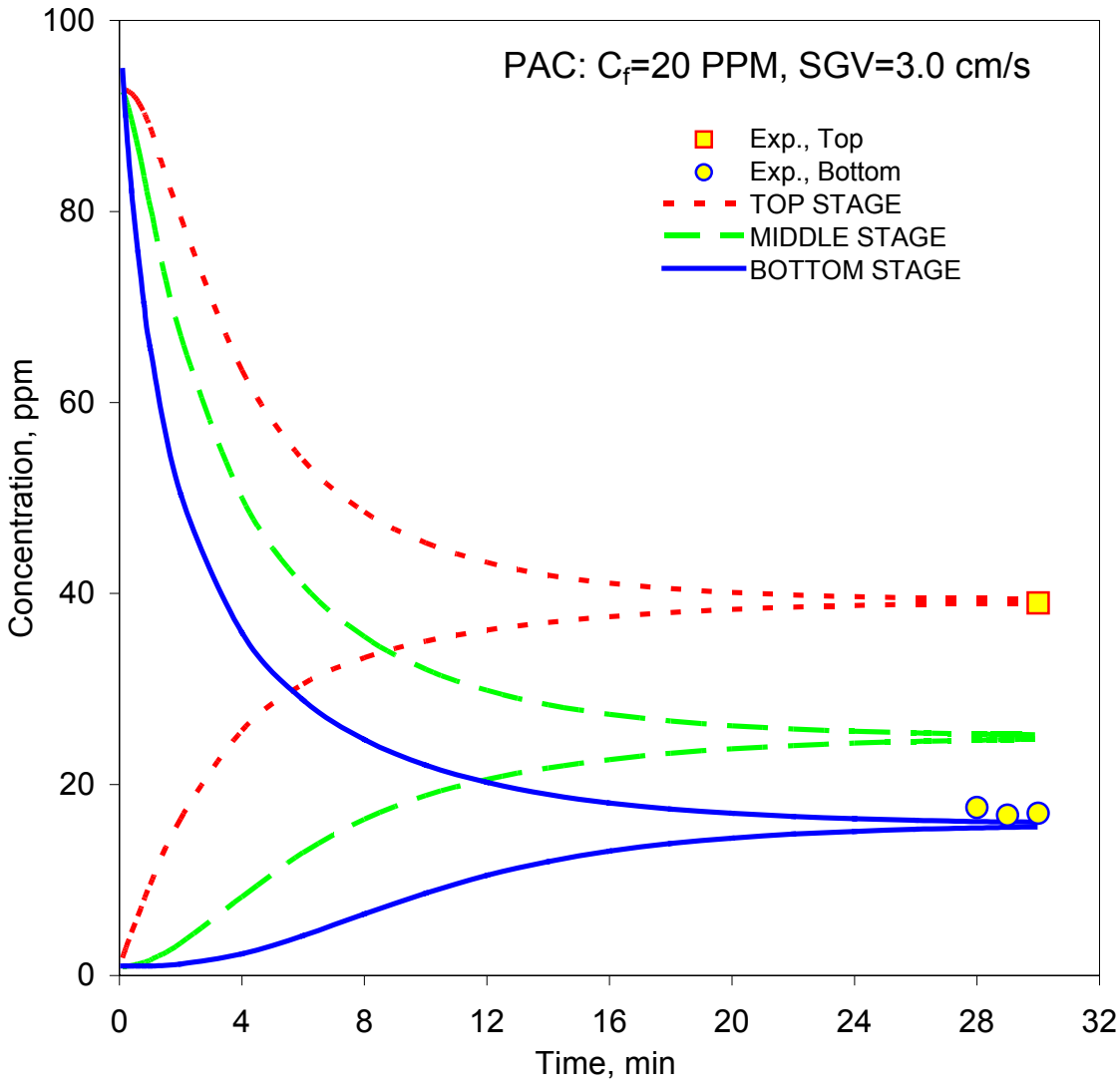

Figure 49 Simulation Results of PAC Removal under Continuous Operation in a 4-in Column (SGV=3.0 cm/s, C_f=20 ppm)

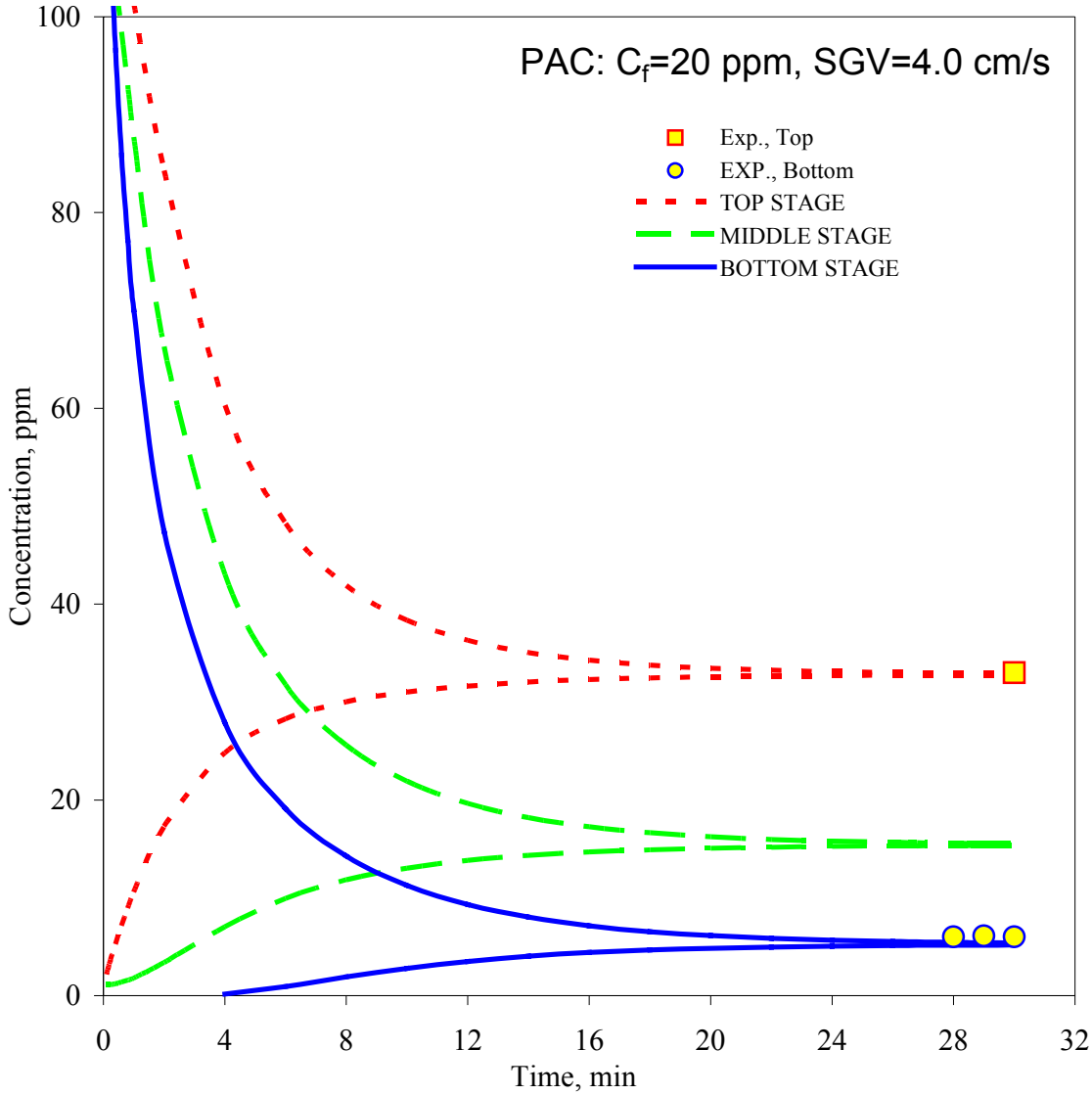

Figure 50 Simulation Results of PAC Removal under Continuous Operation in a 4-in Column (SGV=4.0 cm/s, C_f=20 ppm)

It is noted that the removals of fine particles mostly take place in the top stage in either batch or continuous operations. This is because favorable hydrodynamic conditions in the bottom stage keep on driving particles to the upper stages. For example, the PAC separation illustrated in Figure 50, when 20 ppm frother and 4.0 cm/s SGV are applied, 70% of PAC particles are in the top stage, and while less than 20% and 5% of particles are in the middle and bottom stages, respectively. Similar results are found under other operating conditions. Therefore, additional stage (beyond three stages) in the column provides no significant improvement in fine particle separation. In other words, a three-stage MSTLFLO column under proper operating conditions is sufficient to provide effective removal of fine particles from water.

9.2 PROCESS SIMULATION FOR OIL REMOVAL IN THE 12-IN MSTLFLO COLUMN

The same simulation strategy as that used for the particle separation simulation in 4-in MSTLFLO column has been applied to for the oil removal in a three-stage 12-in MSTLFLO column. Equations (20 a-c) are employed in the simulations. Similar Fortran codes shown in Appendix F are used for obtaining numerical solutions for continuous oil separations. The following initial and boundary conditions are applied:

$$\text{i.c.: } t = \sqrt[k]{\frac{1}{a(C - C_\infty)}},\ C_T = C_M = C_B = 0 \quad \text{or } 500 \tag{24}$$

$$b.c.: t = \infty,\ \frac{dC_i}{dt} < \lambda, i = T, M, B \tag{25}$$

As discussed before, the same "shifted" start point is applied, which is defined as $\sqrt[k]{\frac{1}{a(C-C_{\infty})}}$. The boundary conditions remain the same as those in the solid separations simulations. In this simulation, feeding rate (F) is 10 L/min.

Simulated oil concentration profiles for continuous operation in all three stages are plotted in Figures 51 and 52. Different types of curves represent simulated oil concentration profiles in different stages with two different initial oil concentrations at 0 and 500 ppm, respectively. Solid symbols represent experimentally measured oil concentrations in the treated water under steady state conditions. Two different SGV in the presence of 20 ppm of frother are simulated. Excellent agreements between simulation results and experimental data in term of oil residual concentrations in the bottom stages are found in all cases.

Similar to the simulations of solid separations in the 4-in column, in each stage of 12-in column, oil concentration profiles converge to the steady state operation. As indicated earlier, gas holdups in all three stages are not all the same, which gives different kinetic values. Hence, in different stages, it took from 30 to 50 minutes before oil concentration profiles converge to steady state operations, which is different from the simulation of the 4-in column. This is likely due to the difference in residence time in the two columns. Also, the curves representing the cases with initial oil concentration at 0 are expected to require much longer time to reach steady state operation.

In addition, it is also noted that the oil removal efficiency in a three-stage 12-in column is greater than 90%. Any additional stage beyond the three-stage configuration is considered to be unnecessary for oil removal in the MSTLFLO column. In other words, a three-stage MSTLFLO column is sufficient to provide effective removal of oil as well as fine particles from water (see discussion in the last section).

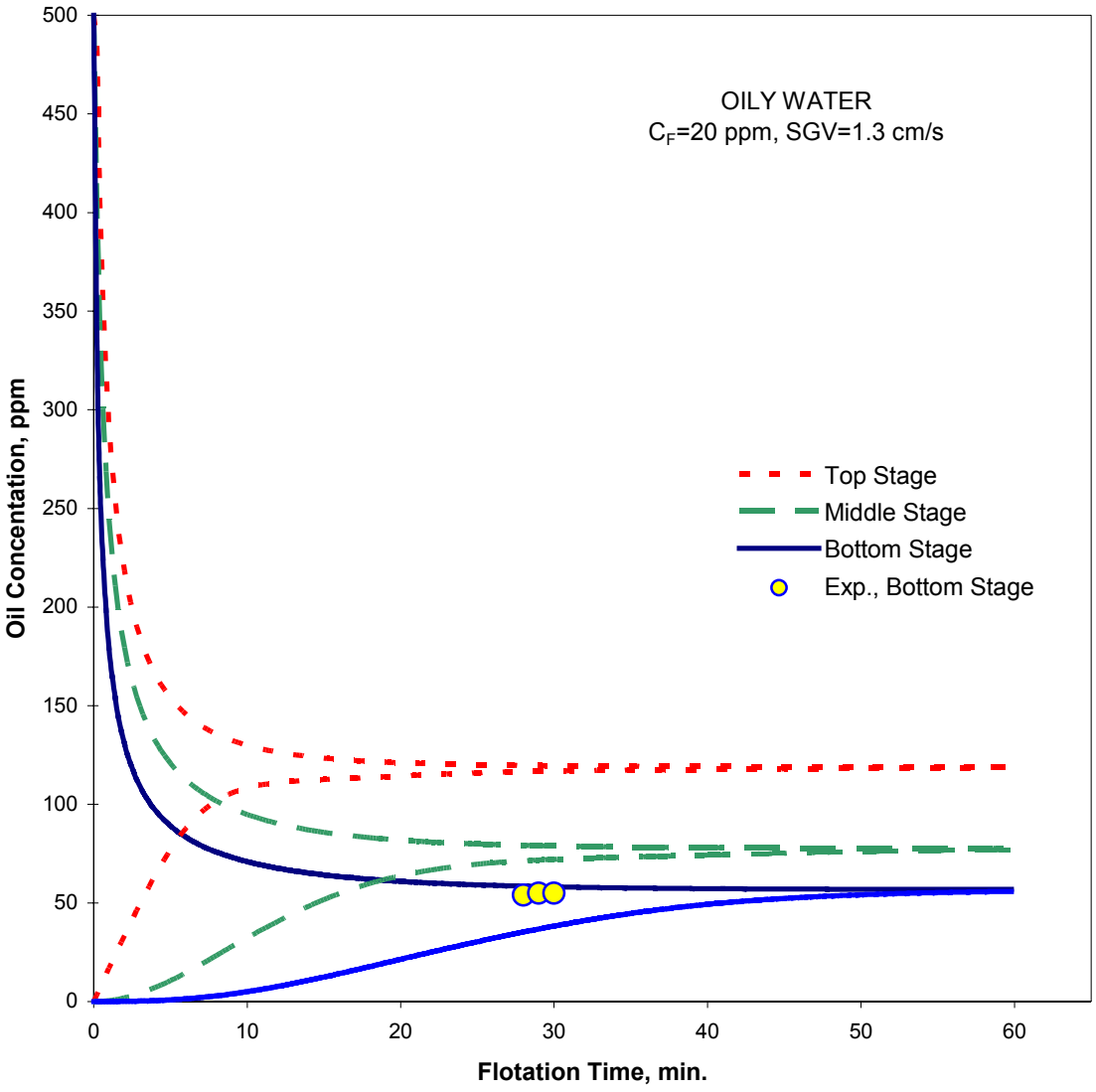

Figure 51 Simulation Results of Oil Removal under Continuous Operation in a 12-in Column (SGV=1.3 cm/s, C_f=20 ppm)

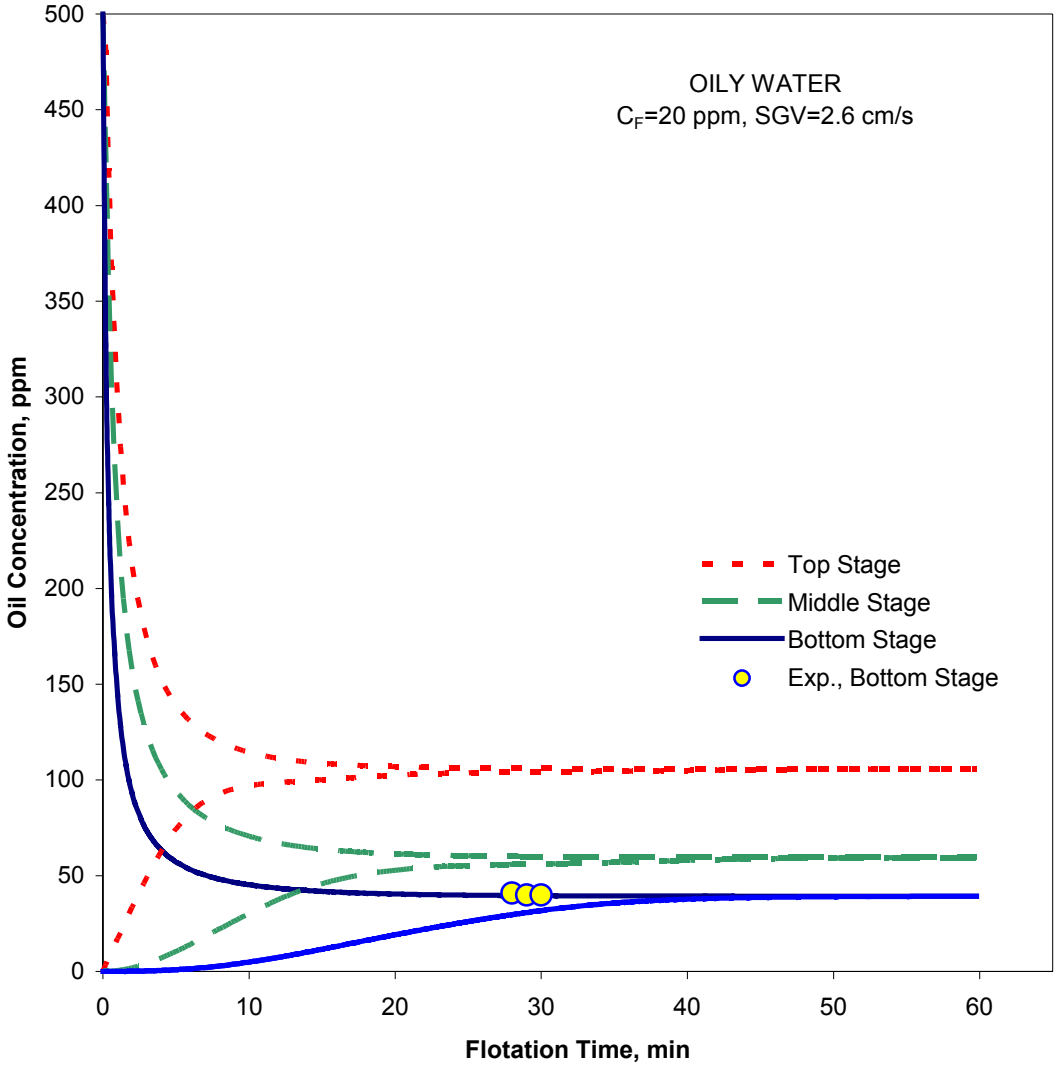

Figure 52 Simulation Results of Oil Removal under Continuous Operation in a 12-in Column (SGV=2.6 cm/s, C_f=20 ppm)

9.3 PROCESS SIMULATION FOR SIMULTANEOUSLY REMOVAL OF PAC AND OIL

The same numerical simulation method as that used for the single component separation has been applied to the simultaneously removal of PAC and oil in a 4-in MSTLFLO column. Equations (24) and (25) are employed as the initial and boundary conditions.

Numerical simulation is carried out for the continuous operation of simultaneously removal of PAC and oil in the presence of 20 ppm of frother at 3.0 SGV. Simulated oil and PAC concentration profiles in all three stages are plotted in Figure 53. Different curves represent simulated oil and PAC concentration profiles in the three stages with two different initial concentrations at 0 and 500 ppm. Also shown are experimentally measured oil and PAC concentrations in the treated water as designated by solid symbols. Once again, excellent agreements are observed between simulation results and experimental data at steady state.

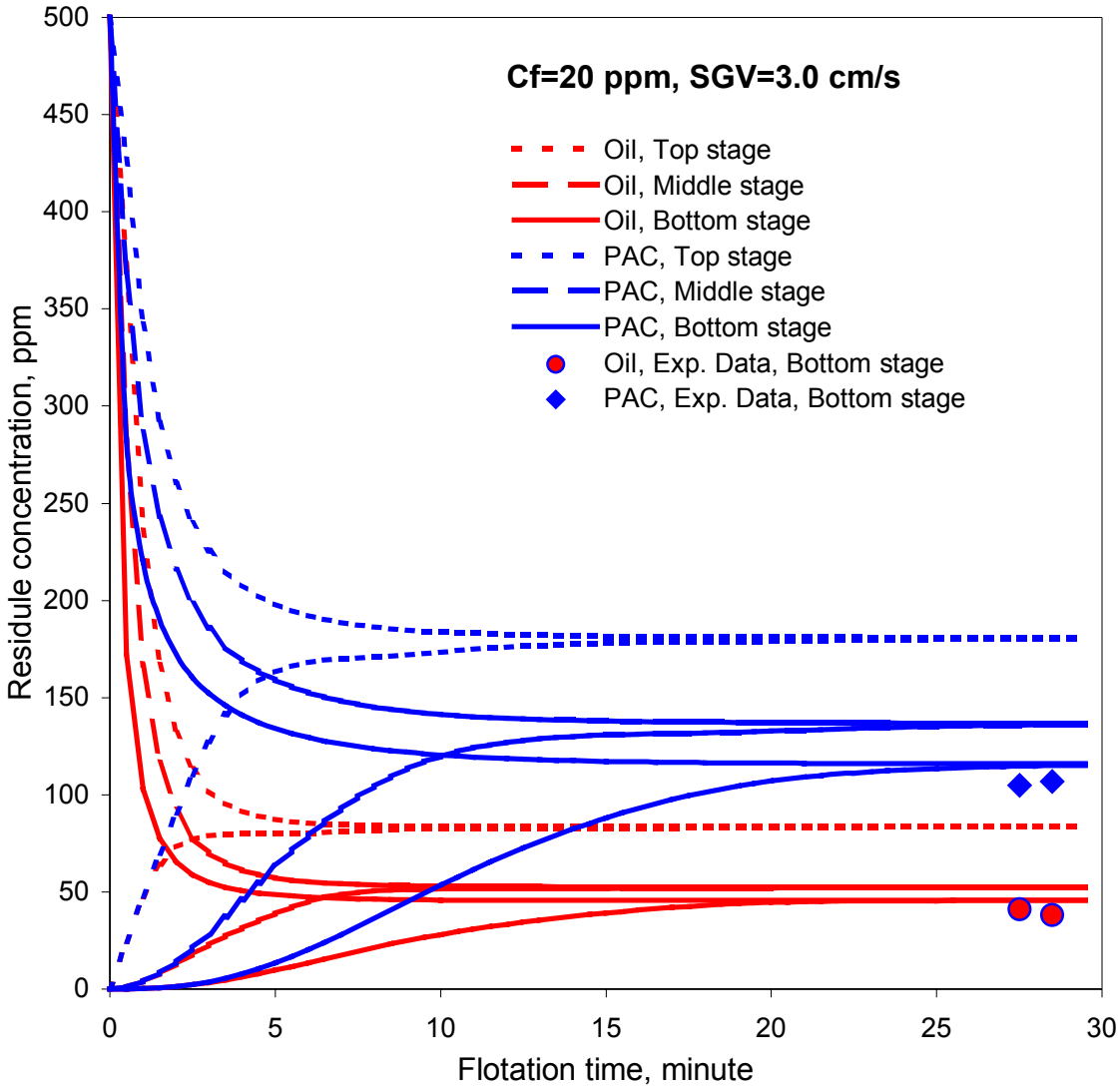

Figure 53 Simulation Results of Simultaneous Removal of Oil and PAC under Continuous Operation in a 4-in Column (SGV=3.0 cm/s, C_f=20 ppm)

10.0 SCALE-UP STUDY

This section presents a discussion of a simple geometric scale-up scheme based on experimental results and kinetic behaviors in MSTLFLO column operations. This is followed by a design of a large size MSTLFLO column using the scale-up scheme developed here. Based on the scale-up criteria, a set of parameters for the column design and operation of future commercial scale units are recommended.

10.1 SCALE-UP OF THE MSTLFLO PROCESS

For the scale-up study, two different sizes of the MSTLFLO flotation column with similar internal structure and space velocity have been used: a 4-in column with 0.102 m O.D. and a 12-in column with 0.306 m O.D. Geometric dimensions of major components of these two columns and key operating conditions are given in early sections. It is shown that the ratios of two columns diameters and two draft tubes diameters are approximately 3. However, due to the head room limitation in our laboratory, the height of the 12-in column cannot exceed 7 meters. Therefore, the ratio of draft tube height to its diameter in the 12-in column is smaller than that in the 4-in column. It should also be noted that the range of liquid feed rates in the 12-in column is 10 times of that in the 4-in column because the same space velocity is applied for both columns.

As reported in early discussions (Section 7.1 and 7.2), both 12-in and 4-in columns have shown comparable superior performance in the removal of emulsified oil. Experimentally determined kinetic constants have been correlated with operating conditions in terms of the same set of hydrodynamic parameters. These results validate the use of a simple geometric ratio as the basis for scale-up of the MSTLFLO column design to large size commercial units.

10.2 DESIGN GUIDELINES FOR LARGE SCALE MSTLFLO PROCESS

Based on the results of the experimental and theoretical study, design guidelines for the scale-up of the MSTLFLO process for future commercial applications are proposed. The design of a commercial size 90-in MSTLFLO column (with a capacity of 0.77 MGD) is based on the simple scale up scheme in term of the ratio of column diameter, which has been confirmed in the 12-in column, and the comparable space velocity in the 4-in and 12-in columns. The preferred ranges for the scale-up design parameters are presented in Table 23.

Table 23 Recommended Parameters for Scale-up MSTLFLO Column

Scale-up Parameter	**Recommended Range**	**Objective**
Space velocity, s^{-1}	0.0020-0.0025	Removal efficiency > 90%
Column Diameter, m	2.3	Meet the design capacity
Column Height, m	35 - 45	Meet the design capacity
Area ratio, AR	0.9 – 1.1	Maximize liquid circulation
Draft tube diameter, m	1.5	Meet the design capacity
Draft tube height, m	15	Meet the design capacity
D_{tube}/L_{tube}	10	Enhance liquid circulation
Distance between cone and draft tube	$\leq 0.25\ D_{tube}$	Direct rising bubbles and minimize backmixing
Clearance between cone edge and inner wall, m	≤ 0.001	Minimize backmixing
Angle of cone, degree	40° - 60°	Direct rising bubbles and minimize backmixing
Sparger Pore size, m	$\leq 10 \times 10^{-6}$	Generate small bubbles

10.3 RECOMMENDED OPERATING CONDITIONS FOR THE MSTLFLO PROCESS

In addition, the recommended ranges of operating conditions and key hydrodynamic parameters for the simultaneous removal of multi-component, including emulsified oil, suspended fine particles (both hydrophobic and hydrophilic) and dissolved chemicals, from wastewater are listed in Table 24.

Table 24 Recommended Operating Parameters for Scale-up MSTLFLO Column (for simultaneous removal of multi-component pollutants from wastewater)

Operating Parameter	**Recommended Range**	**Objective**
SGV, m/s	0.03 – 0.04	Create large gas holdup
Frother Concentration, ppm	20 - 30	Maintain small bubbles
Gas Holdup	0.3 - 0.4	Create large interfacial area
Bubble size, d_{32}, m	≤ 0.001	Enhance collision probability and increase interfacial area
PAC concentration, ppm	300-500	Provide large adsorption capacity of dissolved chemicals
PAC particle size, d_{50}, m	$< 20\times10^{-6}$	Increase the adsorption capacity of dissolved chemicals in column

11.0 CONCLUSIONS

The MSTLFLO flotation column is shown to be an efficient one-step separation process for simultaneous removal of the mixed types of contaminants, including fine solid particles, dissolved phenol and emulsified oil droplets. Based on the results of experimental measurements and process simulation, the following conclusions can be drawn:

1. MSTLFLO process shows high efficiency in removing fine particles smaller than 50 μm. Under optimum operating conditions, as much as 99% of fine particles, including PAC particles and glass beads, can be removed.
2. An adsorptive MSTLFLO flotation process has been successfully tested using PAC particles as an adsorbent, showing promising results for the removal of dissolved chemical, such as phenol from water.
3. MSTLFLO process is effective for simultaneously removing mixed types of contaminants from wastewater, including emulsified oil, dissolved phenol and suspended fine solids particles (both hydrophobic and hydrophilic particles). Removal efficiency is greater than 90% for both emulsified oil and solid particles, and 80% for phenol.
4. The experimental results obtained in the 12-in column compare favorably with that in the 4-in column in terms of the oil removal efficiency and kinetics as well as the operating capacity.

5. A generalized correlation for kinetic constants has been established in terms of hydrodynamic parameters (gas holdups and bubble size) for both oil removal and fine particles separations in the MSTLFLO flotation column.
6. A tank-in-series process model has been successfully applied to simulate the operations for fine particle separation and oil removal in a three-stage MSTLFLO flotation column.
7. The experimental results and process simulation show that the optimum configuration of the MSTLFLO process is a column with three stages.
8. A comparison of performance data and kinetic constants obtained in two MSTLFLO columns of different sizes (a 12-in and a 4-in column) indicates that a simple geometric scale-up scheme based on the ratio of column diameter can be used for the design of large commercial units.

APPENDIX A

SELECTED RESULTS OF 4-IN MSTLFLO COLUMN

A brief summary of the results of gas holdup, bubble size and column applications in a 4-in MSTLFLO column are summarized below [36].

a. Gas Holdup

The gas holdups in the 4-in MSTLFLO column are shown in Figure A-1. It can be found that most of the gas holdups are in the range of 20% to 45%. The MSTLFLO column has a significantly higher gas holdup (up to 45%) than that of conventional column (no more than 30%).

b. Bubble Size Distribution

The gas bubbles generated in the 4-in MSTLFLO column were relatively small and spherical in the presence of frother. A typical bubble size distribution is shown in Figure A-2. The Sauter mean diameter is as small as 1.01 mm, when 15 ppm frother and 2.0 cm/s superficial gas velocity are applied. Meanwhile the average bubble size is found about 2~4 mm in the conventional flotation devices when similar operation conditions are applied.

c. Column Applications

The MSTLFLO column demonstrates its superior efficiency for oily water treatment. More than 95% removal efficiency can be achieved in case of 500 ppm initial emulsified oil. Furthermore, its potential application for solid removal was demonstrated, as shown in Figure A-3. When MSTLFLO was used to treat a simulated DECON water from nuclear power plant, 97% metal oxide particles were removed.

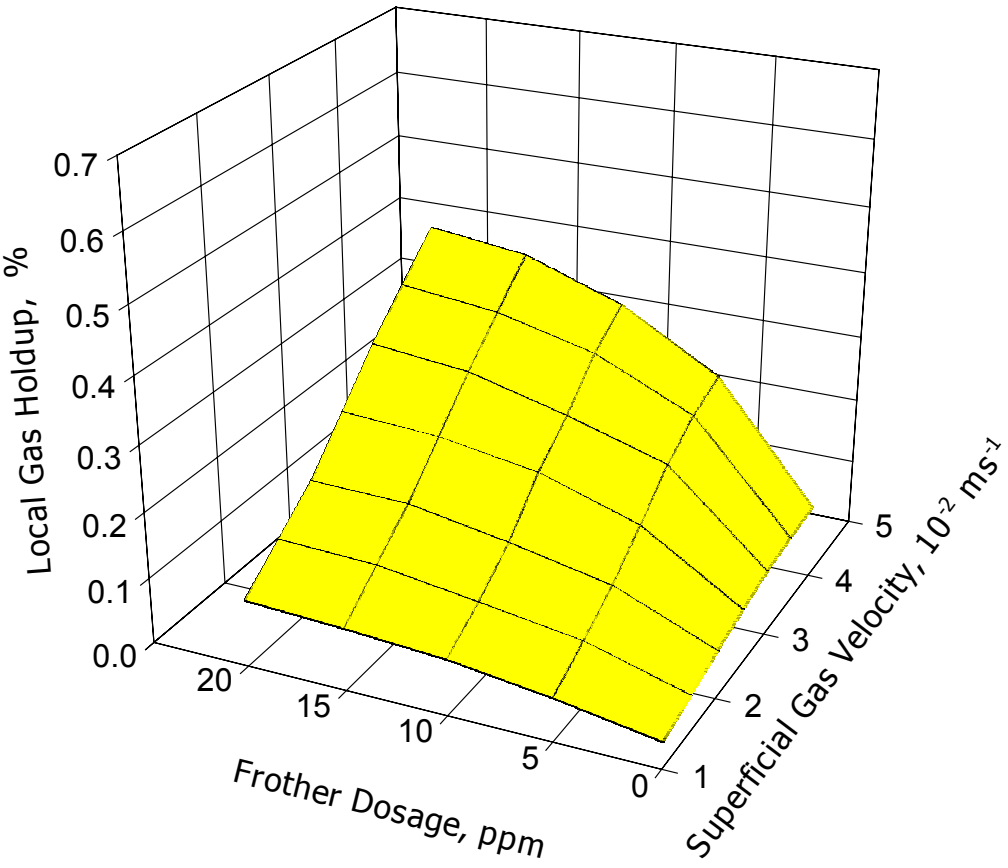

Figure A-1 Gas Holdups in the 4-in MSTLFLO Column

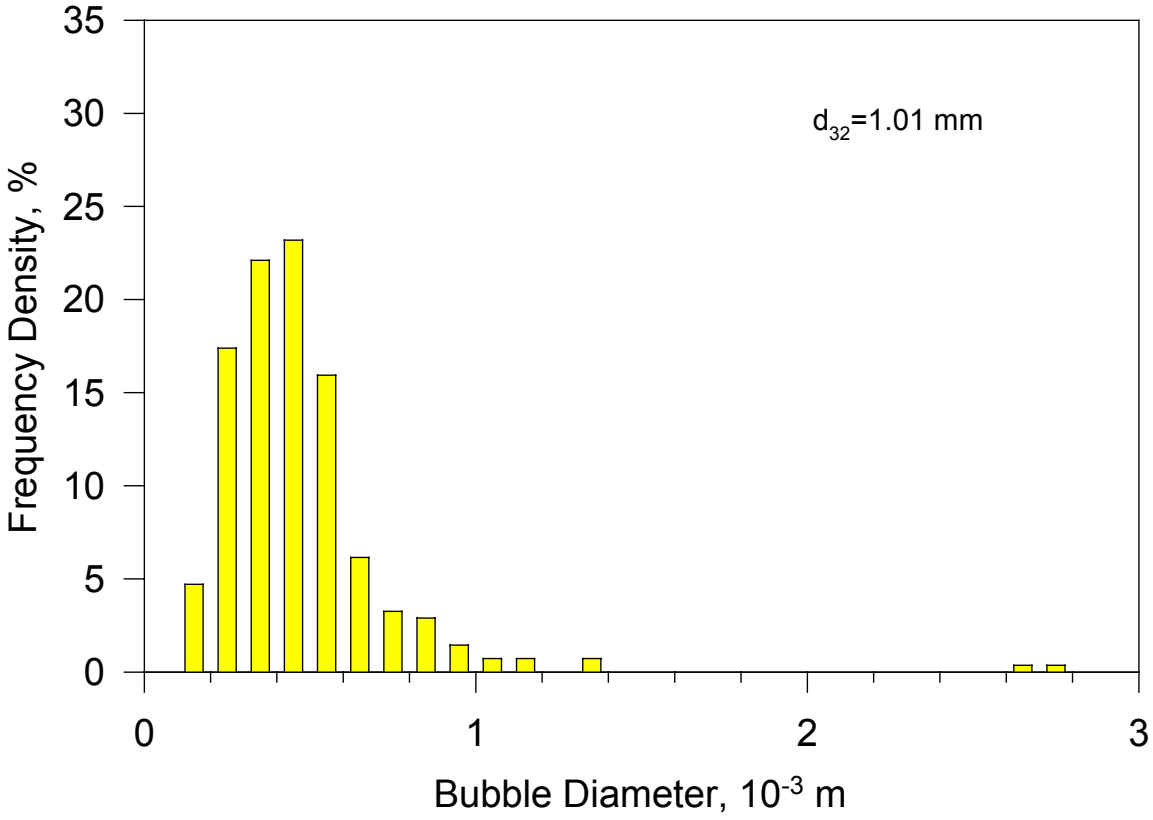

Figure A-2 The Bubble Size Distribution at 15 ppm of Frother

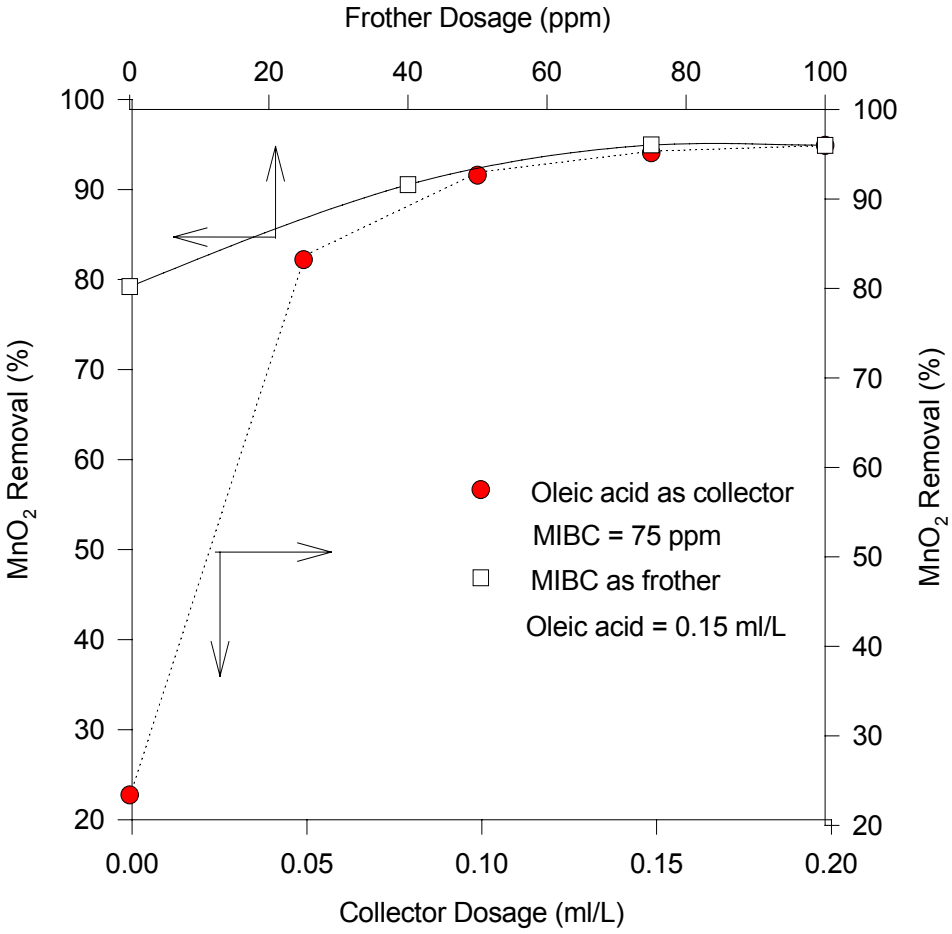

Figure A-3 Removal of Metal Oxide using MSTLFLO Column

APPENDIX B

GAS HOLDUP MEASUREMENT

In this study, gas holdup is measured by using hydrostatic pressure method: measuring the pressure difference between two set points.

Schematics of gas holdup measurement devices in the riser and downcomer are shown in Figure B-1. Inverted U-tube manometers are installed for gas holdup measurements with two pairs of ∅ 1 mm probes into the bulk of the riser and downcomer.

Following equation is used to calculate, $\varepsilon_{g:\,r,d}$, gas holdup in the riser or downcomer, respectively:

$$\varepsilon_{g:r,d} = \frac{H_m}{H_L} \tag{B-1}$$

where, H_m denotes manometer reading; H_L is a distance between two probes.

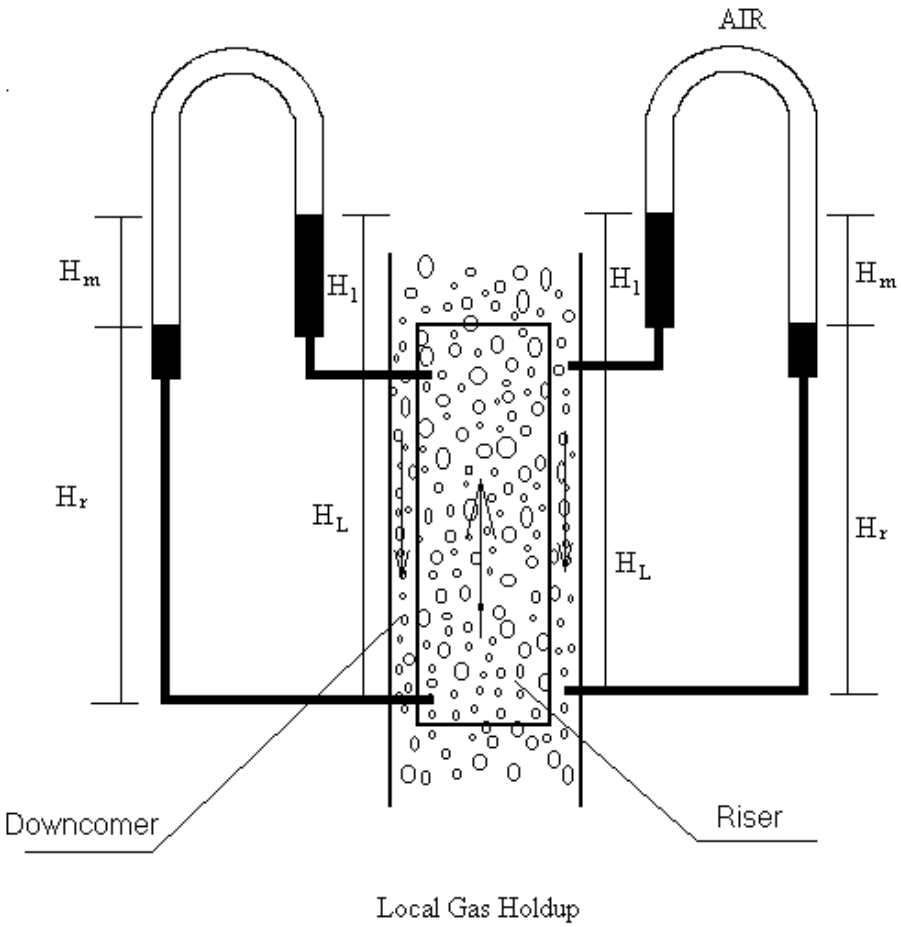

Figure B-1 Manometer for Gas Holdup Measurements

APPENDIX C

LIQUID CIRCULATION VELOCITY MEASUREMENT

Liquid circulation velocity is measured using tracer response technique. Measurement setup is illustrated in Figure C-1. Two sets of digital conductivity meter (Cole-Parmer 1481-61) and flow type conductivity probes(Cole-Parmer 1481-66) are used in measurements. In order to avoid small bubbles entering the conductivity cell and to cause interference, tips of probes are covered with fine screen caps. Saturated Potassium Chloride (KCl) solution at room temperature is used as a tracer because of its high solubility and conductivity. The response is detected at a location down stream from the point of tracer injection. Time difference t_d between peaks on two conductivity meters is taken as average linear time.

Average liquid linear velocity can be calculated using following equation:

$$u_L = \frac{d_e}{t_d} \tag{B-1}$$

where d_e is a distance between two electrodes.

Superficial liquid velocity U_L can be obtained using following expression:

$$U_L = u_L(1-\varepsilon) \tag{B-2}$$

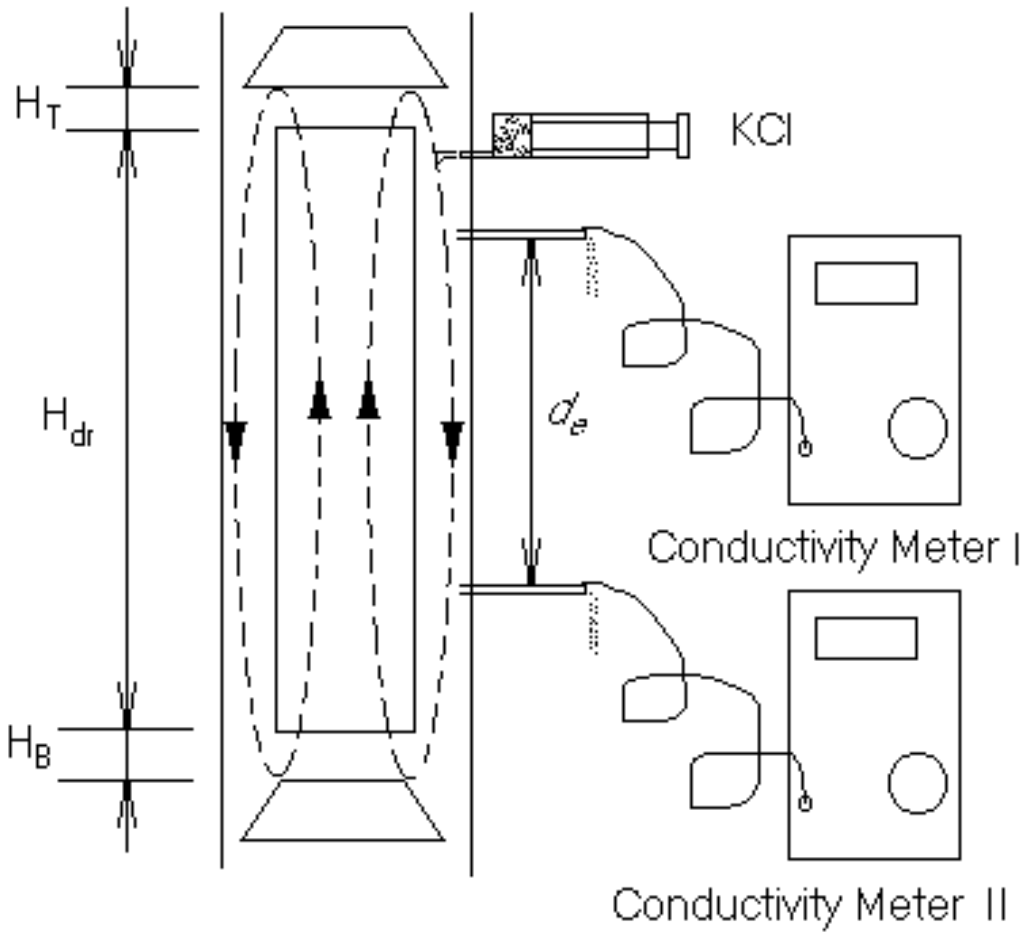

Figure C-1 Experiment Setup for the Measurement of Liquid Circulation

APPENDIX D

CORRELATIONS FOR KINETIC CONSTANTS

A software STATISTICA is used to perform the correlations for solid separation kinetic constant, K_p, with selected variables.

Five different empirical correlations (as shown in Table D-1) have been tested for both PAC and glass beads. Four different regression methods, including quasi-Newton, Simplex, Rosenbrock pattern search and Hooke-Jeeves pattern moves, are used to determine the stabilization of empirical constants involved in these correlations. The least square method is used to examine the variation between estimated values and experimental results.

Correlation results for PAC and glass beads are shown in Table D-1 and D-2, respectively. Determination coefficients R^2 are used to verify the robustness of a given correlation. The value of R^2 ranges from 0 to 100%, while 100% represents a perfect positive correlation between model and experiment results.

Table D-1 Regressed Constants for Kinetic Constant of the Removal of PAC Particles

Model	Regress method*	PAC					
		a	*b*	*c*	*d*	*e*	R^2, %
$K_p = \frac{a\varepsilon_g^b}{d_b^e}$	H-J	0.808	0.210			3.60	99.9
	R-P	0.645	0.150			1.35	96
	Q-N	0.810	0.209			3.63	99.9
$K_p = \frac{a\varepsilon_g^b E_{cg}^c}{d_b^e}$	H-J	1.90	0.31	0.099		4.49	97
	R-P	1.42	0.21	0.101		1.033	92
	Q-N	0.12	-0.01	-0.23		2.20	99
	Splx	1.57	0.23	0.12		0.96	98
$K_p = \frac{a\varepsilon_g^b E_{cg}^c V_g^d}{d_b^e}$	H-J	3.24	0.103	0.1	0.206	4.42	99
	R-P	1.93	0.17	0.096	0.087	2.53	98
$K_p = \frac{aE_{cg}^c V_g^d}{d_b^e}$	H-J	4.29		0.1	0.31	4.50	97
	R-P	1.8		0.07	0.2	0.95	98
	Splx	1.7		0.07	0.18	0.66	97
$K_p = \frac{aV_g^d}{d_b^e}$	H-J	1.43			0.213	3.79	99.9
	R-P	1.43			0.213	3.79	99.9
	Q-N	1.43			0.213	3.79	99.9

*Q-N: quasi-Newton; Spl: Simplex; H-J: Hooke-Jeeves pattern moves; R-P: Rosenbrock pattern search

Table D-2 Regressed Constants for Kinetic Constant of the Removal of Glass Beads

Model	Regress method*	Glass beads					
		a	*b*	*c*	*d*	*e*	R^2, %
$K_p = \frac{a\varepsilon_g^b}{d_b^e}$	H-J	1.10	0.075			0.766	98
	R-P	1.12	0.073			0.792	98
	Q-N	1.11	0.075			0.766	98
	Splx	1.07	0.084			0.760	98
$K_p = \frac{a\varepsilon_g^b E_{cg}^c}{d_b^e}$	H-J	1.42	0.16	0.1		0.69	98
	R-P	1.57	0.12	0.099		0.705	97
	Q-N	1.47	0.16	0.11		0.68	99
	Splx	0.92	0.04	-0.06		0.81	98
$K_p = \frac{a\varepsilon_g^b E_{cg}^c V_g^d}{d_b^e}$	H-J	1.65	0.1	0.1	0.055	0.716	99
	R-P	1.675	0.099	0.103	0.060	0.720	98
	Q-N	0.00001	5.35	0.511	-4.95	-1.84	99
	Splx	0.82	0.116	-0.04	-0.07	0.76	98
$K_p = \frac{aE_{cg}^c V_g^d}{d_b^e}$	H-J	2.14		0.1	0.156	0.76	97
	R-P	1.73		0.053	0.119	0.78	99
	Q-N	1.73		0.053	0.119	0.78	99
$K_p = \frac{aV_g^d}{d_b^e}$	R-P	1.35			0.08	0.79	99.9
	Q-N	1.35			0.08	0.79	99.9
	H-J	1.35			0.08	0.79	99.9

APPENDIX E:

TANK-IN-SERIES MODEL FOR MSTLFLO PROCESS

MSTLFLO process can be simulated using a classic tank-in-series model, assuming each stage as a well mixed Continuous Stirred Tank Reactor (CSTR).

In MSTLFLO process, solid particles are transported from lower stages to upper ones, while net liquid flow is in the opposite direction. A sketch of this process model for a three-stage MSTLFLO process is shown in Figure E-1.

In the Figure, water with particle concentration C_0 is fed into a column from the top. Solid particles laden foam overflows from the top of column and clean water is discharged from the bottom. Based on mass conservation, the accumulation of solid concentration in each stage is equal to the amount of solid input subtracting that of output. For example, in the middle stage, input streams are: 1) net fluid flow bringing in solids from the top stage; 2) rising bubbles transporting solids from the bottom stages. Similarly, output streams are: 1) net fluid flow carrying solids to the bottom stages; 2) rising bubbles transporting solids of current stage to the top ones. Such a model is based on the assumption that solid concentration in each stage is uniform and back mixing is negligible.

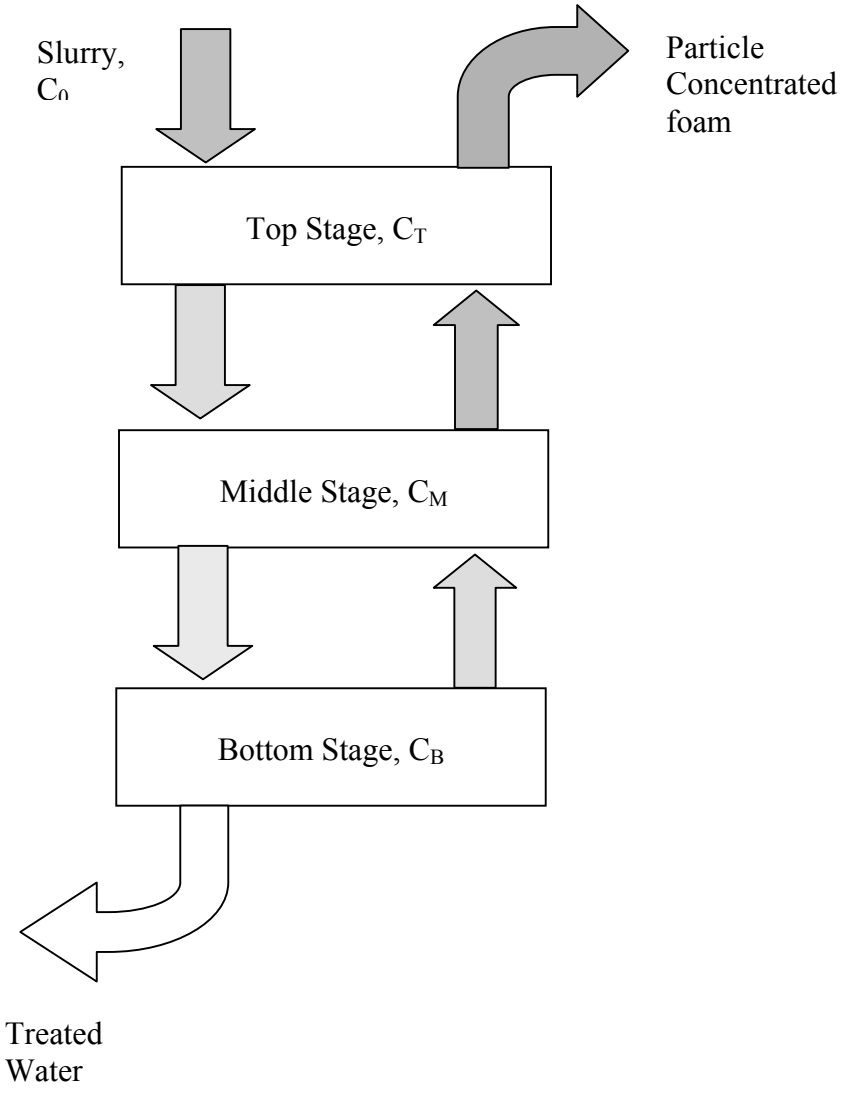

Figure E-1 A Sketch of the Physical Model for MSTLFLO Process

The mathematical expressions for above discussion can be written as follows:

$$\frac{dC_T}{dt} = \frac{C_0 - C_T}{\tau_T} - RF(C_T) + RF(C_B) \qquad \text{(top stage)} \qquad \text{(E-1a)}$$

$$\frac{dC_M}{dt} = \frac{C_T - C_M}{\tau_M} - RF(C_M) + RF(C_B) \qquad \text{(middle stage)} \qquad \text{(E-1b)}$$

$$\frac{dC_B}{dt} = \frac{C_M - C_B}{\tau_B} - RF(C_B) \qquad \text{(bottom stage)} \qquad \text{(E-1c)}$$

where τ_i and C_i are mean residence time and solid concentration of stage *i (i=T,M,B)*; *RF* is solid particle removed from each stage, which is a function of the concentration of that stage (C_i).

APPENDIX F

FORTRAN CODE FOR MSTLFLO PROCESS

```
************************************************************
*    FORTRAN CODES FOR SOLVING CONCENRATION
*    PROFILES IN A MSTLFLO CONTINUOUS OPERATION
*
****************************************************
*
*    INITIAL CONCENTRATION AND HYDRODYNAMIC
*    DATA ARE READ FROM "INPUT.DAT".
*
*-------------------------------------------------
*
*    DECLARATION OF VARIABLES
*
*-------------------------------------------------
*    DB=SAUTER MEAN DIAMETER, DB32
*    L=VOLUMETRIC LIQUID FLOW RATE, QL
*    F=FEED RATE, FL
*    GH=GAS HOLDUP
*    CO=INITIAL CONCENTRATION
*    CM=ASYMPTOTE OF CONCENTRATION at DIFFERENT CONDITIONS
*    CO=INITIAL CONCENTRATION
*    X=FLOTATION TIME
*    Y=OIL CONCENTRATION
*    NVAR=NUMBER OF STAGES
*    NSTEP=NUMBER OF INTEGRATION STEPS
*    TAU=MEAN RESIDENCE TIME
*    V(I)=VOLUME OF THE ITH STAGE
*    AK=KINETIC CONSTANT
*    SGV=SUPERFICIAL GAS VELOCITY
*    VSTART=0, FILLED IN WITH CLEAN WATER
*    A,B,D=CORRELATION CONSTANTS FOR KINETICS
```

```
*    PPM=INITIAL CONCENTRATION, NOT IN CALCULATIONS
*    AK=PRE-DECIDED KINETIC CONSTANT



*-------------------------------------------------
*
*     MAIN PROGRAM
*
*-------------------------------------------------
      PROGRAM OIL_CONT_GK_00
      INTEGER NVAR, NSTEPMX,NSTEP
      REAL*8 K, GH, L, DB, VSTART, TAU, V, C0, CM
     &    ,A, B, C, D, X, Y, F, X1, X2,SGV,PPM,AK
      PARAMETER(NVAR=3,NSTEPMX=1000)
      PARAMETER(NSTEP=300)
      DIMENSION K(NVAR),GH(NVAR),L(NVAR),DB(NVAR),
     &          VSTART(NVAR),TAU(NVAR),V(NVAR)
      EXTERNAL DERIVS
      COMMON /PATH/X(NSTEPMX),Y(NVAR,NSTEPMX)
      COMMON /CONT1/TAU,K
      COMMON /CONT2/C0,CM(3)
*4"      DATA GH(1),GH(2),GH(3)/0.3772,0.3888,0.3975/
*4"      DATA L(1),L(2),L(3)/9.46,9.7,9.84/
*4"      DATA DB(1),DB(2),DB(3)/1.25,1.24,1.22/
*4"      DATA A,B,C,D/0.9865,0.7536,0.8037,-1.4294/
*4"      DATA C0,CM/500.0,20.02/
*4"      DATA C0,CM/500.0,0.02/

***  12-IN MSTLFLO SIMULATIONS  ***
** SGV =1.3 cm/s **
*    DATA GH(1),GH(2),GH(3)/9.2, 10.7, 13.1/
*      DATA DB(1),DB(2),DB(3)/0.922, 0.96, 0.983/
** SGV =2.6 cm/s **
     DATA GH(1),GH(2),GH(3)/16.3, 24.8, 42.0/
      DATA DB(1),DB(2),DB(3)/1.155, 1.22, 1.30/
** SGV =3.9 cm/s **
*    DATA GH(1),GH(2),GH(3)/30.0, 47.5, 65/
*     DATA DB(1),DB(2),DB(3)/1.23, 1.27, 1.30/

*** Kinetic constants, SGV=1.3, 2.6, 3.9 cm/s ***
      DATA A,B,D/0.129, 0.659, -1.043/

      OPEN(UNIT=2,FILE='INPUT.DAT',STATUS='OLD')
      READ(2,*) SGV, PPM, F,AK,C0,CM,X2
*      READ(2,*) GH
*      READ(2,*) L
```

```
*      READ(2,*) DB
*      READ(2,*) AK
*      READ(2,*) CM
*      READ(2,*) C0
      X1=0.0
*      X2=10.0
*
      V(1)=110.0
      V(2)=66.0
      V(3)=88.0
      DO 200, I=1,NVAR
*    K(I)=A*GH(I)**B*L(I)**C*DB(I)**(D)
     K(I)=A*GH(I)**B*DB(I)**(D)
*      K(I)=AK
200   CONTINUE
      WRITE(*,*)'INPUT VSTART VALUE'
      READ(*,*)VSTART_TEMP
      DO 100 I=1,NVAR
      TAU(I)=V(I)/F
      VSTART(I)=VSTART_TEMP
 100  CONTINUE
*
*
      CALL RKDUMB(VSTART,NVAR,X1,X2,NSTEP,DERIVS)
      OPEN (UNIT=1, FILE='OIL_RT.DAT', STATUS='UNKNOWN')
      WRITE(1,13) SGV,PPM,F
  13  FORMAT(2X,'SGV, cm/s=',F8.4,2X,'PPM=',F8.4,2X,
     &'FEED, L/min=',F5.2)
     WRITE(1,*)'Flotation time  C(T)     C(M)      C(B)'
 130  FORMAT(2X,'SGV=',F8.4,2X,'PPM=',F8.4,2X,
     &'FEED, L/min=',F5.2)

      DO 11 I=1,NSTEP
      WRITE(*,12) X(I),Y(1,I),Y(2,I),Y(3,I)
      WRITE(1,12) X(I),Y(1,I),Y(2,I),Y(3,I)
 12   FORMAT(2X, 4(E13.6,1X))
 11   CONTINUE
      CLOSE(1)
      CLOSE(2)
      END
C
C
C    SUBROUTINE FOR CALCULATING DERIVATIVES, DY/DX
C
C
      SUBROUTINE DERIVS(X,Y,DYDX)
      REAL*8 C0, CM, K, TAU, TS, Y, DYDX
```

```
      INTEGER I
      DIMENSION K(3), TAU(3),TS(3), Y(3),DYDX(3), CM(3)
      COMMON /CONT1/TAU,K
      COMMON /CONT2/C0,CM(3)
      PARAMETER(A = 0.006)
      DO 100 I=1,3
       IF (Y(I).LE.CM(I)) THEN
      TS(I)=1000
        ELSE
          TS(I)=(A*(Y(I)-CM(I)))**(-1.0D00/K(I))
      ENDIF
100   CONTINUE
      DYDX(1)=(C0-Y(1))/TAU(1)-(Y(1)-CM(I))/TS(1)*K(1)
     ++(Y(2)-CM(I))/TS(2)*K(2)
      DYDX(2)=(Y(1)-Y(2))/TAU(2)-(Y(2)-CM(I))/TS(2)*K(2)
     ++(Y(3)-CM(I))/TS(3)*K(3)
       DYDX(3)=1/TAU(3)*(Y(2)-Y(3))-(Y(3)-CM(I))/TS(3)*K(3)
        RETURN
      END
C
C
C     RUNGE-KUTTA DRIVER
C
C
      SUBROUTINE RKDUMB(VSTART,NVAR,X1,X2,NSTEP,DERIVS)
      INTEGER NSTEP,NVAR,NMAX,NSTPMX
      PARAMETER (NMAX=3,NSTPMX=1000)
      REAL*8 X1,X2,VSTART(NVAR),XX(NSTPMX),Y(NMAX,NSTPMX)
      EXTERNAL DERIVS
      COMMON /PATH/ XX,Y
C     USES RK4
      INTEGER I,K
      REAL*8 H,X,DV(NMAX),V(NMAX)
      DO 11 I=1,NVAR
        V(I)=VSTART(I)
        Y(I,1)=V(I)
11    CONTINUE
      XX(1)=X1
      X=X1
      H=(X2-X1)/NSTEP
      DO 13 K=1,NSTEP
        CALL DERIVS(X,V,DV)
        CALL RK4(V,DV,NVAR,X,H,V,DERIVS)
        IF(X+H.EQ.X)PAUSE 'STEPSIZE NOT
     & SIGNIFICANT IN RKDUMB'
*
        X=X+H
```

```
        XX(K+1)=X
        DO 12 I=1,NVAR
          Y(I,K+1)=V(I)
12      CONTINUE
13    CONTINUE
      RETURN
      END

C
C
C     4TH ORDER RUNGE-KUTTA METHOD
C
C
      SUBROUTINE RK4(Y,DYDX,N,X,H,YOUT,DERIVS)
      INTEGER N,NMAX
      REAL*8 H,X,DYDX(N),Y(N),YOUT(N)
      EXTERNAL DERIVS
      PARAMETER (NMAX=3)
      INTEGER I
      REAL*8 H6,HH,XH,DYM(NMAX),DYT(NMAX),YT(NMAX)
      HH=H*0.5
      H6=H/6.
      XH=X+HH
      DO 11 I=1,N
        YT(I)=Y(I)+HH*DYDX(I)
11    CONTINUE
      CALL DERIVS(XH,YT,DYT)
      DO 12 I=1,N
        YT(I)=Y(I)+HH*DYT(I)
12    CONTINUE
      CALL DERIVS(XH,YT,DYM)
      DO 13 I=1,N
        YT(I)=Y(I)+H*DYM(I)
        DYM(I)=DYT(I)+DYM(I)
13    CONTINUE
      CALL DERIVS(X+H,YT,DYT)
      DO 14 I=1,N
        YOUT(I)=Y(I)+H6*(DYDX(I)+DYT(I)+2.*DYM(I))
14    CONTINUE
      RETURN
      END
```

APPENDIX G

SUMMARY OF EXPERIMENTAL DATA

Fine Particles Size Distributions

	Percentage Density, %		
Particle size, μm	PAC_A	PAC_B	Glass beads
1.4	1.1		
1.9	5.6		
2.8	15.4	1.9	
3.9	37.8	9.8	
5.5	60.9	21.1	1.3
7.8	72.2	27.4	5.7
11	84.6	33.8	14.5
16	94.4	48.3	20.5
22	100	68.4	33.7
31		74.2	49.9
44		92.2	69.7
62		100	81.3
89			95.1
127			100

Gas Holdups in Single Stage Operation in the 4-in Column

	Gas holdups, %		
C_f, ppm / SGV, cm/s	10	15	20
1.50	16	18	19
2.00	24	24	25
2.50	29	32	33
3.00	35	40	41
3.50	41	47	48

Gas Holdups in Single Stage Operation in the 12-in Column

	Gas holdups, %		
C_f, ppm / SGV, cm/s	10	15	20
1.30	15	17	18
1.95	23	24	25
2.60	29	33	33
3.25	38	42	43
3.90	45	48	52

Gas Holdups in the 12-in Column using Different Spargers (C_f=10 ppm)

	Gas holdups, %			
SGV, cm/s	Disk sparger		Stick sparger	
1.3	5	5	4.6	5
2.6	8.3	7.5	9.2	13.3
3.9	11.6	10	14.6	23.3

Gas Holdups in the 12-in Column using Different Cones (C_f=10 ppm)

	Gas holdups, %					
SGV, cm/s	Long cone baffle			Short cone baffle		
1.3	5.83	6.67	7.92	5	4.6	5
2.6	10.83	13.33	19.17	7.5	9.3	13.3
3.9	15.42	18.33	32.92	10	14.6	23.3

Gas Holdup in Different Stages the 12-in Column with Different Frothers

SGV, cm/s	Frother, ppm	Gas holdups, %					
		MIBC			2 EH		
		B	M	T	B	M	T
1.30	5	6.25	7.92	10.00	5.83	6.67	7.92
2.60		10.83	12.92	16.67	10.89	13.33	19.17
3.90		15.00	18.75	24.58	15.42	18.33	32.75
1.30	10	6.25	8.33	9.58	7.50	9.17	11.67
2.60		12.09	15.00	19.17	14.17	16.25	22.08
3.90		17.50	21.25	31.67	22.08	33.33	48.80
1.30	20	7.08	9.17	11.25	7.50	8.75	10.89
2.60		18.33	25.83	44.58	19.58	22.92	39.58
3.90		35.83	53.33	67.92	33.33	45.00	60.00
1.30	30	7.50	9.58	11.67	10.42	11.25	14.17
2.60		20.00	26.67	46.67	37.50	58.33	N/A
3.90		45.83	60.00	N/A	64.17	68.33	N/A

PAC Residual Concentrations in the 4-in column (Different PAC Feed Positions)

PAC concentrations, ppm	Central Top Stage			Annular Top Stage			Middle Stage		
C_f, ppm / SGV, cm/s	20	30	40	20	30	40	20	30	40
1	57	44	21	65	52	34	59	47	20
2	31	18	10	36	25	17	34	20	13
3	18	11	5	22	17	11	20	14	9
4	7	4	1	14	10	6	10	8	5

Glass Beads Concentrations Profile in the 4-in Column

PAC concentrations, ppm	Frother 10 ppm			Frother 20 ppm		
SGV, cm/s / Time, min	1.0	2.0	3.0	1.0	2.0	3.0
1	454	409	372	287	264	222
2	421	354	305	194	169	128
5	344	219	174	121	96	47
8	305	147	122	104	85	26
10	297	138	113	95	64	16
15	252	134	104	91	62	11

Glass Beads Residual Concentrations in the 4-in Column

C_f, ppm / SGV, cm/s	10	20
1	52	72
2	73	88
3	81	98

Oil Removal in the 12-in Column

PAC concentrations, ppm	Frother, 20 ppm			Frother, 30 ppm		
SGV, cm/s / Time, min	1.3	2.1	2.6	1.3	2.1	2.6
1	360	306	254	152	106	74
2	260	175	140	70	55	48
5	150	95	80	53	45	38.5
10	93	63	59	50	43	37
20	66	55	54	48	42	36
30	54	49	48	47	40	36

BIBLIOGRAPHY

1. Ives, K. J., ed., The Scientific Basis of Flotation, "The Froth Flotation Process: Past, Present and Future – In Brief, by Kitchener, J.A." (Hague: Martinus Nijhoff Publishers, 1982), pp. 3-51

2. Feng, D and Aldrich, C, Removal of diesel from aqueous emulsions by flotation, SEPARATION SCIENCE AND TECHNOLOGY, Vol. 35(13), 2000, pp2159-2172

3. Zhang, L, Somasundaran, P, et al, Flotation of hydrophobic contaminants from soil, COLLOIDS AND SURFACES A-PHYSICOCHEMICAL AND ENGINEERING ASPECTS, Vol. 177(2-3), 2001, pp235-246

4. Puget, FP, Melo, MV and Massarani, G, Wastewater treatment by flotation, BRAZILIAN JOURNAL OF CHEMICAL ENGINEERING, Vol. 17, 2000, pp407-413

5. Caixeta C., Cammarota M.C., and Xavier A.M.F., Slaughterhouse wastewater treatment: evaluation of a new three-phase separation system in a UASB reactor, BIORESOURCE TECHNOLOGY, Vol. 81(1), 2002, pp. 61-69

6. Gu. X. and Chiang, S. H., A Novel Flotation Column for Oily Water Clean-up, SEPARATION AND PURIFICATION TECHNOLOGY, Vol. 16, 1999, pp. 193-201

7. Ives K. J., 1982, Op. Cit., pp. 9

8. Svarovsky, L., Solid-liquid separation processes and technology, (Amsterdam: Elsevier, 1985), pp. 103-106

9. Ibid., pp. 610

10. Finch, J. A., and Dobby, G. S., Column Flotation (Oxford: Pergamon Press, 1990), pp. 1

11. Jameson, G., US Patent 4938865, 1990

12. Yoon, R., US Patent 5167798, 1992

13. Yang, D. C., US Patent 4592834, 1986

14. Miller, J.D. and Kinneberg, D. J., US patent 4744890, 1988

15. Lai, Ralph, and Patton, R. A., US patent 6056125, 2000

16. Chiang, S. H., He, D., and Ding, F., US Patent 5897772, 1999

17. Shi, F., Chiang, S. H., "Removal of metal oxides precipitates from nuclear plant waste water using multistage column flotation", 11th annual conference, American Filtration & Separation Society, St. Louis, Missouri, May 4-7,1998

18. He, D.X., Chiang, S.H., " A study of a novel multi-stage agitated column for precombustion coal cleaning", The proceedings of 3rd Asia-Pacific International Symposium on combustion and energy utilization, Hong Kong, 11-15 Dec., 1995, pp. 775-780

19. Leeden, F. Van der, Troise, F. L., Todd, D. K., The Water Encyclopedia, Second Edition, (Lewis Publishers, 1990), pp.510-520

20. Corbitt, Robert A., Standard handbook of environmental engineering, 2nd ed. (McGraw-Hill, 1998), pp. 5.1-5.6

21. Ibid., pp. 5.69-5.75

22. Patterson J., W., Wastewater treatment technology, (Ann Arbor: Ann Arbor Science Publisher, 1975), pp. 199-201

23. Svarovsky, 1990, Op. Cit., pp. 593

24. Matis, K. A., ed., Flotation science and engineering, An overview of the process, by Matis, K. A., and Zouboulis, A. I., (New York: Marcel Dekker, Inc., 1995), pp. 82-83

25. Zeta-Meter Manual, ZM-80, (New York: Zeta-meter, Inc.), 1980

26. Crozier, R. D., Flotation: theory, reagents, and ore testing, (Oxford: Pergamon Press, 1992), pp. 9-10

27. Klassen, V. I., and Mokrousov, V. A., An introduction to the theory of flotation [by] Translated [from the 2d Russian ed.] by J. Leja and G. W. Poling, (London: Butterworths, 1963), pp. 153-155

28. Fuerstenau, M. C., Miller, J. D., Kuhn, M. C., Chemistry of flotation, (New York: Society of Mining Engineering, 1985), pp. 2

29. Svarovsky, L., ed., Solid-liquid separation, "Flotation", by Gochin, R. J., (London: Butterworths, 1990), pp. 593-600

30. Reay D. and Ratcliff G., Removal of fine particles from water by dispersed air flotation: effects of bubble size and particle size on collection efficiency, CAN. J. CHEM. ENG., Vol. 51 (1973), pp. 179

31. Lai, R. W., et al, The modern proportionality law for science, Medicine, and engineering applications, (Pittsburgh: Toshi Company, 1995)

32. Shi, F. and Chiang, S.H., Emulsified Oil Separation by using MSTLFLO process, 17th Pittsburgh Coal Conference, November 11-14, 2000, Pittsburgh, PA

33. Chiang, S.H., Shi, F. and Gu X., A New Development In Flotation Process, JOURNAL OF CHINESE INST. OF CHEM. ENGINEERS, Vol.34 (1), 2003, 1-9

34. Cooney, David O., Adsorption design for wastewater treatment, (Boca Raton, FL: Lewis Publishers, 1998), pp 45-50

35. Calgon Carbon Corp. product Report, 2000, (Pittsburgh, Calgon Carbon Corp.)

36. Gu, X., A novel multi-stage flotation column for oily wastewater treatment, (Ph. D. Thesis, Dept. of Chemical and Petroleum Engineering, Univ. of Pittsburgh, 1998), pp. 56-101

37. Gu, X., Op., Cit., pp. 123-127

38. Shi, F., Gu, X. and S.H. Chiang, A Study of Hydrodynamic Behaviors in a Multi-stage Loop-Flow Flotation Column, the Fluid/Particle Separation Journal, Vol.14 (3), 2002, 185-198

39. Bentham, R., McClure N., et al, Biotreatment of an industrial waste oil condensate, Water Science Technology, Vol. 36(10), 1997, pp.125-129

40. Sato, Y., Murakami, Y., et al, Removal emulsified oil particles by dispersed air flotation, J. of Chemical Engineering of Japan, Vol. 13(5), 1980, pp. 385-389

41. Takahashi, T., Miyahara, T., Nishizaki, Y., Separation of oily water by bubble column, J. of Chemical Engineering of Japan, Vol. 12(5), 1979, pp. 394-399

42. Montgomery, J. H., Groundwater chemicals desk reference (CRC Press LLC, 2000), pp. 859-864

43. Kroschwitz, J. I., ed., Encyclopedia of chemical technology, (New York: Wiley, 1996), pp. 599

44. Surface TensioMeter Users' Manual, 1990 (Fisher Scientific Corp., USA)

45. Levenspiel, O., Chemical reaction engineering, (New York: Wiley, 1962), pp.260-267

46. Adobe PhotoShop 5.0 users' manual, Adobe System Incorporation 1998-2002.

47. ImageJ 1.20s, by National Institutes of Health, USA, 2001 (http://rsb.info.nih.gov/ij/)

48. MICROTRAC analyzer, Model 7995-11 users' manual, 1980 (New York, Leeds & Northrup Co., USA)

49. Oil content analyzer, OCMA-220 users' manual, 1996, (Horiba Co., USA)

50. Greenberg, A. E., Lenore, S. C., Eaton A. D., Franson M. A. H., Standard methods for the examination of water and wastewater (American Public Health Association, 18th ed., 1992)

51. UV/Vis spectrophotometer, DU-600 users' manual, 1998 (Beckman Coulter Inc., USA)

52. Davies J. T. and Rideal E.K., Interfacial Phenomena (New York: Academic Press, 1963)

53. Matis K. A., Op., Cit., pp.481

54. Frederick M. F., ed., Contact angle, wettability and adhesion, "Relation of equilibrium contact angle to liquid and solid constitution", by Zisman W. A. (Washington, American Chemical Society, 1964), pp. 13-31

55. Frederick M. F., ed., Contact angle, wettability and adhesion, "Contact angle hysteresis. II. Contact angle measurements on rough surfaces to liquid and solid constitution", by Dettre R. H. and Johnson R. E. (Washington, American Chemical Society, 1964), pp.139-143

56. Matis K. A., Op., Cit., pp.72-111, pp. 484

57. Neumann A. W. and Spelt J. K. ed., Surfactant Science Series, Volume 63: Applied Surface Thermodynamics, (New York: Marcel Dekker, Inc. 1989), pp. 396

58. Botsaris G. D. and Glazman Y. M. ed., Surfactant Science Series, Volume 32: Interfacial Phenomena in Coal Technology, (New York: Marcel Dekker, Inc. 1989), pp. 41

59. Neumann A. W. and Spelt J. K., Op., Cit., pp. 599

60. Ibid., pp. 421

61. PPG technical report, http://www.ppg.com/gls_aquapel/about.htm, 2000 (PPG Corp., USA)

62. Couvert A., Roustan M., and Chatellier P., Two–phase hydrodynamic study of a rectangular air-lift loop reactor with an internal baffle, Chemical Engineering Science, Vol. 54, 1999, pp5245-5252.

63. Bakker W., Vancan H., and et al., Hydrodynamics And Mixing In A Multiple Airlift-Loop Reactor, Biotechnology And Bioengineering, Vol. 42 (8), 1993, pp994-1001

64. Bello, R. A., Robinson, C. W., and Young, M. M. Liquid circulation and mixing characteristics of airlift contactors. The Canadian Journal of Chemical Engineering, Vol. 62, 1984, pp573-577

65. Choi, K. H., and Lee, W. K., Circulation liquid velocity, gas hold-up and volumetric oxygen transfer coefficient in external-loop airlift reactors, Chemical Technology and Biotechnology, Vol. 56, 1993, pp51-58.

66. Gravilescu, M., and Tudose, R. Z., Study of the liquid velocity in external-loop airlift bioreactors, Bioprocess Engineering, Vol. 14, 1995, pp33-39.

67. Snedecor, G.W., Statistical Methods, (Ames: The Iowa State College Press, 1953), pp 31-54

68. MiniTab 13 Users' Manual, 2000 (MiniTab Inc., USA)

69. F. Shi, S.H. Chiang, Modeling of the Multi-stage Loop-flow Flotation Column, Proceedings Advances in Filtration and Separation Technology Volume 14, 830-833, American Filtration & Separations Society, 2001

70. Lai R. W., The Overlooked Law of Nature: A New Concept in Kinetics Analysis, (Pittsburgh: Toshi Company, 1990), pp. 7-16

71. Statistica Users' Manual 2000 (StatSoft Inc., USA)